Sound transmission through framed buildings

Craik, R. J. M.; Steel, J. A.; Nightingale, T. R. T.

Internal Report (National Research Council of Canada. Institute for Research in Construction); no. IRC-IR-672, 1995-05-01

National Research Council Canada
Conseil national de recherches Canada

NRC·CNRC

Sound Transmission Through Framed Buildings

A report on collaboration between Heriot-Watt University and National Research Council of Canada

Robert J.M. Craik, John A. Steel and Trevor R.T. Nightingale

IRC Internal Report
IRC-IR-672

May 1995

Published by
Institute for Research in Construction
IRC

CONTENTS

LIST OF SYMBOLS USED

A	=	total absorption of a room in metric sabins	m^2
B	=	bending stiffness of a plate	Nm
B_f	=	bending stiffness of the sire stop	Nm
C_L	=	longitudinal wave speed in a plate	m/s
C_o	=	speed of sound in air (taken to be 350 m/s^2)	m/s
D	=	sound pressure level difference	dB
Y	=	Young's modulus	N/m^2
E	=	energy	Joules
f	=	frequency	1/s
f_c	=	critical frequency	1/s
H	=	stiffness of a plate when ribs are present	Nm
k	=	wave number of a wave in a plate	1/m
L_{12}	=	length of the joint between Susbystem 1 and Subsystem 2	m
l_x, l_y	=	length of a floor bay in the x and y directions respectively	m
M	=	moment of inertia	N/m
m	=	total mass of a building element	m
n	=	thickness of a plate	m
n(f)	=	number of modes at frequency f	dimensionless
R	=	sound reduction $-10\log\tau$	dB
S	=	surface area	m^2
T	=	reverberation time of a cavity or structure	s
T_1	=	amplitude of a wave in a plate 1	m

T_{n1}	=	near field amplitude of a wave in a plate 1	m
V	=	room volume	m^3
ϕ	=	slope of a deformed plate	dimensionless
ξ	=	displacement of a deformed plate	m
μ	=	poissons ratio	dimensionless
θ	=	angle of incidence for a wave	radians
η	=	total loss factor	dimensionless
υ	=	normal surface velsity	m/s
σ	=	radiation factor	dimensionless
η_{12}	=	coupling loss factor from Subsystem 1 to Subsystem 2	dimensionless
τ_{12}	=	transmission coefficient from Susbystem 1 to Subsystem 2	dimensionless
ρ_s	=	surface density of a building element	kg/m^2

LIST OF FIGURES

At the bottom of most of the figures is a reference number together with the date of generation. This number refers to the location of the data on the disk. For example, Figure 3.6 has the reference FIG24. The data for this figure can be found in a directory on the data disk called FIG24. The data is then held in files FIG24.A, FIG24.B, FIG24.C, etc. The data is stored as ASCII characters and there is a separate file for each curve. The FIG24.BAT file and the FIG24.SET file were used with the GRAPH program to generate the figures.

LIST OF TABLES

ACKNOWLEDGEMENTS

This report is a result of collaboration between Heriot-Watt University and the National Research Council Canada.

The initial work on sound transmission across fire stops was undertaken at Heriot-Watt University when T. Nightingale visited Scotland in May 1994. This work was developed during a visit by R. Craik and J. Steel in October and November 1994.

The work was carried out at the Institute for Research in Construction at NRC in Ottawa and was funded by the NRC and by Heriot-Watt University, Edinburgh, Scotland.

ABSTRACT

This report looks at sound transmission through walls and floors in a flanking laboratory at NRC Canada.

A statistical energy analysis (SEA) model was developed to predict sound transmission both for direct transmission through the walls and floors and for flanking transmission either due to a specially introduced fire stop material or from flanking due to the construction of the laboratory.

The theoretical model was able to predict most of the characteristics of transmission and that the direct transmission through a wall is dominated by non-resonant transmission into and out of the cavity below the critical frequency and by resonant transmission into and out of the cavity above the critical frequency.

When a fire stop was placed in the test facility there was a considerable decrease in both the measured and predicted transmission. The dominant path at the higher frequencies was then from the source room into the floor, across the fire stop and finally radiated by the floor. The path can be largely eliminated by the use of a floating floor as was confirmed both theoretically and experimentally.

Airborne sound transmission through the floors also gave good agreement between the measured and predicted results.

A more detailed study of the flanking transmission associated with the fire stop was undertaken. It was found that the joists at the joint reduced transmission at the higher frequencies and that at very high frequencies provided an almost total block on transmission across the fire stop.

A study of vibration propagation across a timber joist floor was also undertaken. Measurements showed that there was considerable attenuation

with distance except at 250 Hz. A further examination of the modal properties of the floor and transmission at a joist showed that there was considerable spatial filtering and that, as was measured, vibration would only be transmitted at some frequencies.

1 INTRODUCTION

1.1 INTRODUCTION

In order to understand sound transmission through framed buildings, a collaborative study was undertaken between Heriot-Watt University, Edinburgh, Scotland and the National Research Council Canada, Ottawa, Canada.

The aim of the collaboration was initially to develop a theoretical model to predict the effect of fire stops on sound transmission through walls. This was extended to include prediction of all transmission paths between rooms in standard constructions. This included horizontal transmission through a wall, vertical transmission through floors, and diagonal transmission where there is no common wall and all transmission is flanking transmission.

2 OUTLINE OF THEORY

2.1 INTRODUCTION

The basic theory that was used to predict the performance of the structures is Statistical Energy Analysis. This is a powerful framework of analysis ideally suited to this type of problem where deterministic solutions are not possible. This section does not include the basic theory of SEA but does include the specific equations that were used to perform the calculations.

The actual calculations were carried out using a program called PPC. This runs batch type programs which are included in Appendix B for reference together with the actual coupling loss factors computed for the basic model.

2.2 SUBSYSTEM PROPERTIES

Damping

For each subsystem the reverberation time was measured. These values are discussed in more detail in Chapter 3 where the basic model is described. The total loss factor, η, (often referred to as the system damping) was computed from the reverberation time, T, using the equation

$$\eta = \frac{2.2}{fT} \tag{2.1}$$

where f is the frequency.

Modal densities

The modal density is required for some of the calculations of coupling loss factor.

The modal density of a room was computed from the equation

$$n(f) = \frac{4\pi f^2 V}{c_0^3} + \frac{\pi f S}{2c_0^2} + \frac{L}{8c_0} \tag{2.2}$$

where V is the room volume, c_0 is the speed of sound, S is the surface area, and L is the perimeter length. At low frequencies, cavities behave as two dimensional spaces and the modal density is given by

$$n(f) = \frac{2\pi f S}{c_0^2} \qquad (2.3)$$

Above the first cross mode where a half wavelength fits into the depth of the cavity, the cavity behaves like a room and equation (2.2) was used.

The modal density of walls and floor cladding was determined from

$$n(f) = \frac{\sqrt{3} S}{h c_L} \qquad (2.4)$$

where S is the surface area, h is the thickness of the material, and c_L is the longitudinal wave speed.

Energy

Although not often used in this report, energy is used in SEA as the parameter representing dynamic response. For a room the energy (in dB re 10^{-12} J) is given by

$$L_e = L_p + 10 \log V - 25.4 \qquad (2.5)$$

where L_p is the sound pressure level in dB re 2×10^{-5} N/m^2 and V is the volume.

For walls and floors the energy is given by

$$E = m v^2 \qquad (2.6)$$

where m is the total mass and v is the normal surface velocity.

2.3 COUPLING LOSS FACTORS

Wall to room/cavity coupling

The coupling loss factor from a wall to a room or to a cavity is computed from

$$\eta_{12} = \frac{\rho_0 c_0 \sigma}{2\pi f \rho_s} \qquad (2.7)$$

where σ is the radiation efficiency. The equations used for σ were those given by Leppington *et al* (1982) as

$$\sigma = \frac{U c_0}{4\pi^2 f^{1/2} f_c^{1/2} S(\mu^2-1)^{1/2}} \left(\ln\left(\frac{\mu+1}{\mu-1}\right) + \frac{2\mu}{\mu^2-1} \right) \qquad f<f_c \quad (2.8)$$

$$\sigma = \left(\frac{2\pi f}{c_0}\right)^{1/2} l_x \left(0.5 - 0.15\frac{l_x}{l_y}\right) \qquad f=f_c \quad (2.9)$$

$$\sigma = \left(1 - \frac{f_c}{f}\right)^{-1/2} \qquad f>f_c \quad (2.10)$$

where l_x and l_y are the plate dimensions ($l_x \leq l_y$), U is the plate perimeter, f_c is the critical frequency and $\mu=(f_c/f)^{1/2}$. These are the same as the expressions given by Maidanik except that a correction has been made for frequencies below f_c setting the "g_1" term to zero and correcting the values at f_c.

The value of perimeter length used in the calculations is discussed further in Chapter 3.

The expressions above are for simply supported panels in an infinite baffle. The radiation efficiency was increased by a factor of 4 below the critical frequency to account for radiation into a quarter space and to account for clamping of the edges. The correction is x2 for each.

Although these expression are for radiation into free space, it was assumed that the same equations could be used to give radiation into a cavity.

Room/cavity to wall coupling

In all cases, the coupling loss factors describing power flow from an acoustic space to a structure can be found using the consistency relationship given by

$$n_1 \eta_{12} = n_2 \eta_{21} \qquad (2.11)$$

Thus, if the coupling from a wall to a room is known, then the coupling in the opposite direction can be readily computed.

For large rooms where the modal density can be approximated by the first term of equation (2.2), the coupling loss factor from a room to a plate becomes

$$\eta_{12} = \frac{\rho_0 c_0^2 S f_{c2} \sigma}{8\pi V_1 \rho_{s2} f^3} \qquad (2.12)$$

If a wall is being excited from a cavity, taking equation (2.3) as the modal density of the cavity gives the CLF from a cavity to a wall as

$$\eta_{12} = \frac{\rho_0 c_0 f_c 2\sigma_2}{4\pi f^2} \quad (2.13)$$

Non-resonant transmission between rooms

When modelling sound transmission through a wall, there will be non-resonant transmission modelled as direct transmission between two rooms.

Transmission from one room to another space is given by

$$\eta_{12} = \frac{c_0 S \tau_{12}}{8\pi f V_1} \quad (2.14)$$

and transmission from a cavity to another space is

$$\eta_{12} = \frac{\tau_{12}}{4\pi} \quad (2.15)$$

The transmission coefficient, τ, to be used with these equations is more commonly given as a transmission loss, R, defined as $10\log(1/\tau)$. This can be found from the mass law using equations such as

$$R_0 = 10\log\left(1 + \frac{2\pi f \rho_s}{2\rho_0 c_0}\right) - 20\log\left(\frac{2\pi f \rho_s}{2\rho_0 c_0}\right) = 20\log(f \rho_s) - 42 \quad (2.16)$$

or one of the many variations. However, as this is the dominant transmission path over much of the frequency range, the more accurate equations by Leppington *et al* were used giving the transmission coefficient as

$$\tau = \left(\frac{\rho_0 c_0}{\pi f \rho_s \left(1 - f^2/f_c^2\right)}\right)^2 \left(\ln\left(\frac{2\pi f\sqrt{S}}{c}\right) + 0.160 + U(l_x, l_y)\right.$$

$$+ \frac{1}{4\mu^6}\left[(2\mu^2 - 1)(\mu^2 + 1)^2 \ln(\mu^2 - 1) + (2\mu^2 + 1)(\mu^2 - 1)^2 \ln(\mu^2 + 1)\right. \quad (2.17)$$

$$\left. \left. - 4\mu^2 - 8\mu^6 \ln(\mu)\right]\right)$$

where $U(l_x, l_y)$ is a function of shape and can be ignored for normal shaped structures and $\mu^2 = f_c/f$ as in equation (2.8). This equation is the same as the equation by Sewell but has additional terms which increase the accuracy close to the critical frequency. These terms (the second and third line) can usually be ignored except close to the critical frequency so that the term in the square bracket can be set to zero.

Structure to structure coupling

The structural coupling was obtained from the equation

$$\eta_{12} = 0.1365\left[\frac{h_1 c_{L1}}{f}\right]^{1/2} \frac{L_{12}}{S_1}\tau_{12} = \frac{c_0}{\pi^2\sqrt{f f_{c1}}} \frac{L_{12}}{S_1}\tau_{12} \quad (2.18)$$

where τ is the transmission coefficient and L_{12} is the common boundary length of the joint.

This transmission coefficient is described in more detail in Chapter 5.

2.4 TRANSMISSION PATHS

Although SEA can be used to determine the response of all subsystems by the solution of a series of simultaneous equations this requires specialised software. However, the magnitude of a transmission path can be determined by hand.

If the source and receiving subsystem are both rooms, then the airborne level difference, D, due to transmission along a path 1-2-3-4-...n can be given by

$$D_{1-2-3-4-\ldots n} = 10\log\frac{\eta_2\eta_3\eta_4\cdots\eta_n}{\eta_{12}\eta_{23}\eta_{34}\cdots\eta_{n-1n}}\frac{V_n}{V_1} \quad (2.19)$$

The level difference can be expressed in a normalised form as a Transmission Loss (or Sound Reduction Index), R, as

$$R = D + 10\log\frac{S}{A} = L_1 - L_2 + 10\log\frac{ST_2}{0.161V} \qquad 2.20)$$

where T_2 is the reverberation time of the receiving room 2.

One of the most important paths is non-resonant transmission through the double wall involving non-resonant transmission into the cavity of the double wall followed by non-resonant transmission out again. Inserting the expressions for the coupling and total loss factors into equation (2.18) gives the Transmission loss for the path as

$$R_{1\text{-}5\text{-}2} = R_{15} + R_{52} + 10\log\frac{1}{T_2 f} + 14.4 \qquad (2.21)$$

3 SOUND TRANSMISSION THROUGH WALLS

3.1 INTRODUCTION

The work on sound transmission through walls was split into several parts. The first part was concerned with a basic model to predict sound transmission. This SEA model included all the parts of the flanking laboratory that were thought necessary for the prediction of sound transmission both through the walls and through the floors. This section only contains results for the transmission through the walls.

The initial modelling was carried out for the wall where there was a 0.38 mm steel sheet fire stop. This has the lowest stiffness, and transmission via the flanking paths is not important. The results of this section are given first.

The model was then changed to give predictions for the system with a plywood fire stop and a gypsum fire stop on the flanking wall. These results are given next.

Finally, further work was carried out validating some of the initial assumptions. Due to the time constraints, it was not possible to go back over every prediction but the more important implications of this later work are then discussed.

3.2 THE TEST FACILITY AND SPECIMEN

The test facility was the Flanking Laboratory at the NRC. Details of the basic construction and details of the structure tested are given in Appendix A.

3.3 THE BASIC MODEL

The basic SEA model that was used for the calculations can be seen in Figure 3.1. Each of the major components (the rooms, the cavities between the walls, the floors (both walking surface and joists) and the walls (one for each leaf)) is modelled as a separate subsystem. Some variations on this are given in other sections but this model provides a base from which variations can be determined.

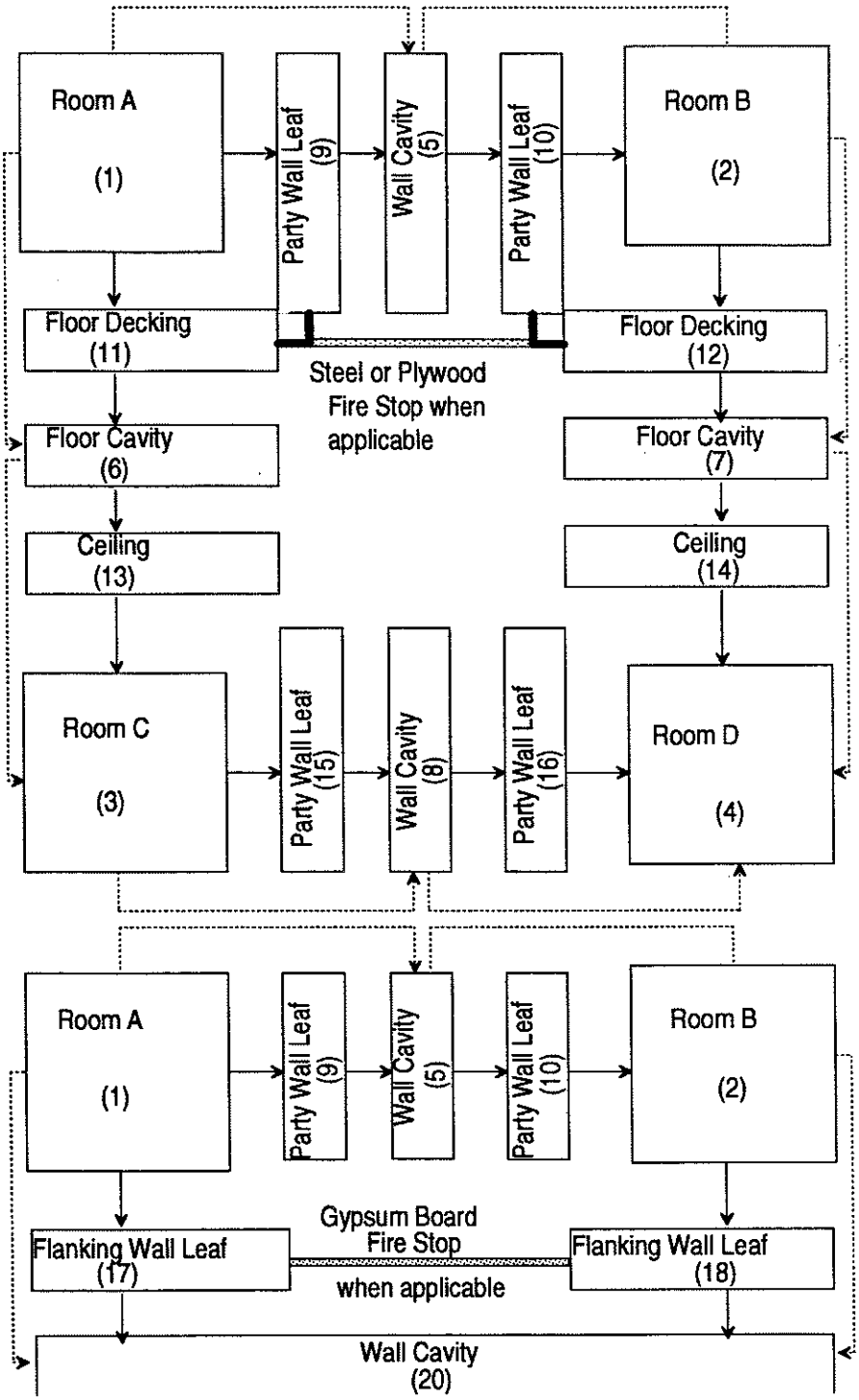

Figure 3.1. Schematic representation of the SEA model and its subsystems used for the calculation of sound transmission.

It was assumed that the floors and the walls were each a single subsystem and that the floor joists and wall framing were not important. This is reasonable as an initial assumption though it does lead to some errors. This is discussed further in Chapter 5.

This model is essentially the same as that used by Price and Crocker in 1970 though some of the assumptions are slightly different and the model has been developed to include other transmission mechanisms.

Material properties

The dimensions and material properties of these subsystems are listed in Table 3.1.

Subsystem		L_x m	L_y m	L_z m	ρ_s kg/m^2	f_c Hz
1	room	4.54	4.60	2.43		
2	room	4.52	4.11	2.43		
3	room	4.38	4.46	2.07		
4	room	4.37	3.96	2.07		
5	upper wall cavity	4.54	2.34	0.191		
6	floor cavity	4.54	4.60	0.240		
7	floor cavity	4.54	4.11	0.240		
8	lower wall cavity	4.64	2.07	0.191		
9	upper party wall	4.54	2.43	0.026	19.2	3000
10	upper party wall	4.54	2.43	0.026	19.2	3000
11	floor	4.54	4.60	0.016	7.22	1600
12	floor	4.54	4.11	0.016	7.22	1600
13	ceiling	4.54	4.60	0.026	19.2	3000
14	ceiling	4.54	4.11	0.026	19.2	3000
15	lower party wall	4.64	2.07	0.026	19.2	3000
16	lower party wall	4.64	2.07	0.026	19.2	3000
17	flanking wall	3.80	2.43	0.26	19.2	3000
18	flanking wall	3.70	2.43	0.026	19.2	3000
20	flanking wall cavity	7.50	2.43	0.191		

Table 3.1. Summary of material properties.

Damping

For the room volumes, the damping was obtained from measured reverberation times. The actual values are not too important as the measured results were normalised (usually as Transmission Loss) and so are independent of the room's damping. The reverberation times used are listed in Table 3.2.

Attempts were made to measure the reverberation times in the cavities. Both the cavities of the wall and the floor have considerable amounts of absorption in the space so that the reverberation time would be expected to be much shorter than for rooms.

Frequency Hz	Room 1 s	Room 2 s	Room 3 s	Room 4 s
50	0.70	0.52	0.45	0.48
63	0.63	0.74	0.70	0.47
80	0.75	0.83	1.08	1.05
100	1.19	1.10	1.27	1.02
125	1.25	1.30	1.44	1.14
160	1.48	1.42	1.72	1.45
200	1.65	1.35	1.61	1.45
250	1.51	1.38	1.47	1.45
315	1.62	1.44	1.74	1.69
400	1.75	1.71	1.88	1.96
500	1.83	1.74	1.85	1.70
630	1.54	1.53	1.84	1.67
800	1.45	1.42	1.59	1.48
1000	1.45	1.36	1.50	1.38
1250	1.38	1.24	1.38	1.33
1600	1.32	1.21	1.35	1.32
2000	1.28	1.17	1.35	1.32
2500	1.30	1.14	1.26	1.30
3150	1.32	1.21	1.27	1.30
4000	1.28	1.18	1.37	1.35
5000	1.21	1.13	1.32	1.31
6300	1.07	1.00	1.23	1.19

Table 3.2 Measured reverberation times for each of the rooms.

Measured values of reverberation time are given in Figure 3.2. High values of around 1 second are likely to be leakage from the rooms. Based on these initial measurements, the reverberation time in the cavity was taken to be

$$T = \frac{3}{\sqrt{f}} \qquad (3.1)$$

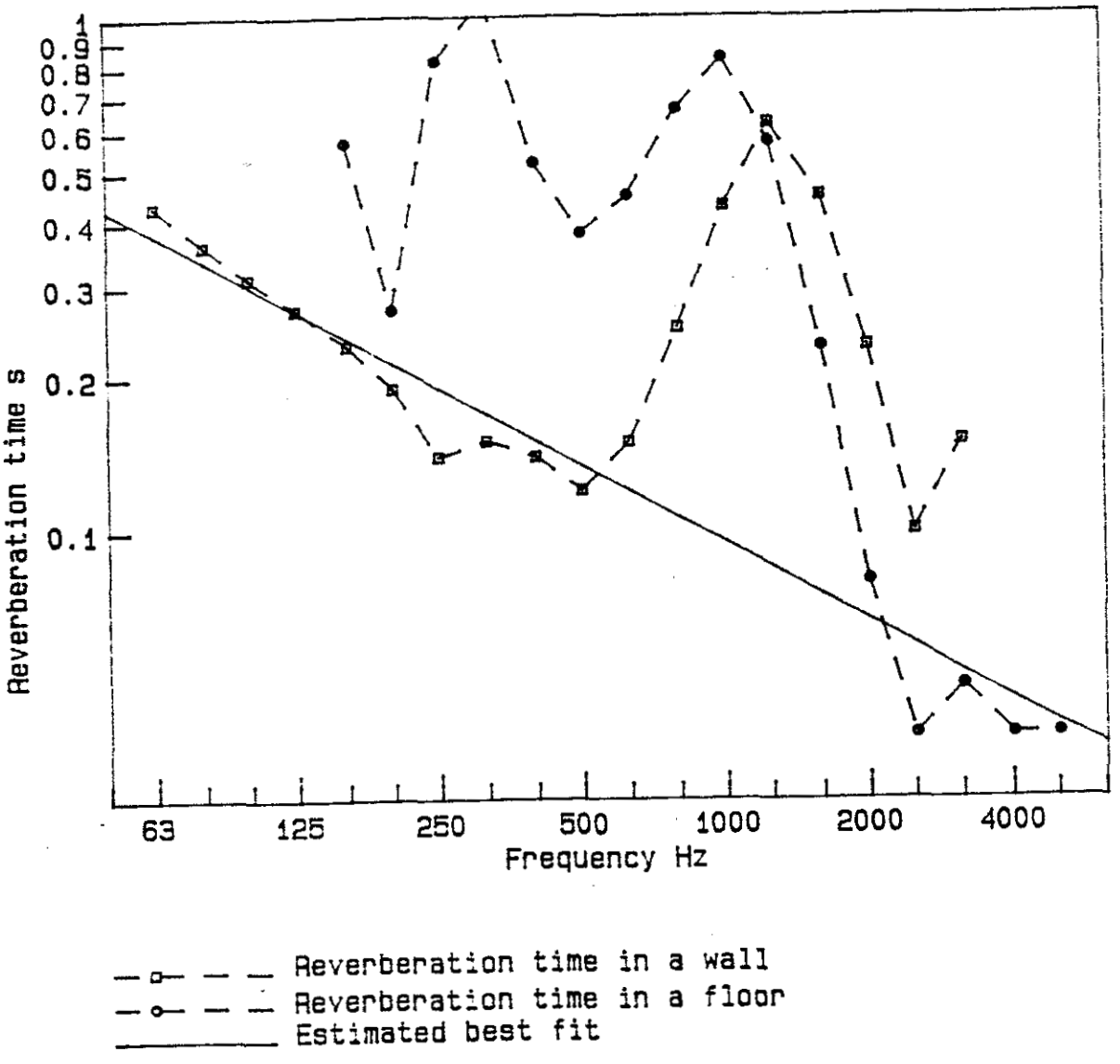

Figure 3.2. Reverberation time measured in the cavity between the walls and in the floor together with a best fitting curve. (PPC FIG3, 26 Oct. 94)

At low frequencies, the sum of the predicted coupling loss factors (CLF) was higher than the total loss factor (TLF) which violates the premise of SEA. Consequently, the TLF at 50 Hz was increased by 3 dB, at 63 Hz it was increased by 2 dB, and at 80 Hz was increased by 1 dB.

These values were used in all initial tests though later measurements are discussed at the end of the chapter.

The reverberation times of the gypsum wall were measured and the values are listed in Table 3.3. The measured data were only available from 100 to 2000 Hz so an average value was obtained by plotting the reverberation times on a log scale and fitting a straight line through the data. This then filled in all the other frequencies. Both the measured and best fit data are shown in Figure 3.3. Attempts to measure the damping of the floor were unsuccessful and so these values were used for all the structural subsystems.

Frequency Hz	Measured s	Best fit line s
50	-	0.47
63	-	0.39
80	-	0.33
100	0.28	0.27
125	0.28	0.23
160	0.19	0.19
200	0.14	0.16
250	0.12	0.13
315	0.11	0.11
400	0.10	0.09
500	0.07	0.08
630	0.06	0.07
800	0.05	0.05
1000	0.04	0.05
1250	0.04	0.04
1600	0.04	0.03
2000	0.03	0.03
2500	-	0.02
3150	-	0.02
4000	-	0.02
5000	-	0.01

Table 3.3. Measured reverberation time of the gypsum board partition wall between rooms 1 and 2 and the best fitting curve.

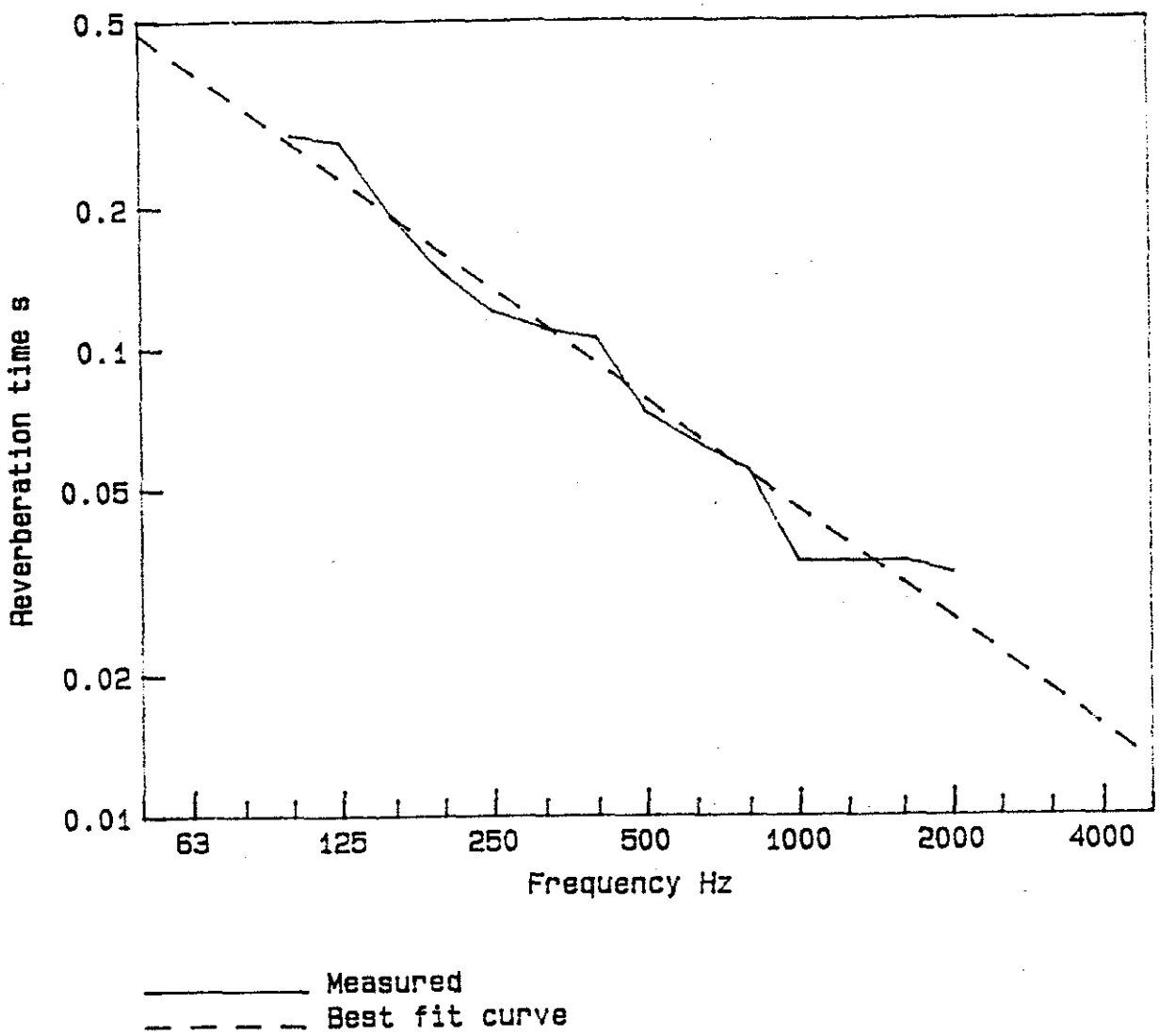

Figure 3.3. Reverberation times measured on the gypsum board partition wall used both for the gypsum walls and the floors. (PPC FIG18, 01 Nov. 94)

The coupling loss factors used were calculated using the above data and the equations given in Chapter 2.

3.4 STEEL FIRE STOP

The first model was run to give the results for a steel fire stop. This fire stop is very soft and produces almost no flanking transmission. Using the model described above, the airborne level difference was computed from transmission between rooms 1 and 2. The results are shown in Figure 3.4 and Table 3.4.

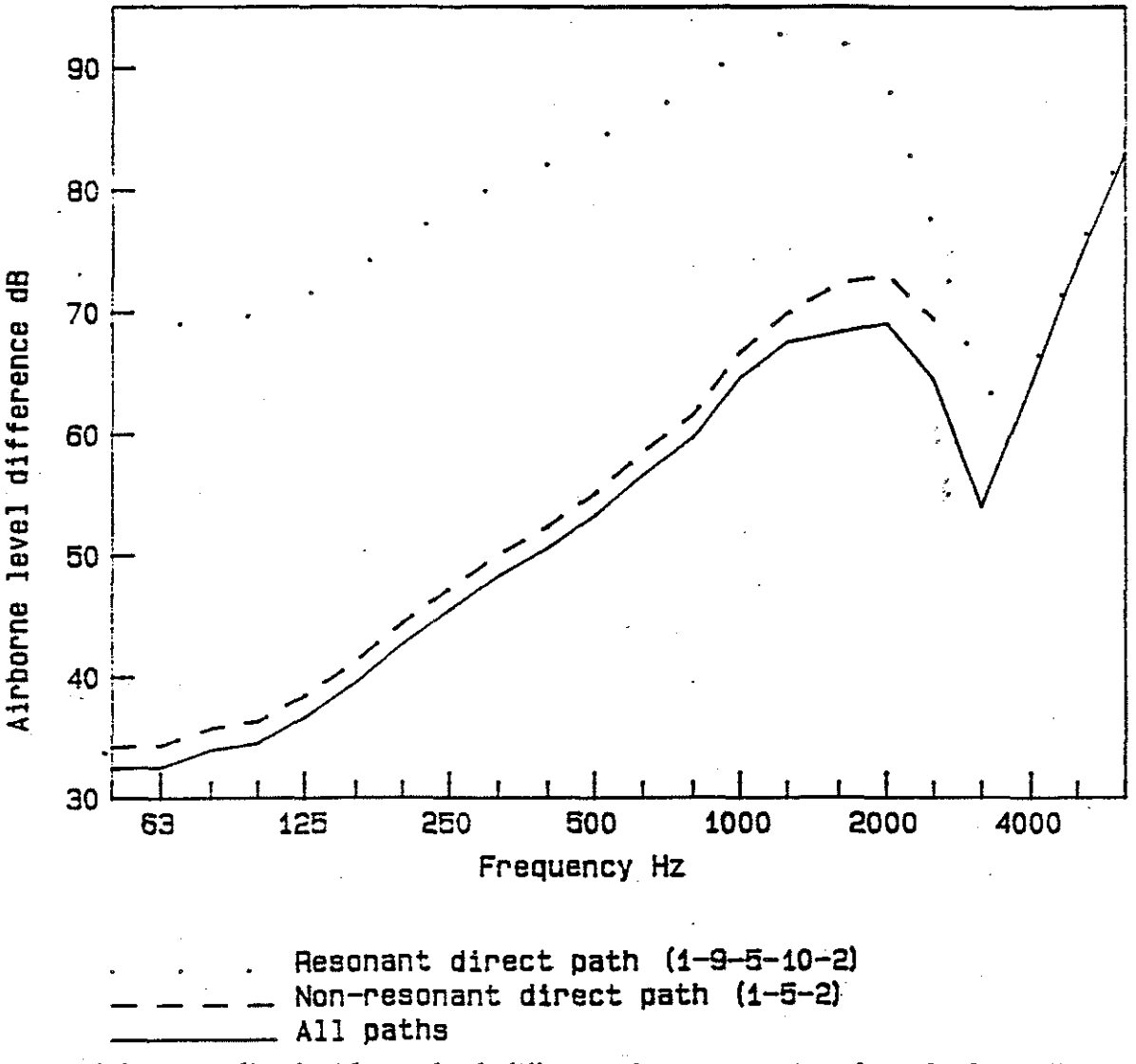

Figure 3.4. Predicted airborne level difference for transmission through the wall between rooms 1 and 2 when there is a steel fire stop together with the two direct transmission paths. (PPC FIG23, 02 Nov. 94)

An analysis of the dominant transmission paths shows that transmission is determined largely by the non-resonant transmission below the critical frequency and by resonant transmission above the critical frequency. These correspond to the paths 1-5-2 and 1-9-5-10-2, respectively. Both these paths are shown in Figure 3.4.

Adding in the flanking along the wall by adding in the paths 1-20-2, etc., makes little difference. The path 1-20-2 is about 4 dB less important than the path 1-5-2. The area of the wall is about the same but the area of the cavity is much larger and this accounts for its lower importance.

The steel fire stop degrades the sound isolation by at most 1.3 dB and is more or less independent of frequency.

One of the properties of the joist floor and framed wall is that the effective perimeter is increased below the critical frequency due to the restraining effect of the beams. For a subsystem like the party wall (9), this would increase the effective perimeter from 13.94 to 67.4 m and the floor (11) would be increased from 18.28 to 118.16 m. This is based on each subsystem being changed to one with 12 independent sections (one for each bay defined by a joist or stud). Below the critical frequency, the radiation efficiency is directly proportional to the perimeter length. The radiation efficiency is therefore increased by about 8 dB which could be important as the radiation occurs 4 times in the path 1-9-5-10-2 giving a decrease in the level difference of about 32 dB. However, most of the individual sections of floor are then placed in a baffle that is in the same plane as the floor so that the multiplier of x4 should be reduced to a multiplier of x2.

Frequency Hz	Measured dB	Predicted dB
50	21.1	32.46
63	28.9	32.56
80	36.8	34.01
100	44.0	34.59
125	44.3	36.74
160	42.1	39.57
200	46.4	42.69
250	47.1	45.49
315	50.4	48.29
400	54.8	50.60
500	57.0	53.34
630	53.5	56.73
800	57.0	59.84
1000	61.0	64.82
1250	61.3	67.72
1600	63.5	68.55
2000	64.4	69.26
2500	63.9	64.49
3150	65.8	54.05
4000	67.3	64.15
5000	70.3	74.15
6300	73.1	83.02

Table 3.4 *Measured and predicted transmission loss between rooms 1 and 2 with a steel fire stop.*

In the model, this caused some difficulty as at low frequencies the sum of the CLFs is then higher than the TLFs which were obtained from measured reverberation times. For the rooms, the reverberation times and hence the TLF can be considered to be very reliable so such a modification to the CLFs cannot be appropriate. The reason is that there are no modes in the floor sub-panels below 125 Hz so that below this frequency the floor acts as a single subsystem and the perimeter is simply that of the entire floor. Above the critical frequency, this correction has no effect but just below the critical frequency the nail spacing is such that the in-line joint with the joists changes from being like a line (which is correct at low frequencies) to being like a series of points. The effective perimeter will obviously be less than for a continuous line but the exact value is not known.

The upper limit for the radiation efficiency was computed increasing the perimeter and reducing the multiplier by 2. The results for the level difference between rooms 1 and 2 can be seen in Figure 3.5. The general trend is for the peak in level difference just below the critical frequency to be reduced by up to 5 dB. Given the uncertainty of the effective perimeter in this region the increased perimeter was not used in other calculations.

For this type of construction, the (steel) fire stop does not produce a particularly strong flanking path. There are 4 dominant paths involving the fire stop:

1-9-10-2
1-9-12-2
1-11-10-2
1-11-12-2

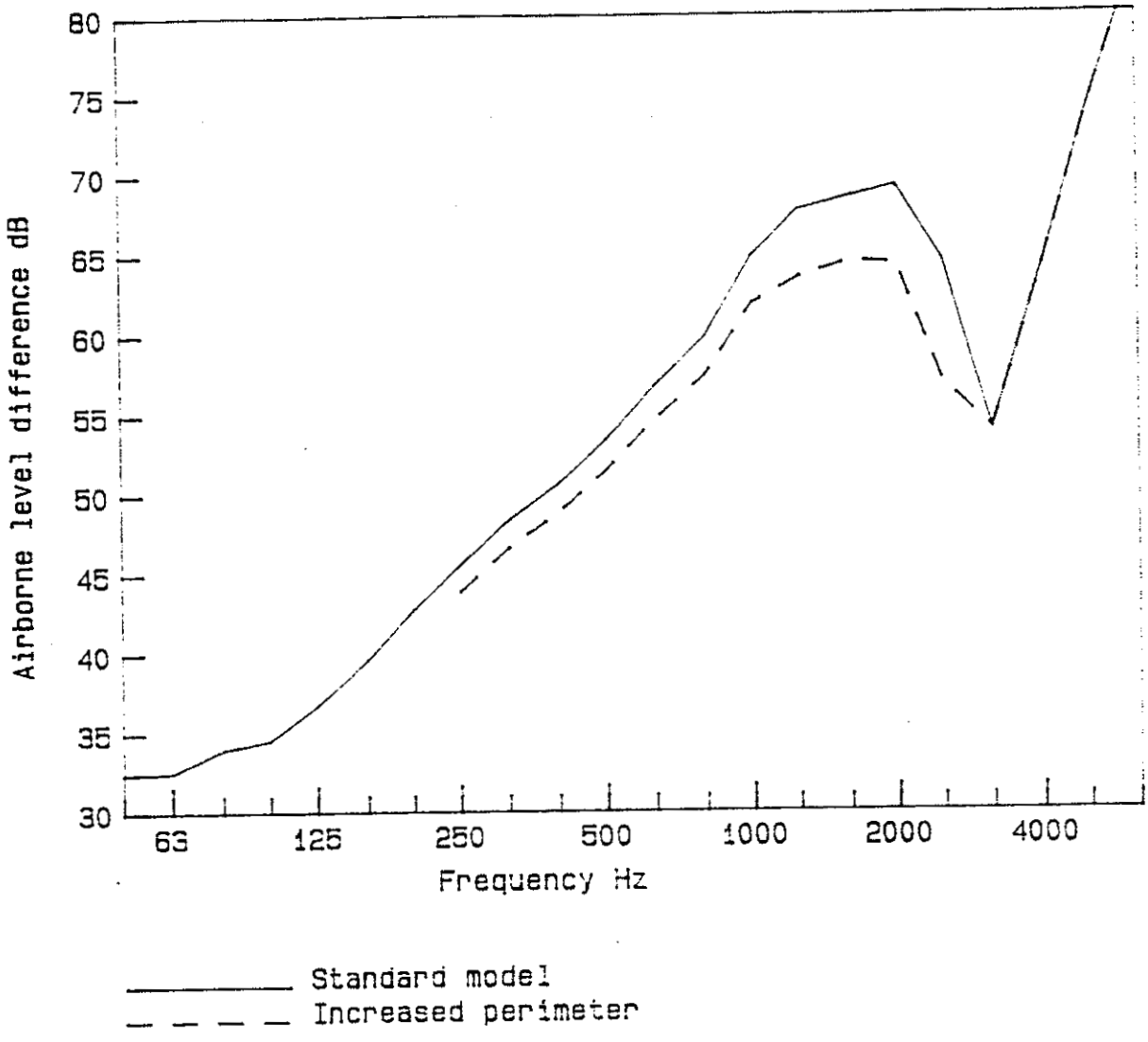

Figure 3.5. *Predicted airborne level difference for the basic model and the model with the effective perimeter of the floors and walls increased. (PPC FIG25, 02 Nov. 94)*

The airborne level difference from these paths was summed and is shown plotted in Figure 3.6 with the overall level difference. It can be seen that the flanking paths can be ignored. This would be expected because the structural transmission loss for this joint is over 60 dB. The transmission coefficients are described in more detail in Chapter 5.

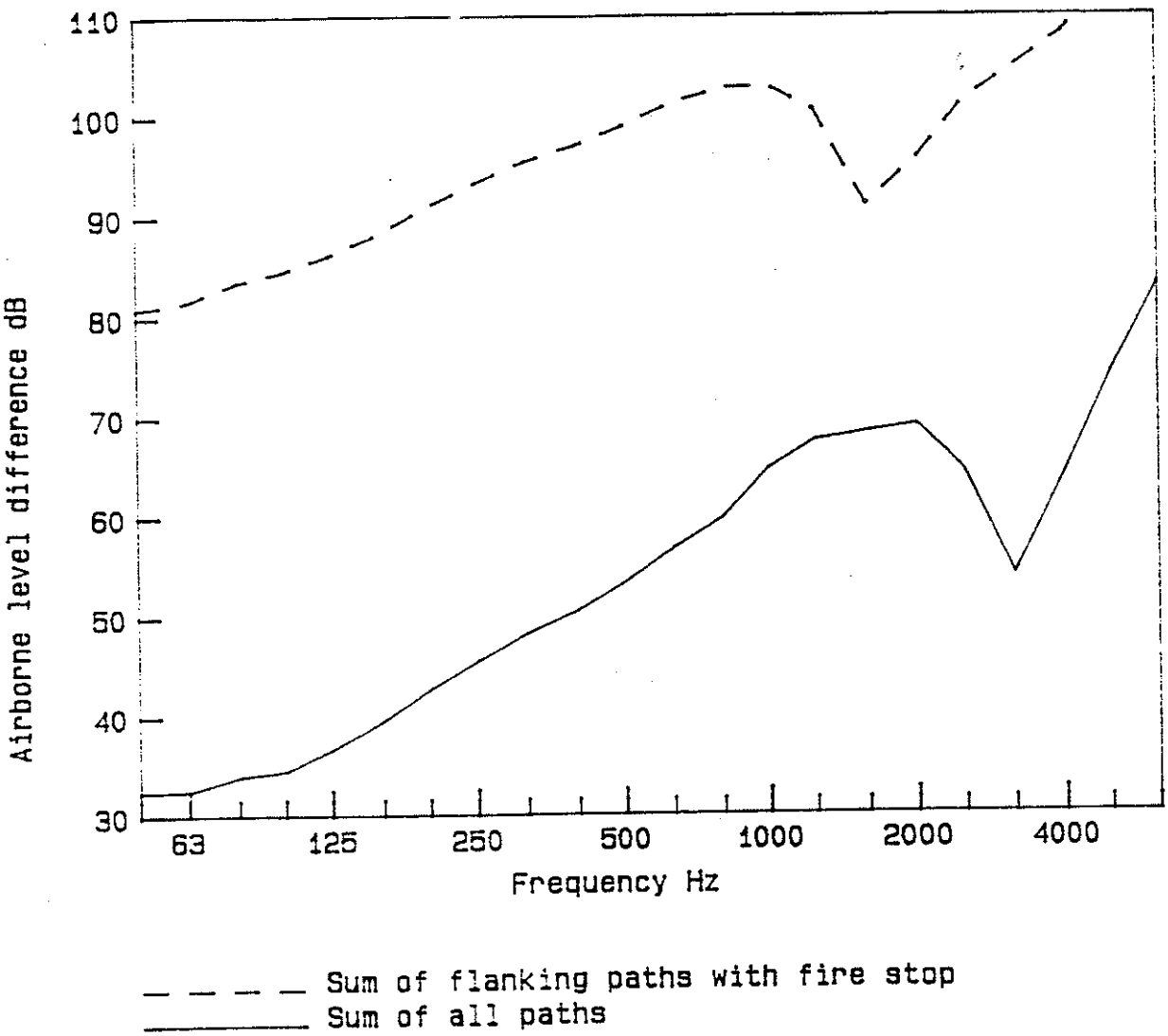

Figure 3.6. Predicted airborne level difference between rooms 1 and 2 showing the contribution of the flanking paths involving the fire stop. (PPC FIG 24, 02 Nov. 94)

A comparison of the measured and predicted results can be seen in Figure 3.7. In this case, the level difference has been normalised to give an airborne transmission loss. The agreement between the results is very good. The predicted dip at 3150 Hz is due to the critical frequency of the gypsum and is probably sharper than it should be. The hump just below f_c would be reduced if the effective perimeter was increased.

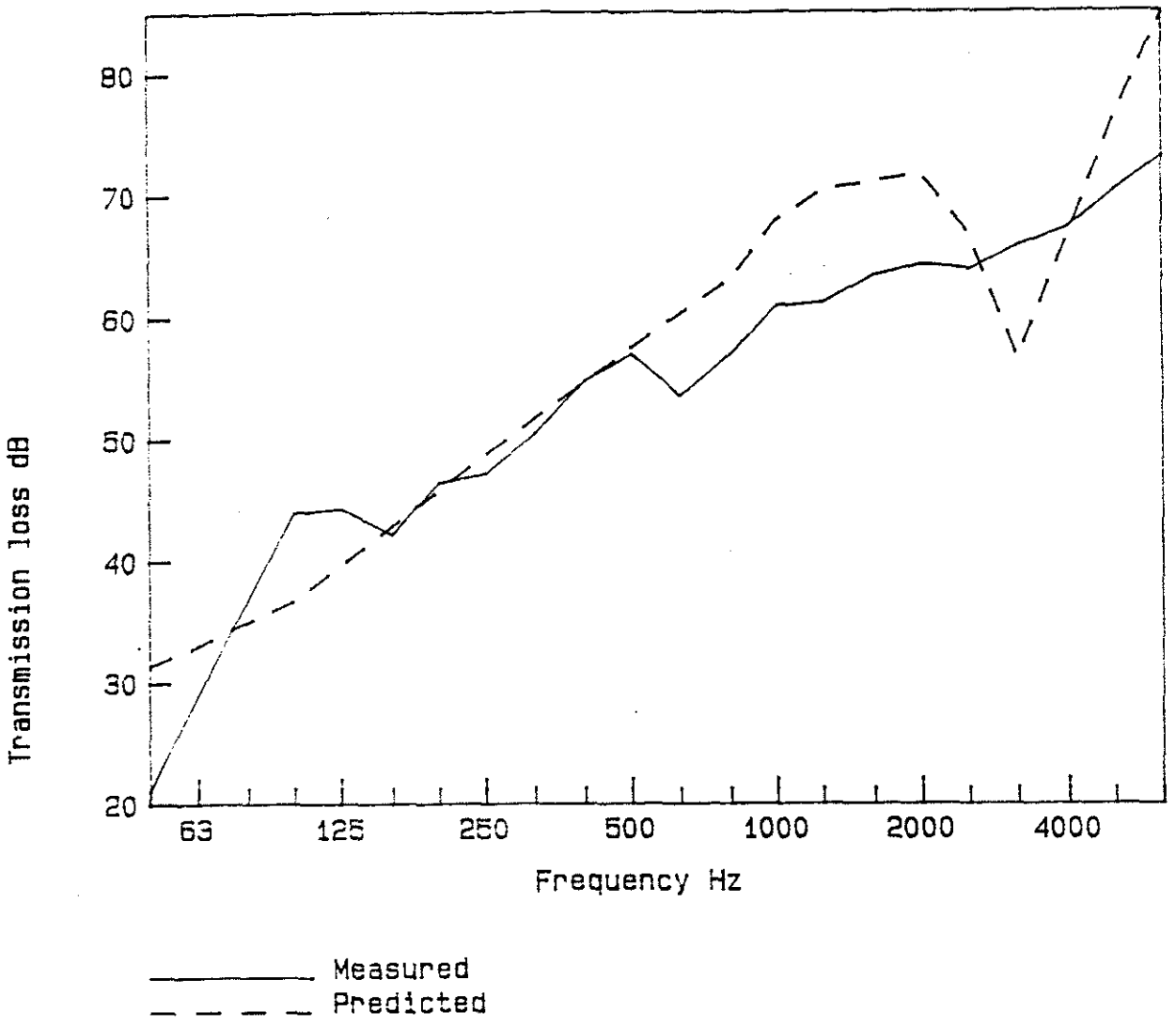

Figure 3.7. Measured and predicted transmission loss from room 1 to 2 for a wall with a steel fire stop. (PPC FIG22, 02 Nov. 94)

3.5 PLYWOOD FIRE STOP

A similar comparison of measured and predicted transmission loss for the wall with the plywood fire stop can be seen in Figure 3.8 and Table 3.5. Again there is good agreement between the results.

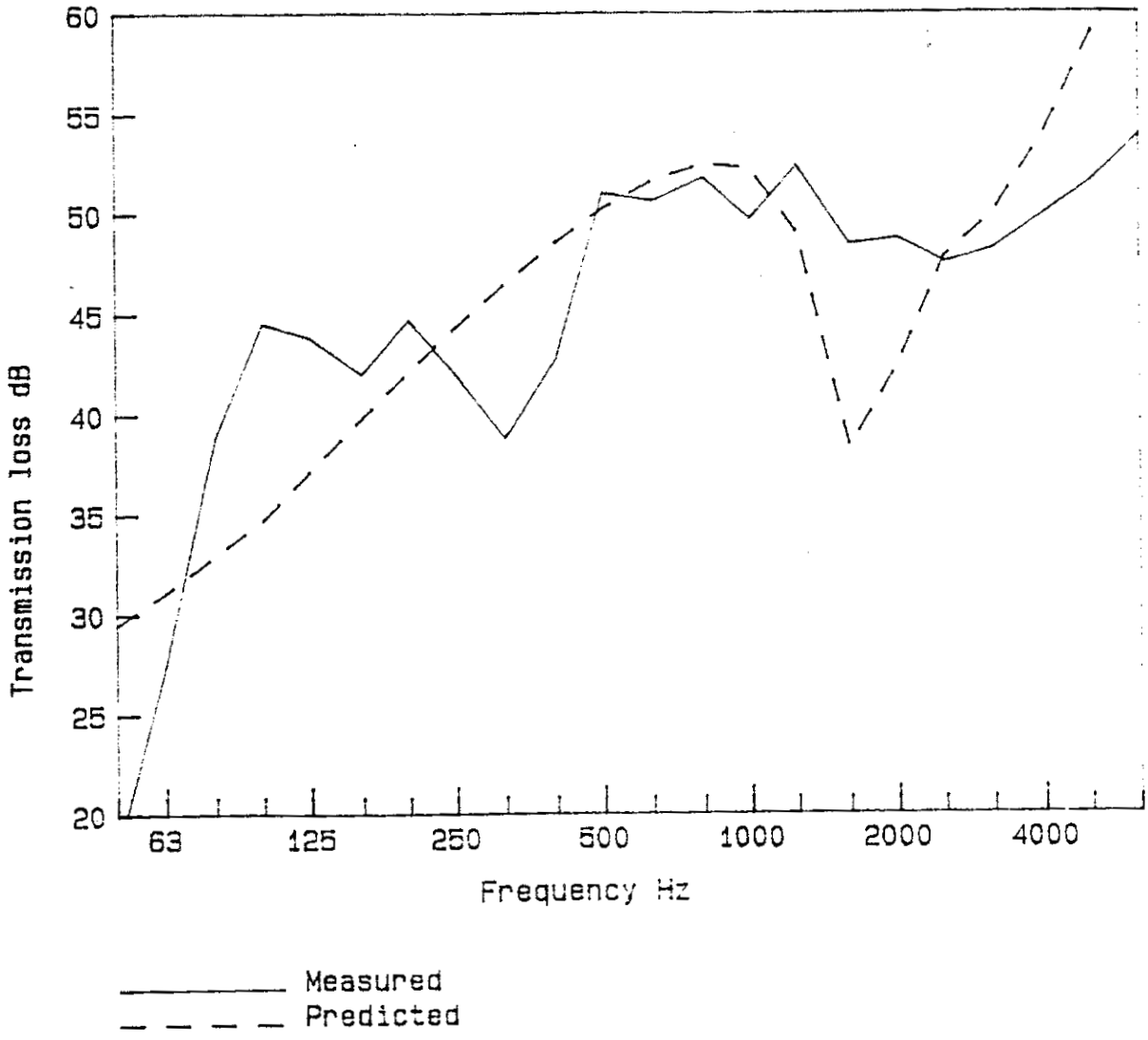

Figure 3.8. Measured and predicted transmission loss from room 1 to 2 for a wall with a plywood fire stop. (PPC FIG25, 02 Nov. 94)

Frequency Hz	Measured dB	Predicted dB
50	18.2	29.49
63	27.4	31.10
80	38.8	32.97
100	44.5	34.71
125	43.8	37.18
160	42.0	39.83
200	44.7	42.14
250	42.0	44.34
315	38.8	46.50
400	42.8	48.54
500	51.0	50.23
630	50.6	51.64
800	51.8	52.49
1000	49.7	52.23
1250	52.4	49.01
1600	48.5	38.36
2000	48.8	42.47
2500	47.6	47.89
3150	48.3	50.07
4000	50.0	54.00
5000	51.6	58.88
6300	53.9	63.34

Table 3.5. Measured and predicted transmission loss from room 1 to 2 with a plywood fire stop.

The relative importance of the transmission paths can be seen in Figure 3.9. Each of the four flanking paths listed above is shown together with the total transmission due to all paths and the result for the steel fire stop (which has effectively no flanking at the fire stop joint).

The most important flanking path is the floor-floor path (1-11-12-2). The two paths floor-wall (1-11-10-2) and wall-floor (1-9-12-2) are more or less the same (the differences being due to small changes in room volumes and reverberation times) they would be identical if the graph showed transmission loss. The least important path is the wall-wall path (1-9-10-2).

At very low frequencies the flanking is not important but in the mid frequencies the flanking dominates transmission.

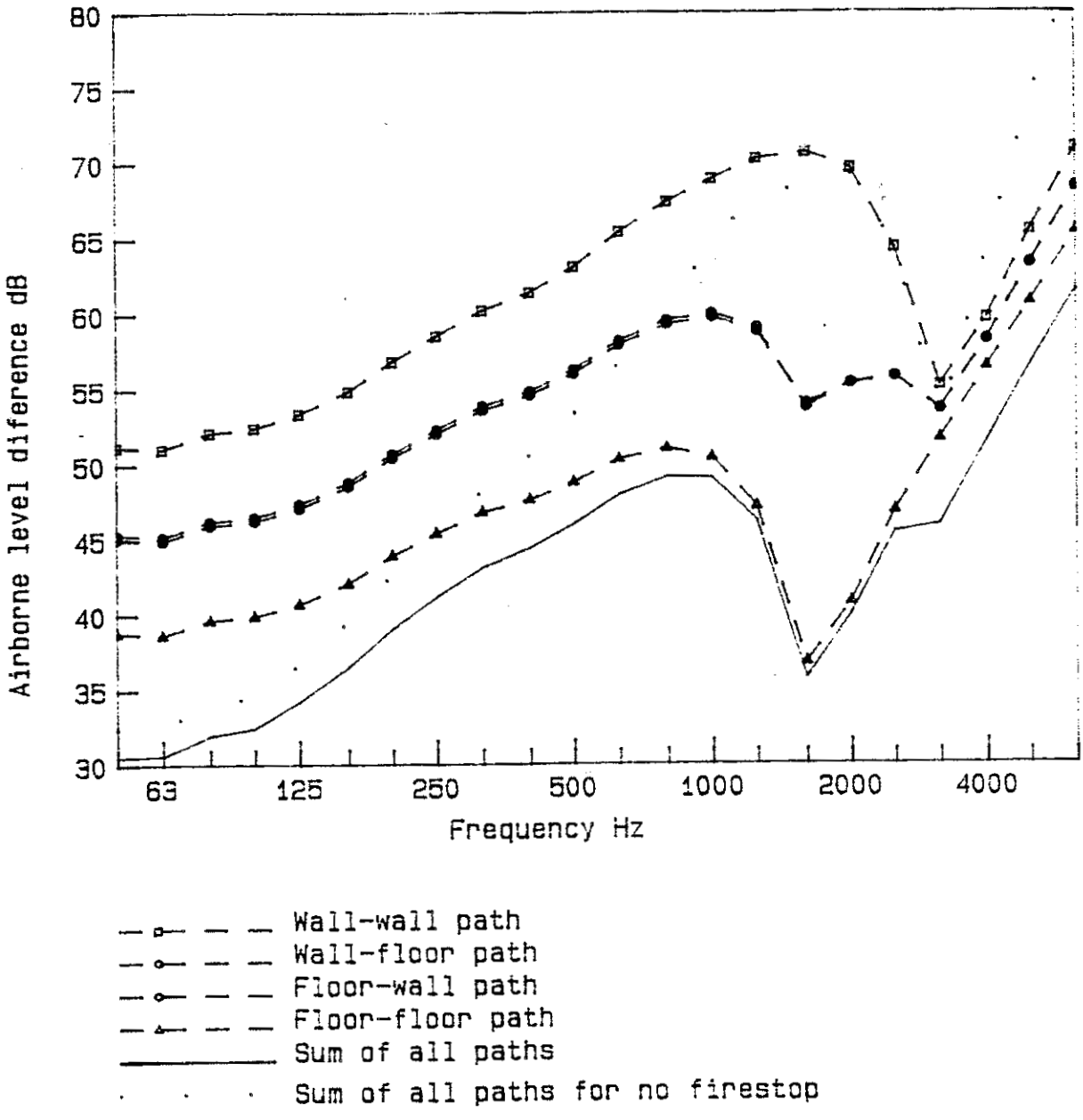

Figure 3.9. Predicted airborne level difference from room 1 to 2 showing the contribution of the paths associated with the plywood fire stop. (PPC FIG27, 02 Nov. 94)

3.6 PLYWOOD FIRE STOP WITH A FLOATING FLOOR

The predicted results were recomputed with a floating floor on top of floor 12 in the receiving room 2. This was assumed to eliminate coupling between the floor and room 2. This will then remove the floor-floor flanking path (1-11-12-2) which was an important path when there was floor to room coupling.

A comparison of the measured and predicted results is given in Figure 3.10 and in Table 3.6. The agreement is reasonable but the prediction is about 6 dB too low. All the trends are correctly predicted.

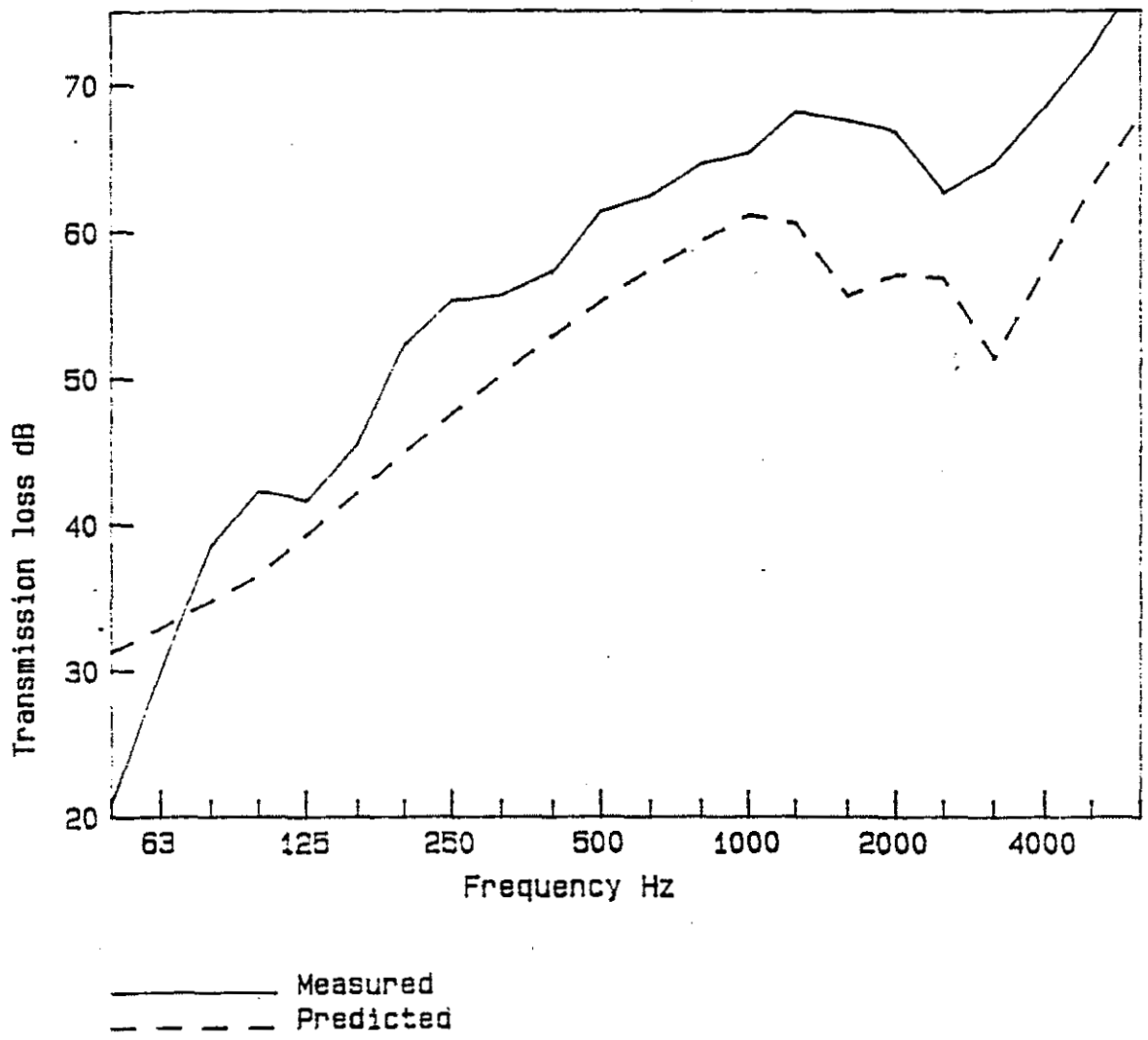

Figure 3.10. Measured and predicted transmission loss from room 1 to 2 for a wall with a plywood fire stop and with a floating floor on the receiving room floor. (PPC FIG29, 02 Nov. 94)

Frequency Hz	Measured dB	Predicted dB
50	20.8	31.32
63	29.9	32.93
80	38.5	34.79
100	42.3	36.55
125	41.6	39.26
160	45.5	42.26
200	52.3	44.95
250	55.3	47.60
315	55.7	50.28
400	57.3	52.95
500	61.4	55.30
630	62.5	57.53
800	64.7	59.45
1000	65.5	61.22
1250	68.2	60.64
1600	67.6	55.71
2000	66.8	57.20
2500	62.7	56.89
3150	64.7	51.47
4000	68.5	57.59
5000	72.4	63.11
6300	77.6	67.89

Table 3.6. Measured and predicted transmission loss from room 1 to 2 with a plywood fire stop and the floating floor in room 2.

The change in the predicted level difference can be seen in Figure 3.11. This shows the predicted overall level difference for the plywood fire stop with and without the floating floor. The addition of the floating floor makes a significant difference at the mid frequencies. The floor-wall flanking path 1-11-10-2 is also shown and as would be expected from Figure 3.9 it is now an important path.

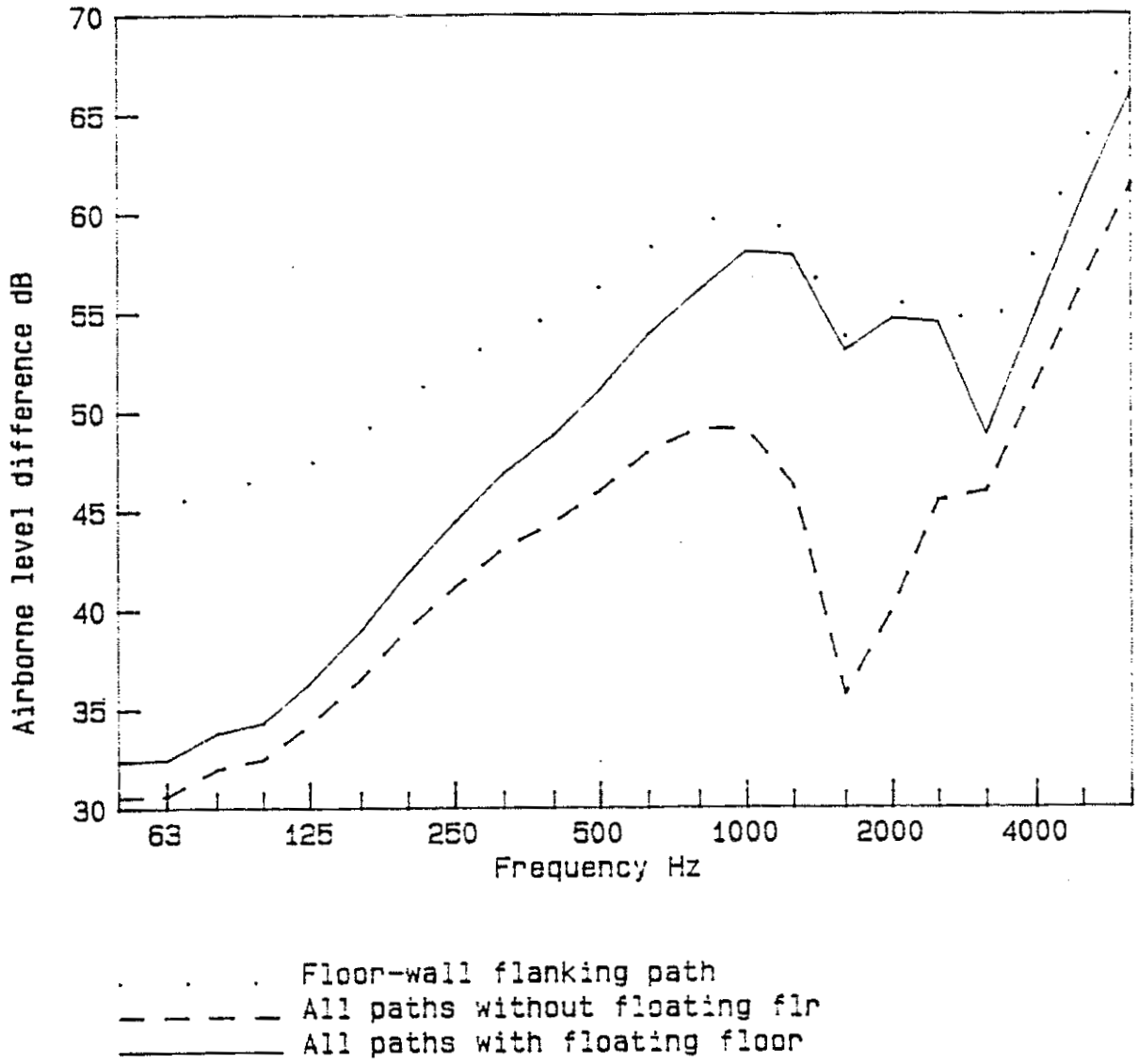

Figure 3.11. Predicted airborne level difference for transmission from room 1 to 2 showing the effect of adding the floating floor and the importance of the flanking path. (PPC FIG28, 02 Nov. 94)

3.7 GYPSUM BOARD FIRE STOP

Measured and predicted airborne transmission loss results are shown in Figure 3.12 for a gypsum board fire stop. The agreement is excellent up to 1000 Hz but thereafter the measured data is lower than predicted. This cannot be explained at present.

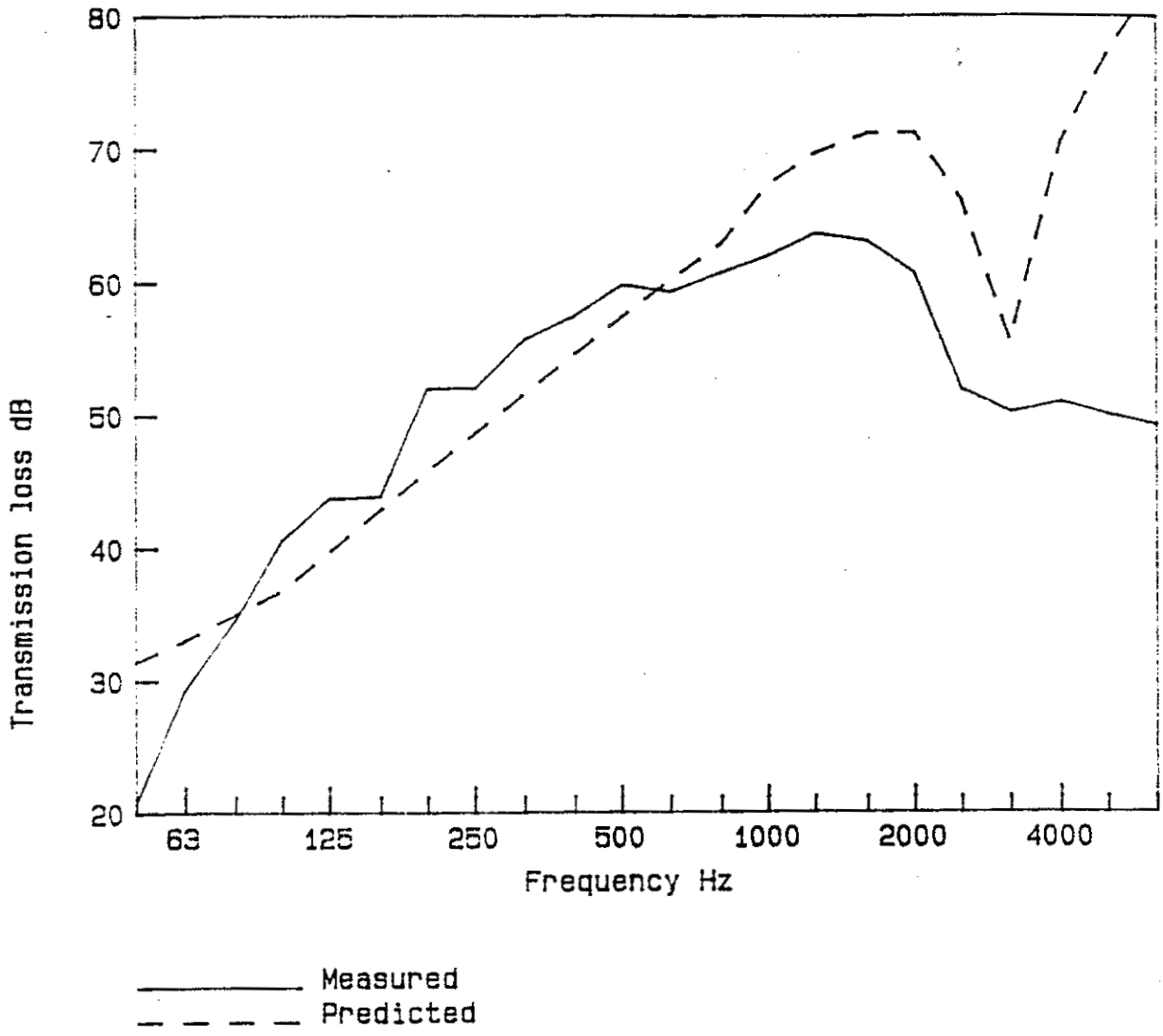

Figure 3.12. Measured and predicted transmission loss from room 1 to 2 for a wall with a gypsum board fire stop on the flanking wall. (PPC FIG30, 02 Nov. 94)

3.8 FURTHER RESULTS AND DISCUSSION

A comparison of the measurements and predictions can be seen in Figure 3.13 for the steel, plywood and gypsum board fire stops. The transmission loss for the case with the gypsum board is unusual in that there is good agreement between measured and predicted results at low frequencies but then measured decreases with frequency.

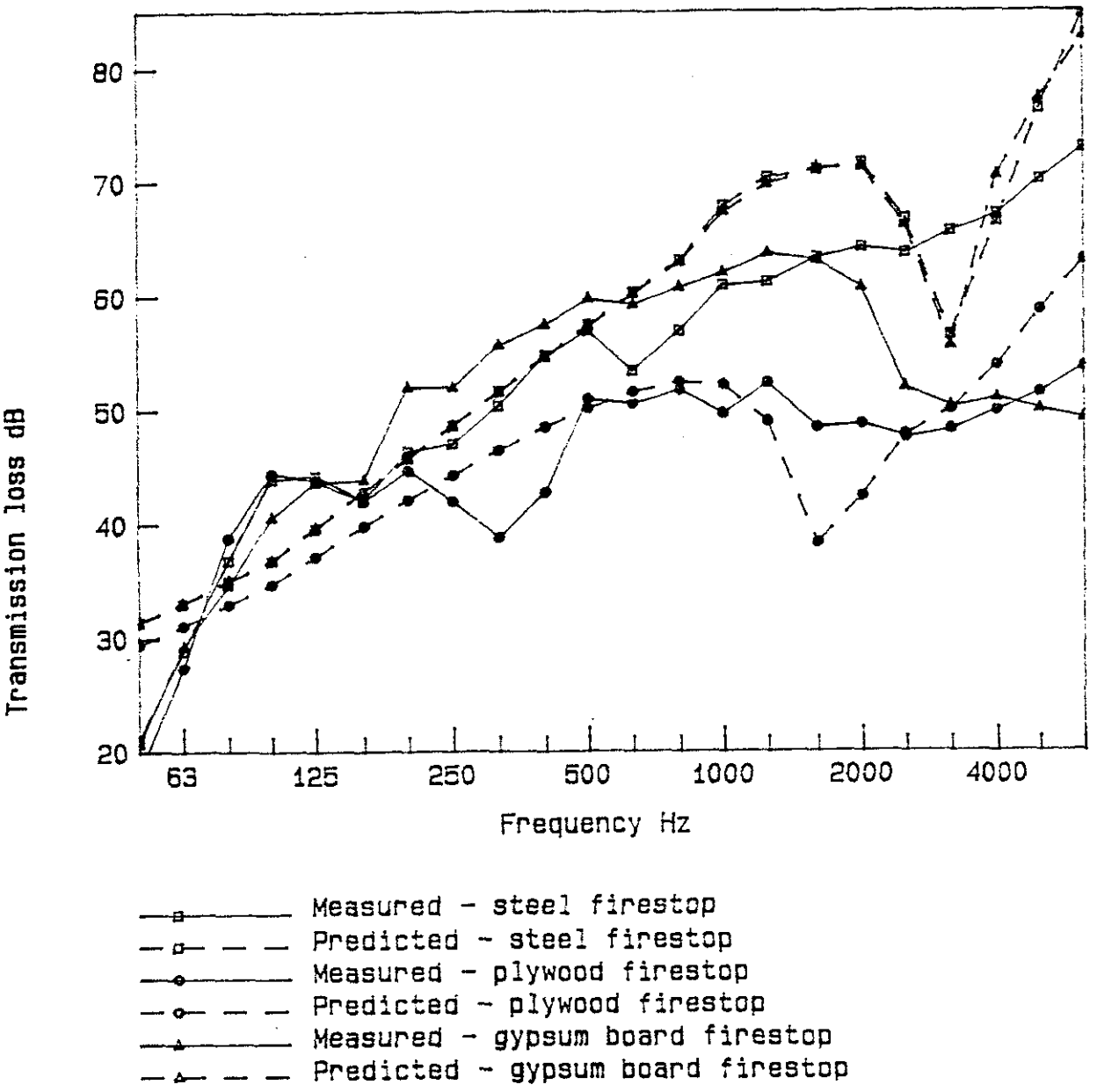

Figure 3.13. Measured and predicted transmission loss from room 1 to 2 for steel, plywood and gypsum board fire stops. (PPC FIG39, 02 Nov. 94)

At 50 Hz there is a dip in all of the results. This could be due to a mass-spring-mass resonance of the wall cavities. This resonance would occur at

$$f_n = \frac{1}{2\pi}\sqrt{\frac{10^5}{d}\left(\frac{1}{\rho_{s1}} + \frac{1}{\rho_{s2}}\right)} \qquad (3.2)$$

where d is the depth of the cavity in metres, and ρ_s is the surface density in kg/m^2. In this case, the resonance would occur at 48 Hz and so could account for the dip. A non-resonant transmission path could be included in the model if necessary to account for this effect.

4 SOUND TRANSMISSION TO OTHER ROOMS

4.1 INTRODUCTION

As well as predicting transmission through the party wall between rooms 1 and 2, the SEA model was used to predict transmission from the source room 1 to the other rooms 3 and 4. The SEA model was the same as was used in Chapter 3.

4.2 VERTICAL TRANSMISSION

Measured and predicted sound transmission through the floor from room 1 to 3 is shown in Figure 4.1. There was no coupling included between the floor surface and the joists, nor between the joists and the ceiling. The ceiling gypsum boards were mounted on resilient channel so that this should have significantly reduced coupling between the joists and the ceiling making any coupling between the plywood and the joists irrelevant.

Despite the simplicity of the model, there is good agreement at frequencies up to 4000 Hz. At higher frequencies, the predicted transmission loss is too high.

4.3 DIAGONAL TRANSMISSION

The model was also used to predict transmission diagonally between rooms 1 and 4. The model was again unchanged from Chapter 3. No additional coupling was introduced into the model apart from that already described. As a result, there is poorer agreement between the measured and predicted transmission loss shown in Figure 4.2 though the correct trends are predicted.

For the calculation of transmission loss, an area of 10 m^2 was assumed.

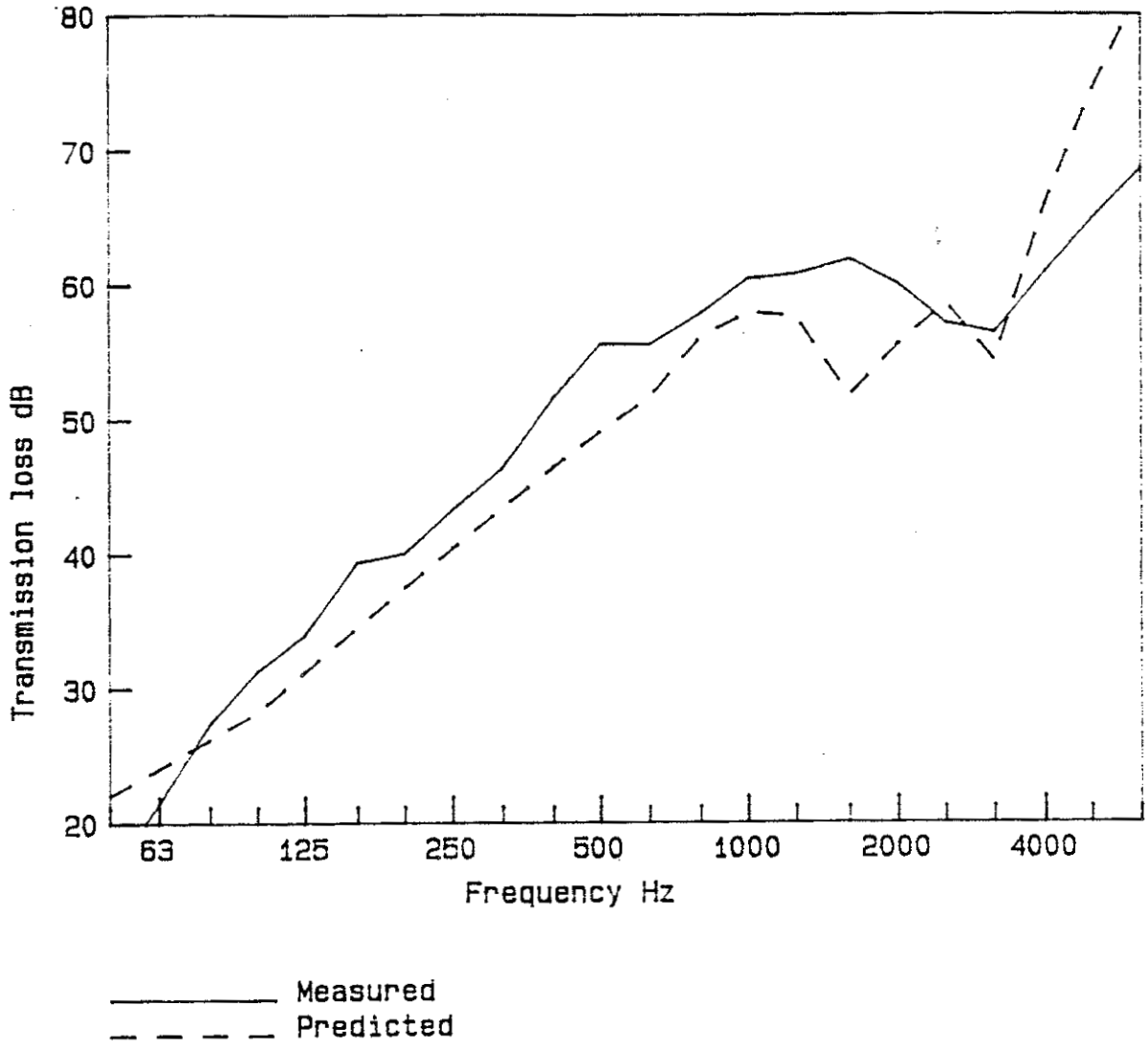

Figure 4.1. Measured and predicted vertical transmission loss between rooms 1 and 3. (PPC FIG31, 02 Nov. 94)

Frequency Hz	Measured dB	Predicted dB
50	16.0	22.08
63	21.5	24.08
80	27.4	26.25
100	31.3	28.24
125	34.0	31.23
160	39.4	34.54
200	40.1	37.51
250	43.3	40.45
315	46.4	43.45
400	51.6	46.46
500	55.6	49.14
630	55.6	51.70
800	57.9	56.16
1000	60.5	58.01
1250	60.9	57.67
1600	62.0	51.87
2000	60.1	55.70
2500	57.2	58.70
3150	56.5	54.47
4000	61.0	65.98
5000	64.9	74.36
6300	68.6	81.94

Table 4.1. Measured and predicted vertical transmission loss from room 1 to 3.

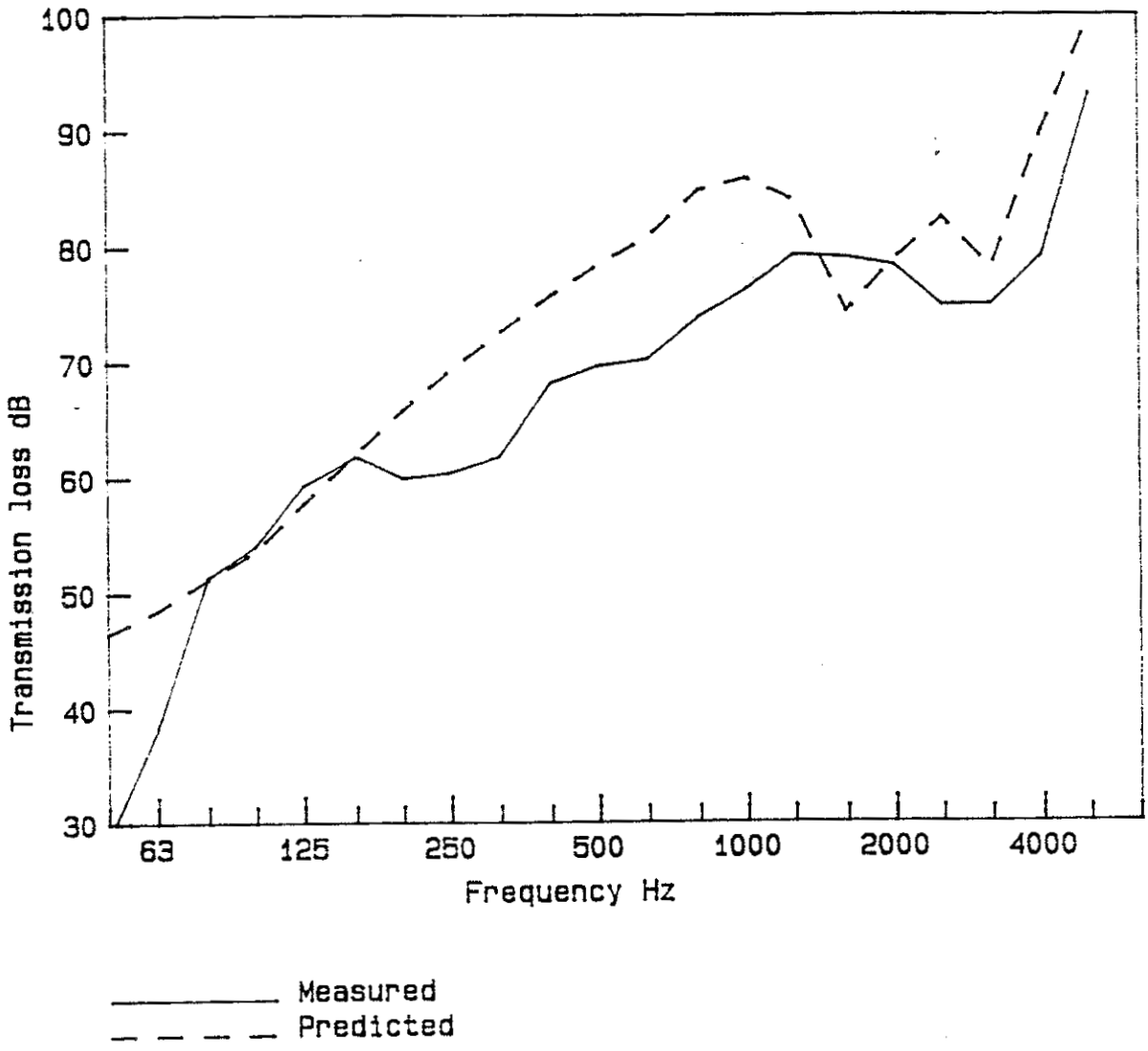

Figure 4.2. *Measured and predicted diagonal transmission loss between rooms 1 and 4 (common surface area of 10 m² assumed). (PPC FIG 32, 02 Nov. 94)*

Frequency Hz	Measured dB	Predicted dB
50	28.7	46.50
63	38.3	48.51
80	51.4	51.24
100	54.1	53.66
125	59.3	57.69
160	61.8	61.99
200	59.9	65.79
250	60.4	69.24
315	61.8	72.54
400	68.2	75.68
500	69.7	78.39
630	70.3	80.80
800	73.9	84.86
1000	76.3	85.91
1250	79.3	83.94
1600	79.0	74.39
2000	78.3	78.89
2500	74.9	82.46
3150	75.0	78.11
4000	79.2	89.96
5000	93.1	99.53
6300	0.0	108.20

Table 4.2. Measured and predicted diagonal transmission loss from room 1 to 4 with a plywood fire stop (common surface area of 10 m² assumed).

5 SOUND TRANSMISSION ACROSS FIRE STOPS

5.1 INTRODUCTION

This section describes the theory that was used to predict the performance of the fire stops. The first part of the chapter describes the waves and conditions that exist on the plates. The second describes a simple model for transmission across the fire stop, and the third section looks at a more complex model that includes the effects of joists at the joint.

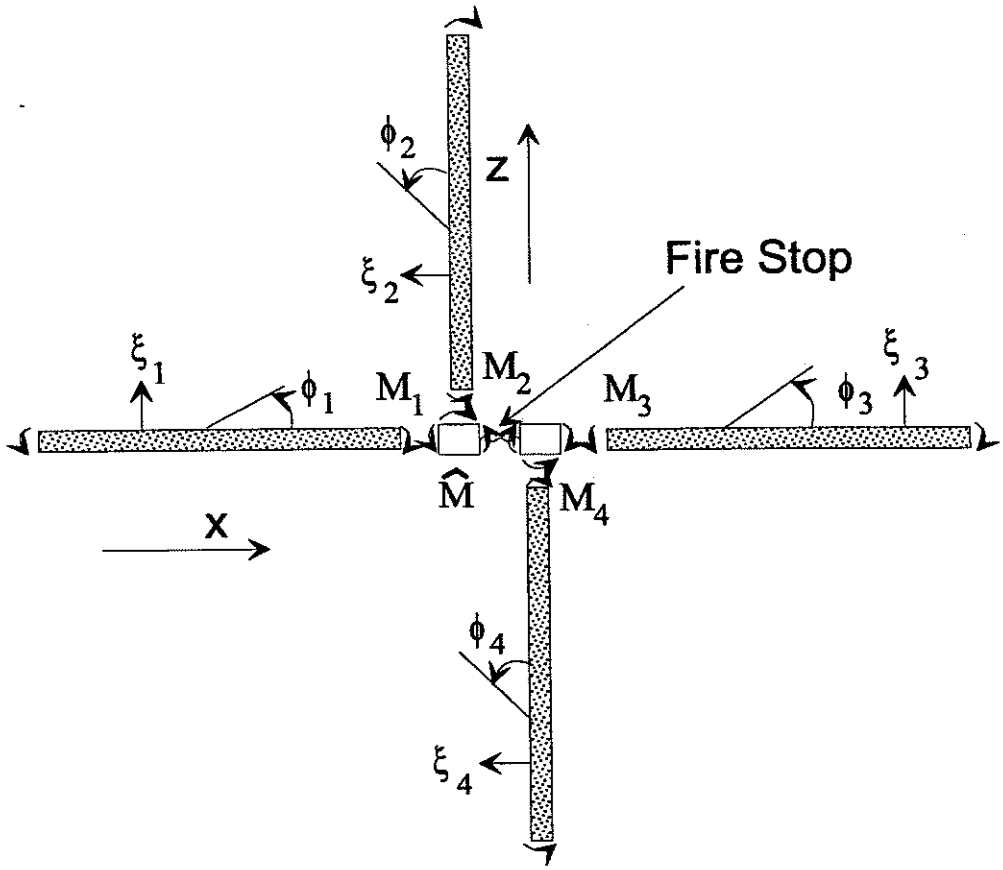

Figure 5.1. Fire stop joint configuration.

5.2 WAVES ON THE PLATES

The basic system that is examined in this section can be seen in Figure 5.1. It consists of four plates, two on each side of the fire stop.

In order to be able to model the system, a number of approximations and assumptions were made about the system. It was assumed that the plates forming the structural joint are homogeneous. In this section, the joists at the joint are ignored but are introduced to each side of the fire stop in the next section.

It is assumed that there are no in-plane waves generated at the joint. This is the same as assuming that the two sides of the joint are pinned

Properties of the waves on the plates

From the derivation of the bending equation, the slope, ϕ, is related to the displacement, ξ, by

$$\phi = \frac{\partial \xi}{\partial x} \tag{5.1}$$

Similarly the moment, M, applied to the boundary is related to the displacement by

$$M = -B\left(\frac{\partial^2 \xi}{\partial x^2} + \mu \frac{\partial^2 \xi}{\partial y^2}\right) \tag{5.2}$$

where μ is Poisson's ratio and B is the bending stiffness of the plate.

On plate 1 there is an incoming wave of unit amplitude at angle ξ_1, with a wave number k_1. There is also a reflected wave with amplitude, T_1, and a near field wave with amplitude, T_{n1}. The equation for the displacement is then

$$\xi_1 = (e^{-ik_1 \cos\theta_1 x} + T_1 e^{ik_1 \cos\theta_1 x} + T_{n1} e^{k_{n1} x})(e^{-ik_1 \sin\theta_1 y} e^{i\omega t}) \tag{5.3}$$

The last term is common to all equations and is not given in subsequent equations.

The term k_{n1} is the near field wave number and is given by

$$k_n^2 = k^2(1 + \sin^2\theta) \tag{5.4}$$

for any plate. The angle at which the waves leave the joint can be found from Snell's law which requires that

$$k_1 \sin\theta_1 = k_m \sin\theta_m \tag{5.5}$$

In a similar manner, there are waves on plates 2, 3 and 4 which can be given by

$$\xi_2 = T_2 e^{-ik_2 \cos\theta_2 z} + T_{n2} e^{-k_{n2} z} \tag{5.6}$$

$$\xi_3 = T_3 e^{-ik_3 \cos\theta_3 x} + T_{n3} e^{-k_{n3} x} \tag{5.7}$$

$$\xi_4 = T_4 e^{ik_4 \cos\theta_4 z} + T_{n4} e^{k_{n4} z} \tag{5.8}$$

Fire stop

The fire stop is subjected to moments and as a result is deformed. A positive moment on either side will, for the co-ordinate system used, give a negative angle of rotation. Thus

$$M_f = (\phi_3 - \phi_1) B_f = -(\phi_1 - \phi_3) B_f \tag{5.9}$$

where B_f is the fire stop bending stiffness.

The stiffness of the fire stop can be found by considering a small element of beam and using fundamental mechanics

$$B_f = \frac{Y h^3}{12(1-\mu^2)L} \tag{5.10}$$

where L is the span of the fire stop (typically 13 or 25 mm), h is the thickness of the fire stop (such as 0.038 mm for the steel plate) and Y is Young's Modulus of the fire stop material.

Typical properties of the fire stop with a span of 25 mm are

Material	Stiffness Nm	Young's Modulus N/m^2	Density kg/m^3
0.038 mm steel	42	$210x10^9$	7800
16 mm plywood	42201	$2.81x10^9$	451
26 mm gypsum board	15900	$2.48x10^9$	740

5.3 BASIC MODEL

At the boundary, a number of continuity and equilibrium conditions exist.

1 At the joint the displacements of all plates are zero.

2 The right angle between plates 1 and 2 is preserved (the slopes are equal).

3 The right angle between plates 3 and 4 is preserved (the slopes are equal).

4 The sum of the moments at the left hand pin is zero.

5 The sum of the moments at the right hand pin is zero.

6 The angular deformation of fire stop is determined by the bending stiffness and the moment.

From these conditions, a number of equations can be generated. The first set of boundary conditions, that the displacements of all plates be zero, gives the amplitude of the near field waves as

$$T_{n1} = -1 - T_1 \tag{5.11}$$

$$T_{n2} = -T_2 \tag{5.12}$$

$$T_{n3} = -T_3 \tag{5.13}$$

$$T_{n4} = -T_4 \tag{5.14}$$

The requirement that the slopes of plates 1 and 2 be equal gives $\phi_1 = \phi_2$ which, expressing the slope as the derivative of the displacement and evaluating, gives

$$T_1[-k_{n1}+ik_1\cos\theta_1] + T_2[-k_{n2}+ik_2\cos\theta_2] = k_{n1}+ik_1\cos\theta_1 \tag{5.15}$$

In a similar manner, the requirement that the slopes of plates 3 and 4 be equal ($\phi_3=\phi_4$) gives

$$T_3[k_{n3}-ik_3\cos\theta_3] + T_4[k_{n4}-k_4\cos\theta_4] = 0 \tag{5.16}$$

The requirement that the moments about the left pin sum to zero can be written as

$$M_1 - M_2 + (\phi_3 - \phi_1)B_f = 0 \tag{5.17}$$

Substituting for M and ϕ gives

$$\begin{aligned} T_1[2B_1k_1^2+B_fk_{n1}-iB_fk_1\cos\theta_1] + T_2[-2B_2k_2^2] \\ + T_3[B_fk_{n3}-iB_fk_3\cos\theta_3] = -2B_1k_1^2-B_fk_{n1}-iB_fk_1\cos\theta_1 \end{aligned} \tag{5.18}$$

The requirement that the moments about the right pin sum to zero can be written as

$$M_4 - M_3 -(\phi_3 - \phi_1)B_f = 0 \tag{5.19}$$

Substituting for M and ϕ gives

$$\begin{aligned} T_1[-B_fk_{n1}-iB_fk_1\cos\theta_1] + T_3[-2B_3k_3^2-B_fk_{n3}+iB_fk_3\cos\theta_3] \\ + T_4[2B_4k_4^2] = B_fk_{n1}+iB_fk_1\cos\theta_1 \end{aligned} \tag{5.20}$$

These four equations — (5.15), (5.16), (5.18) and (5.20) — can be solved simultaneously to give the amplitude of the waves on each plate.

The transmission coefficient can then be found from

$$\tau_{12}(\theta) = \frac{\rho_{s2}k_1\cos\theta_2}{\rho_{s1}k_2\cos\theta_1}|T_2|^2 \tag{5.21}$$

The angular average transmission coefficient is then given by

$$\tau_{av} = \int_0^{\pi/2} \tau(\theta)\cos(\theta)d\theta \tag{5.22}$$

Normal incidence

If it is assumed that all the plates are the same (have the same material properties and thickness) and that only normal incidence is considered, then the equations can be simplified.

Taking the parameter C to be

$$C = \frac{B_f}{Bk} \tag{5.23}$$

the equations for the conditions at the boundary can be solved analytically giving

$$R_{13} = R_{14} = 10\log 8\left(\frac{2}{c^2}+\frac{2}{c}+1\right) \tag{5.24}$$

This gives the transmission loss in non-dimensional form. When C tends to zero, as occurs at very high frequencies or for very soft fires stops, then the transmission loss tends to infinity. When C tends to infinity, then the transmission loss tends to 9 dB.

The transmission loss can be seen in Figure 5.2 for both random and normal incidence. It can be seen that the random incidence curve is higher than normal incidence. The difference is about 1.8 to 1.9 dB, as shown in Figure 5.3

5.4 EFFECTS OF JOISTS

The joists at the joint will resist rotation due to their inertia and torsional stiffness. The orientation of the joist is shown in Figure 5.4. An equation which describes the resisting moments in the joists can be given in terms of the slopes on the connected plates. In a similar manner to the in-line joint at a beam, which is treated by Cremer *et al*, the moments and slopes at the joint are related through a stiffness term, $H=M/\phi$, as

$$H_1 = \frac{M_{J1}}{\phi_1} = -(\omega^2 \rho_{J1} J_{J1} - G_{J1} k_1^2 \sin\theta_1^2) \tag{5.25}$$

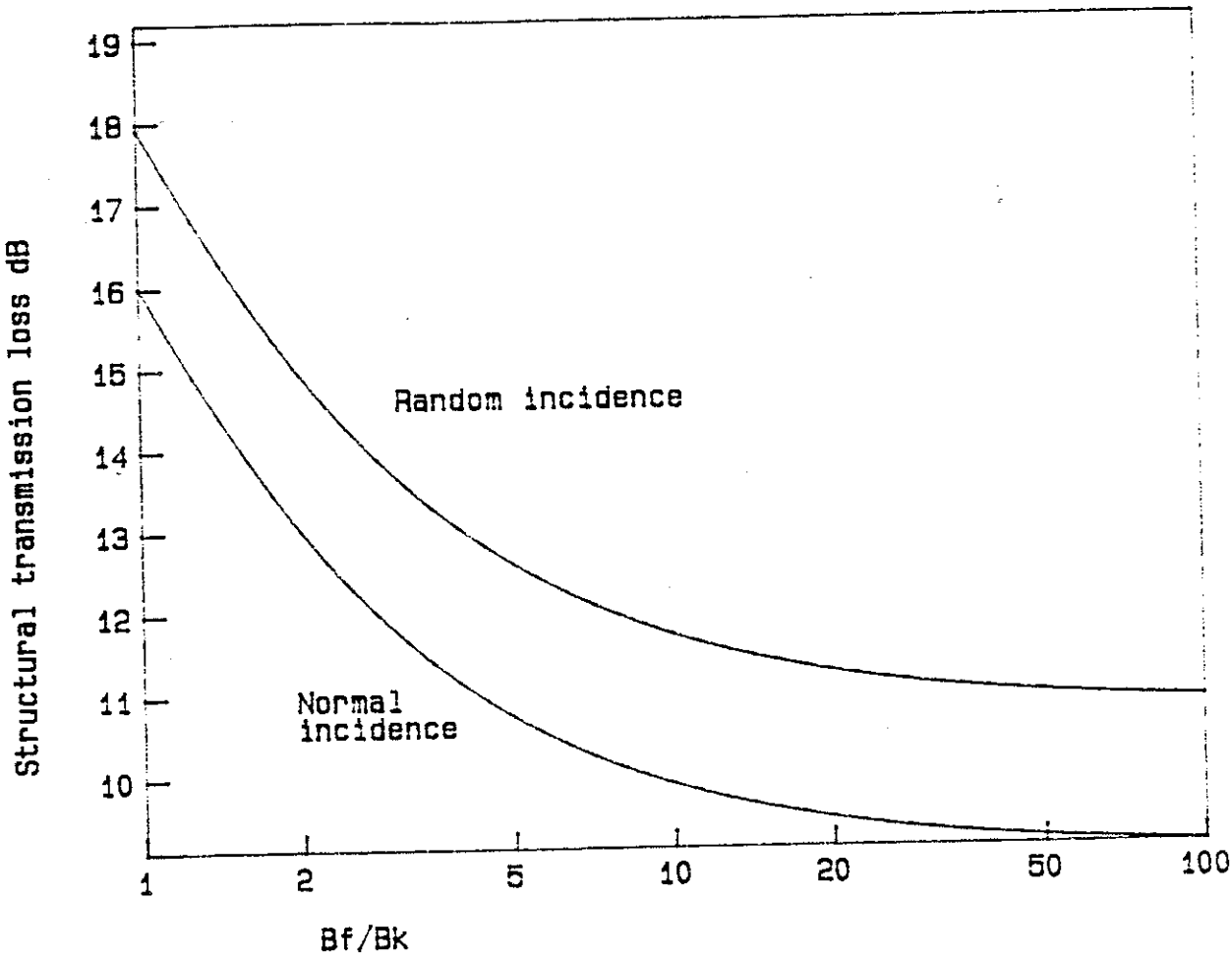

Figure 5.2. *Structural transmission loss as a function of the stiffness of the fire stop and the plate stiffness. (PPC FIG 47, 04 Nov. 94)*

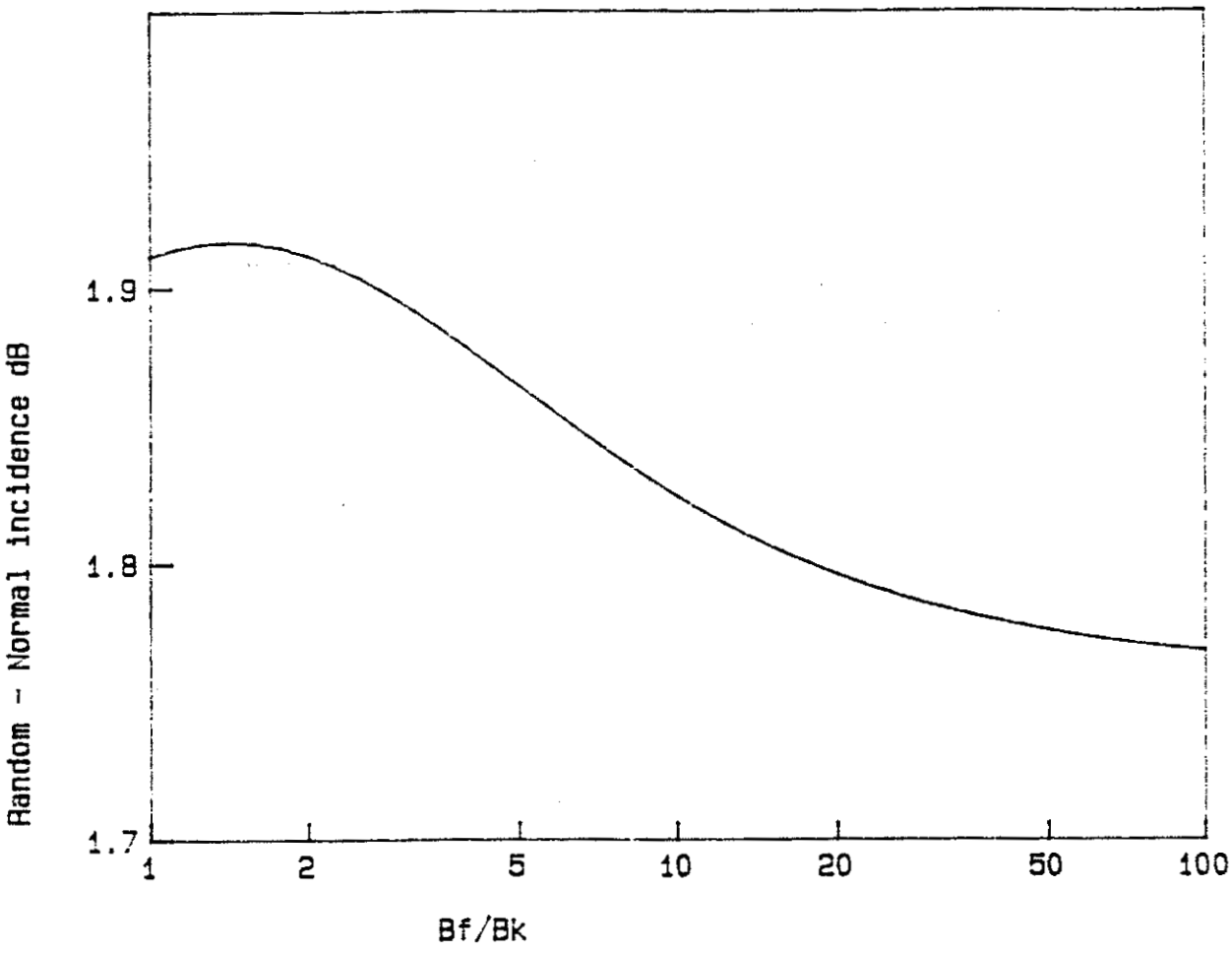

Figure 5.3. Difference between random and normal incidence for the transmission loss across a fire stop. (PPC FIG 48, 04 Nov. 94)

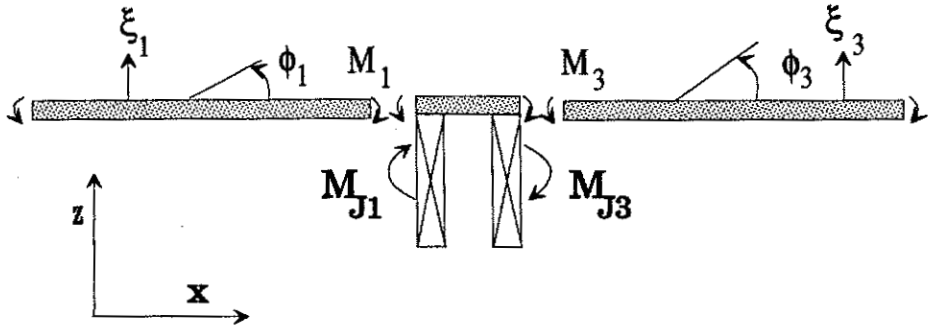

Figure 5.4. Definition of joist properties at fire stop joint.

where the subscript J1 is used to represent the joist. J and G are the polar moment of inertia and elastic modulus, respectively. The second joist is attached to plate 3 and its stiffness is given by

$$H_3 = \frac{M_{J3}}{\phi_3} = -(\omega^2 \rho_{J3} J_{J3} - G_{J3} k_3^2 \sin\theta_3^2) \qquad (5.26)$$

where the subscript J3 is used to represent the joist attached to plate 3.

Introducing these terms into the equilibrium equations (5.17) and (5.19) gives two new equilibrium equations as,

$$M_1 - M_2 + B_f(\phi_3 - \phi_1) + H_1\phi_1 = 0 \qquad (5.27)$$

and

$$M_4 - M_3 - B_f(\phi_3 - \phi_1) - H_3\phi_3 = 0 \qquad (5.28)$$

The transmission coefficients can then be calculated by solving the new set of eight boundary conditions ((5.11), (5.12), (5.13), (5.14), (5.15), (5.16), (5.17), (5.19)) as was described in the previous section.

5.5 RESULTS

The transmission coefficients for vibration transmission at 1000 Hz from floor 11 as a function of angle of incidence are shown in Figure 5.5. The simple model was used where the joists are not considered. The fire stop used was plywood. The transmission coefficients for transmission to wall 9 and 10 fall smoothly from normal incidence to a limiting angle of 37.6°. Strongest transmission is to wall 9.

The transmission coefficients for the same joint are shown in Figure 5.6 but the effects of the joists (38x235 mm finished dimension) are included. The joists reduce transmission at most angles of incidence but two sharp peaks are observed in each curve at an angle of incidence of around 27°.

The angular average structural transmission loss at the joint for the cases with and without joists and for plywood, gypsum and steel fire stops are given in Tables 5.1, 5.2, 5.3 and 5.4 for reference.

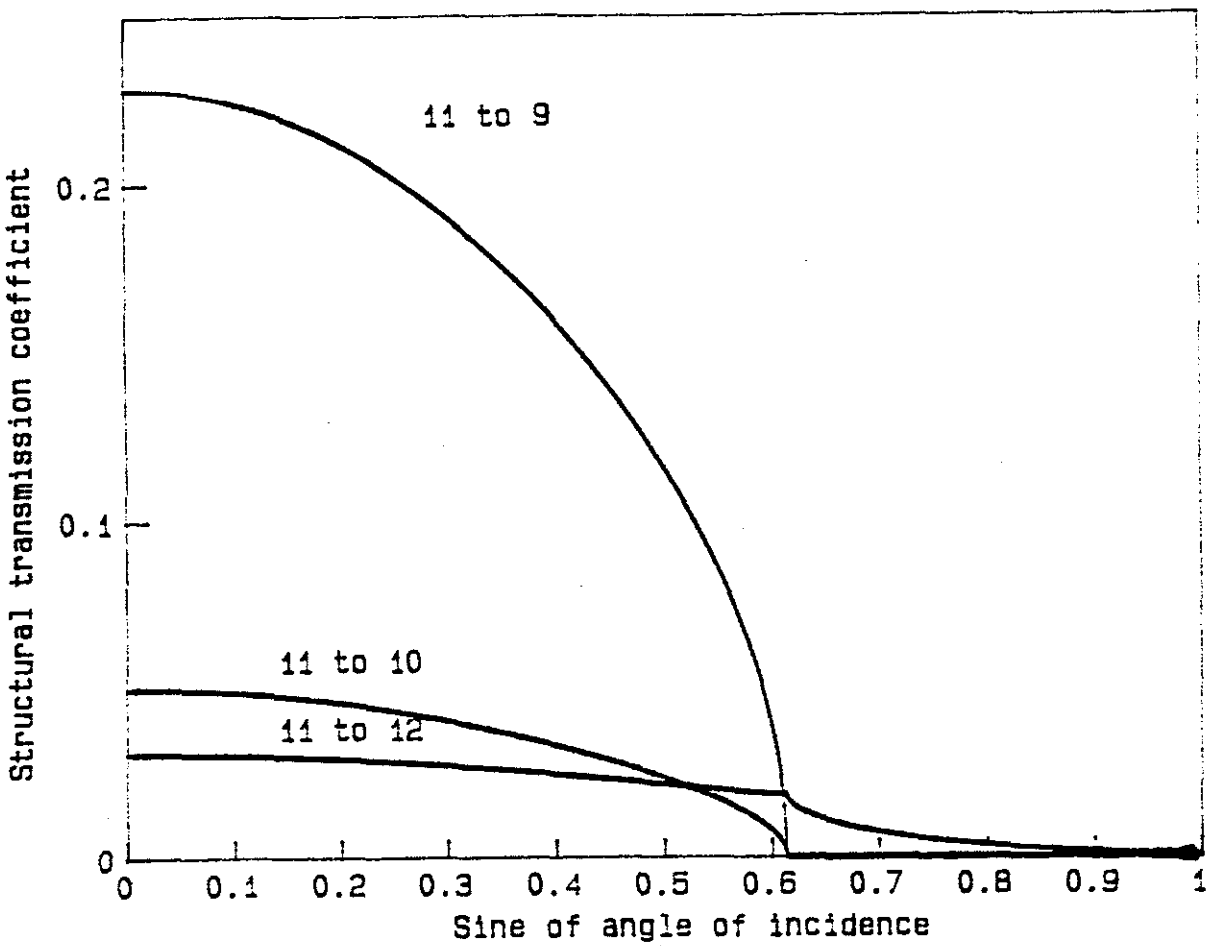

Figure 5.5. Predicted transmission coefficients against angle of incidence at 1000 Hz for transmission from floor 11 with a plywood fire stop (no joists). (PPC FIG 46, 03 Nov. 94)

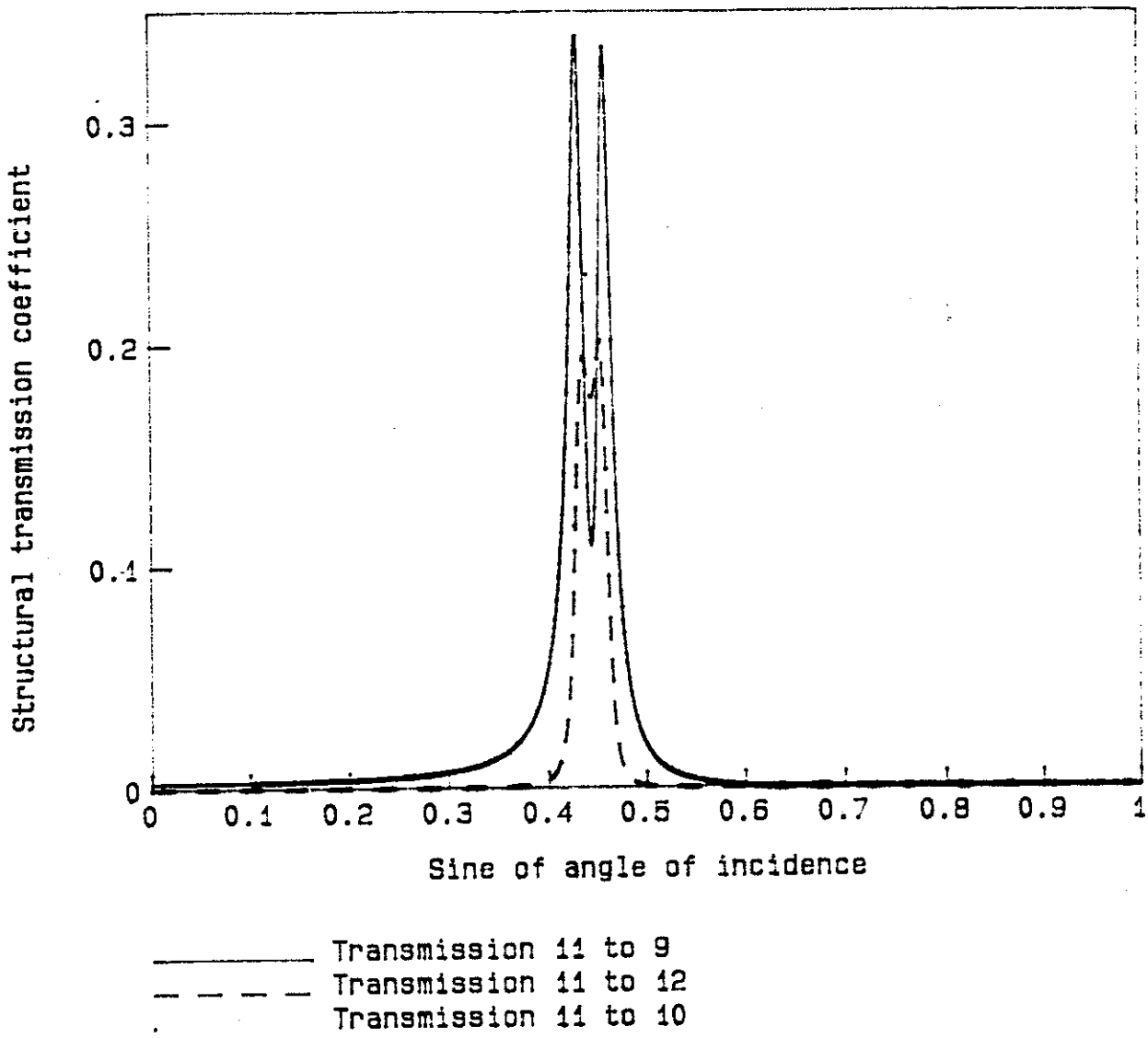

Figure 5.6. *Predicted transmission coefficients at 1000 Hz versus angle of incidence for transmission from floor 11 with a plywood fire stop including the effects of joists. (PPC FIG 45, 03 Nov. 94)*

Freq.	Plywood			Gypsum Board			Steel		
	$\tau_{11,9}$	$\tau_{11,12}$	$\tau_{11,10}$	$\tau_{11,9}$	$\tau_{11,12}$	$\tau_{11,10}$	$\tau_{11,9}$	$\tau_{11,12}$	$\tau_{11,10}$
50	9.6	9.9	11.5	8.5	11.3	12.9	4.5	52.2	53.8
63	9.5	10.0	11.6	8.3	11.6	13.2	4.5	53.2	54.8
79	9.4	10.1	11.7	8.1	11.9	13.5	4.5	54.2	55.8
100	9.3	10.2	11.9	8.0	12.2	13.8	4.5	55.2	56.8
126	9.2	10.4	12.0	7.8	12.6	14.2	4.5	56.2	57.8
159	9.0	10.6	12.2	7.6	12.9	14.6	4.5	57.2	58.8
200	8.9	10.8	12.4	7.4	13.3	15.0	4.5	58.2	59.8
252	8.7	11.0	12.6	7.2	13.8	15.4	4.5	59.2	60.8
317	8.6	11.2	12.8	7.0	14.3	15.9	4.5	60.2	61.8
400	8.4	11.5	13.1	6.8	14.8	16.4	4.5	61.2	62.8
504	8.2	11.7	13.4	6.6	15.3	16.9	4.5	62.2	63.8
635	8.0	12.1	13.7	6.5	15.9	17.5	4.5	63.2	64.8
800	7.9	12.4	14.0	6.3	16.5	18.1	4.5	64.2	65.8
1008	7.7	12.8	14.4	6.1	17.1	18.8	4.5	65.2	66.8
1270	7.5	13.2	14.8	6.0	17.8	19.4	4.5	66.2	67.8
1600	7.3	13.6	15.2	5.9	18.5	20.1	4.5	67.2	68.8
2016	7.1	14.1	15.7	5.7	19.2	20.9	4.5	68.2	69.8
2540	6.9	14.5	16.2	5.6	20.0	21.6	4.5	69.3	70.8
3200	6.7	15.1	16.7	5.5	20.8	22.4	4.5	70.3	71.9
4032	6.5	15.6	17.3	5.4	21.5	23.2	4.5	71.3	72.9
5080	6.4	16.2	17.9	5.3	22.4	24.0	4.5	72.3	73.9
6400	6.2	16.9	18.5	5.2	23.2	24.8	4.5	73.3	74.9
8063	6.1	17.5	19.1	5.2	24.0	25.7	4.5	74.3	75.9
10159	5.9	18.2	19.8	5.1	24.9	23.5	4.5	75.3	76.9
12800	5.8	18.9	20.5	5.0	25.8	27.4	4.5	76.3	77.9

Table 5.1. Predicted angular average transmission loss in dB for transmission from floor 11 for various fire stop materials (no joists).

Freq.	Plywood			Gypsum Board			Steel		
	$\tau_{9,11}$	$\tau_{9,10}$	$\tau_{9,12}$	$\tau_{9,11}$	$\tau_{9,10}$	$\tau_{9,12}$	$\tau_{9,11}$	$\tau_{9,10}$	$\tau_{9,12}$
50	11.8	14.5	13.6	10.6	16.0	15.1	6.7	56.9	55.9
63	11.7	14.6	13.7	10.4	16.3	15.3	6.7	57.9	56.9
79	11.5	14.7	13.8	10.3	16.6	15.6	6.7	58.9	57.9
100	11.4	14.9	14.0	10.1	16.9	15.9	6.7	59.9	58.9
126	11.3	15.1	14.1	9.9	17.3	16.3	6.6	60.9	59.9
159	11.2	15.2	14.3	9.7	17.7	16.7	6.6	61.9	60.9
200	11.0	15.4	14.5	9.5	18.1	17.1	6.6	62.9	61.9
252	10.9	15.7	14.7	9.3	18.5	17.5	6.6	63.9	62.9
317	10.7	15.9	14.9	9.1	19.0	18.0	6.6	64.9	63.9
400	10.5	16.2	15.2	8.9	19.5	18.5	6.6	65.9	64.9
504	10.3	16.5	15.5	8.8	20.1	19.1	6.6	67.0	66.0
635	10.2	16.8	15.8	8.6	20.7	19.6	6.6	68.0	67.0
800	10.0	17.1	16.1	8.4	21.3	20.2	6.6	69.0	68.0
1008	9.8	17.5	16.5	8.3	21.9	20.9	6.6	70.0	69.0
1270	9.6	17.9	16.9	8.1	22.6	21.6	6.6	71.0	70.0
1600	9.4	18.3	17.3	8.0	23.3	22.2	6.6	72.0	71.0
2016	9.2	18.8	17.8	7.9	24.0	23.0	6.6	73.0	72.0
2540	9.0	19.3	18.3	7.7	24.7	23.7	6.6	74.0	73.0
3200	8.8	19.8	18.8	7.6	25.5	24.5	6.6	75.0	74.0
4032	8.7	20.4	19.4	7.5	26.3	25.3	6.6	76.0	75.0
5080	8.5	21.0	20.0	7.4	27.1	26.1	6.6	77.0	76.0
6400	8.3	21.6	20.6	7.4	27.9	26.9	6.6	78.0	77.0
8063	8.2	22.3	21.2	7.3	28.8	27.8	6.6	79.0	78.0
10159	8.0	23.0	21.9	7.2	29.7	28.6	6.6	80.0	79.0
12800	7.9	23.7	22.6	7.2	30.5	29.5	6.6	81.0	80.0

Table 5.2. Predicted angular average transmission loss in dB for transmission from wall 9 for various fire stop materials (no joists).

Freq.	Plywood			Gypsum Board			Steel		
	$\tau_{11,9}$	$\tau_{11,12}$	$\tau_{11,10}$	$\tau_{11,9}$	$\tau_{11,12}$	$\tau_{11,10}$	$\tau_{11,9}$	$\tau_{11,12}$	$\tau_{11,10}$
50	10.2	8.4	10.2	8.2	7.5	9.0	4.3	50.0	51.9
63	10.4	8.6	10.4	8.2	7.8	9.4	4.6	51.4	53.3
79	10.0	8.5	9.9	8.2	8.2	9.9	4.9	52.8	54.7
100	10.0	8.6	10.0	8.2	8.8	10.5	5.3	54.3	56.2
126	10.1	8.8	10.4	8.3	9.5	11.2	5.7	55.9	57.8
159	10.3	9.2	10.8	8.4	10.3	12.1	6.2	57.6	59.5
200	10.6	9.7	11.3	8.7	11.4	13.1	6.8	59.3	61.2
252	11.0	10.4	12.0	9.1	12.5	14.3	7.5	61.1	62.9
317	11.4	11.2	12.8	9.6	13.9	15.6	8.3	62.9	64.7
400	12.0	12.1	13.7	10.2	15.3	17.0	9.1	64.8	66.5
504	12.6	13.2	14.7	11.0	16.8	18.4	10.1	66.7	68.3
635	13.4	14.4	15.8	11.8	18.5	20.2	11.1	68.6	70.1
800	14.2	15.8	17.0	12.8	20.2	21.5	12.1	70.5	71.8
1008	15.3	17.3	18.3	13.9	22.0	23.1	13.3	72.5	73.5
1270	16.5	19.2	19.6	15.1	24.0	24.5	14.6	74.5	75.1
1600	18.1	21.6	21.1	16.8	26.3	25.9	16.2	76.7	76.4
2016	22.6	29.4	24.7	20.6	32.0	27.9	19.6	81.5	77.6
2540	35.0	68.8	67.8	34.9	77.0	75.9	34.8	128.4	127.3
3200	39.3	79.6	79.9	39.2	88.0	88.3	39.2	139.4	139.7
4032	42.9	88.1	89.0	42.9	96.6	97.4	42.9	148.1	148.9
5080	46.3	96.0	97.1	46.3	104.5	105.6	46.3	156.0	157.1
6400	49.6	103.6	104.8	49.6	112.0	113.3	49.6	163.5	164.8

Table 5.3. *Predicted angular average transmission loss in dB for transmission from floor 11 for various fire stop materials using a model that includes the effect of joists.*

Freq.	Plywood			Gypsum Board			Steel		
	$\tau_{9,11}$	$\tau_{9,10}$	$\tau_{9,12}$	$\tau_{9,11}$	$\tau_{9,10}$	$\tau_{9,12}$	$\tau_{9,11}$	$\tau_{9,10}$	$\tau_{9,12}$
50	12.3	11.7	12.3	10.3	12.6	11.1	6.4	55.9	54.0
63	12.5	11.7	12.5	10.3	13.1	11.5	6.7	57.3	55.4
79	12.1	12.8	12.1	10.3	13.7	12.0	7.0	58.8	56.9
100	12.1	13.4	12.2	10.3	14.3	12.6	7.4	60.3	58.4
126	12.2	13.9	12.5	10.4	15.1	13.4	7.8	61.8	59.9
159	12.4	14.5	12.9	10.6	16.0	14.2	8.3	63.5	61.6
200	12.7	15.1	13.5	10.8	17.0	15.3	8.9	65.1	63.3
252	13.1	15.8	14.1	11.2	18.2	16.4	9.6	66.9	65.0
317	13.5	16.5	14.9	11.7	19.4	17.7	10.4	68.6	66.8
400	14.1	17.4	15.8	12.3	20.8	19.1	11.3	70.3	68.6
504	14.7	18.3	16.8	13.1	22.2	20.6	12.2	72.1	70.4
635	15.5	19.3	17.9	13.9	23.6	22.1	13.2	73.7	72.2
800	16.4	20.4	19.1	14.9	24.9	23.6	14.3	75.3	73.9
1008	17.4	21.4	20.4	16.0	26.2	25.2	15.4	76.7	75.6
1270	18.6	22.2	21.8	17.3	27.2	26.7	16.7	77.8	77.2
1600	20.2	22.8	23.3	18.9	27.6	28.0	18.3	78.1	78.5
2016	24.8	21.5	26.8	22.6	25.7	30.0	21.7	75.8	79.7
2540	37.1	21.1	70.0	37.0	23.4	78.1	37.0	77.4	129.4
3200	41.4	25.3	82.1	41.4	27.3	90.4	41.3	83.5	141.9
4032	45.1	26.5	91.1	45.0	29.0	99.6	45.0	87.3	151.0
5080	48.4	27.3	99.3	48.4	29.1	107.7	48.4	71.5	159.2
6400	51.7	98.0	107.0	51.7	106.4	115.4	51.7	157.9	166.9

Table 5.4. Predicted angular average transmission loss in dB for transmission from wall 9 with various fire stop materials using a model that includes the effect of the joist at the joint.

The average structural transmission loss for transmission from wall 9 to floor 12 is shown in Figures 5.7, 5.8 and 5.9. The figures show the results for fire stops made of plywood, gypsum board and steel, respectively. The joists generally reduce transmission at higher frequencies and there is very little transmission above 2000 Hz. The steel fire stop greatly reduces transmission when compared with the results for the plywood and gypsum board fire stops.

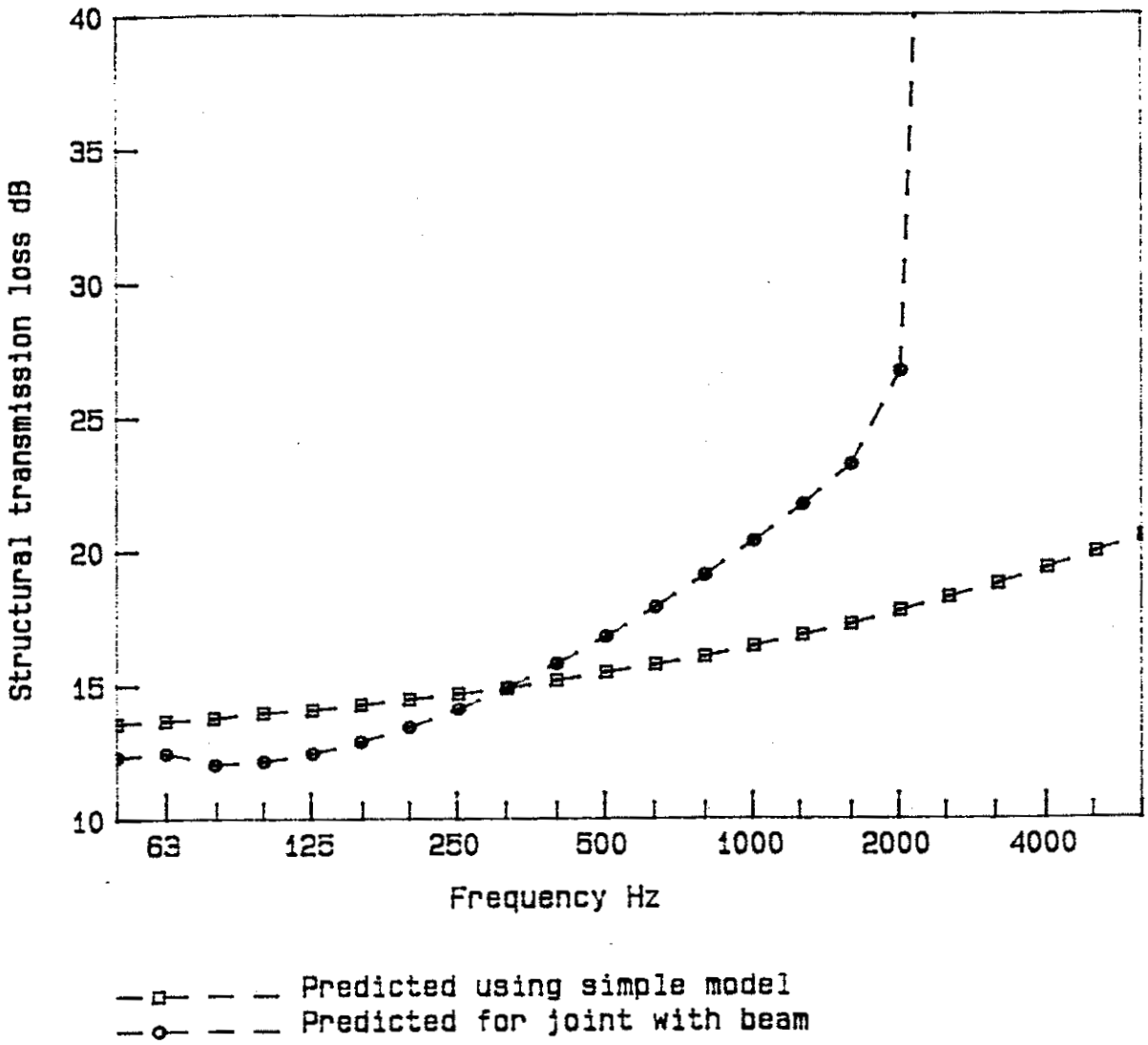

Figure 5.7. Predicted angular average transmission loss for vibration transmission from wall 9 to floor 12 with a plywood fire stop. (PPC FIG 42, 03 Nov. 94)

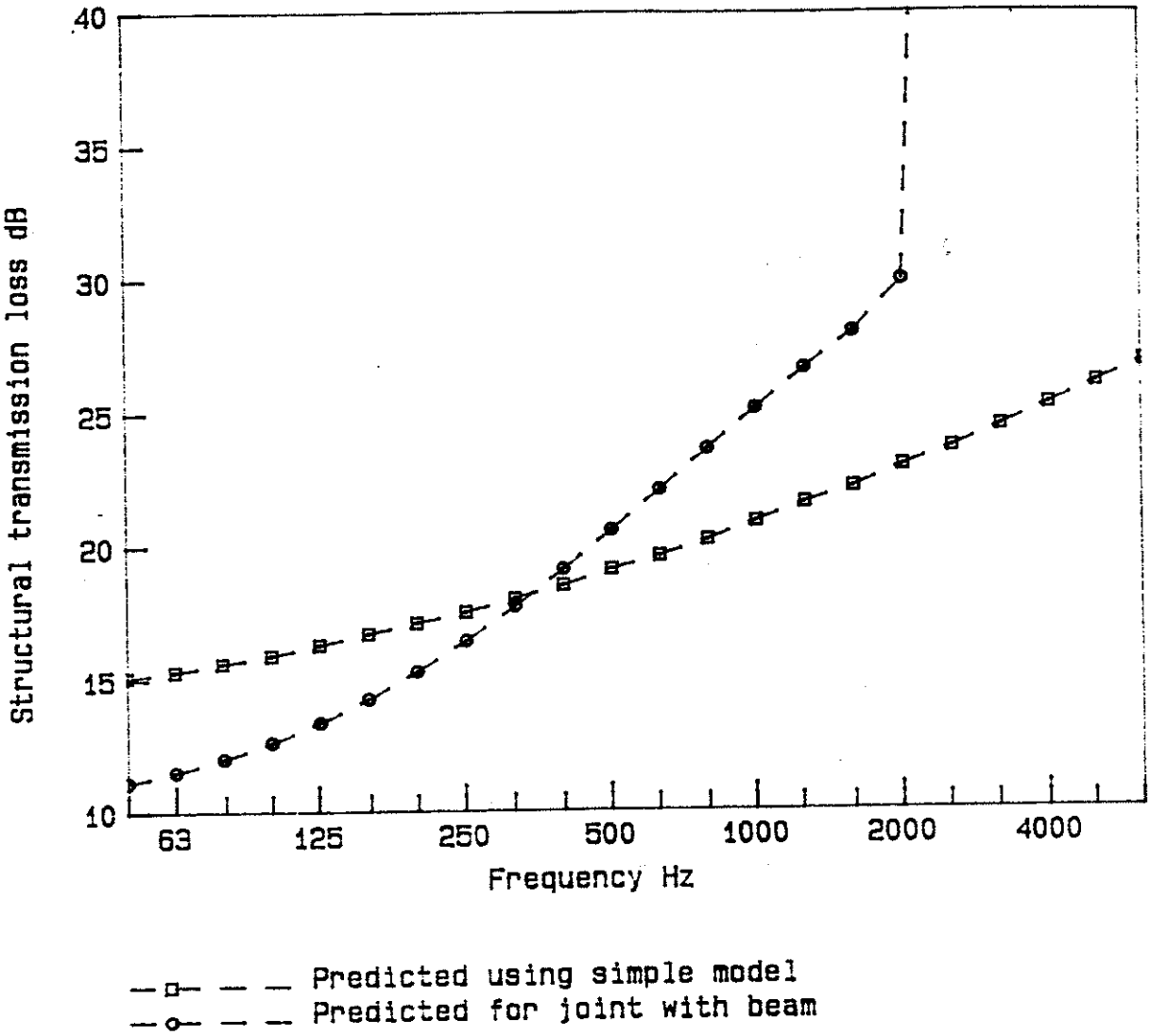

Figure 5.8. *Predicted angular average transmission loss for vibration transmission from wall 9 to floor 12 with a gypsum board fire stop. (PPC FIG 43, 03 Nov. 94)*

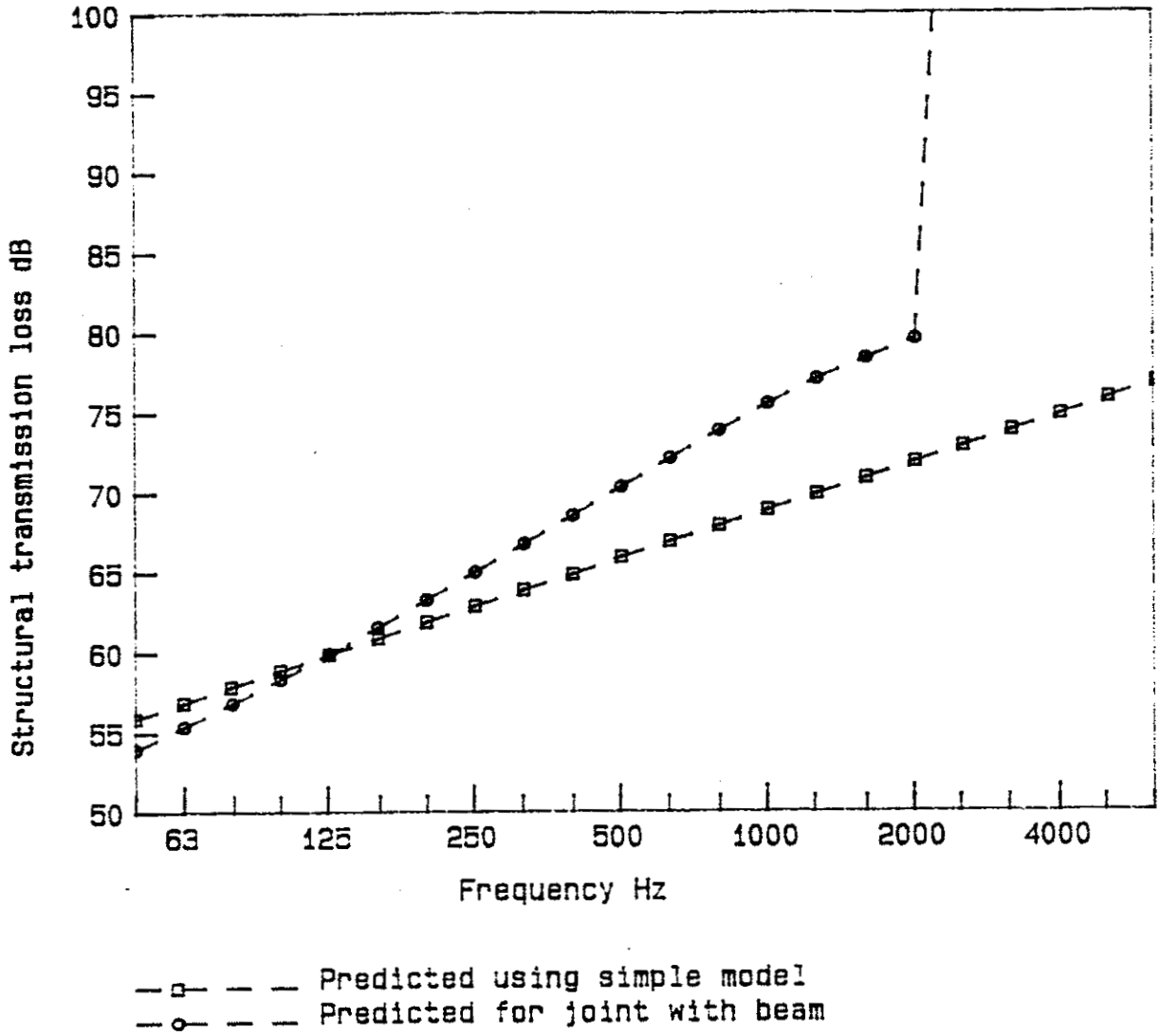

Figure 5.9. Predicted angular average transmission loss for vibration transmission from wall 9 to floor 12 with a steel fire stop. (PPC FIG 44, 03 Nov. 94)

Figure 5.10 shows measured and predicted vibration level differences for transmission from floor 11 to wall 10 with a plywood fire stop. The measurements were carried out using a tapping machine as a noise source on floor 11. The vibration levels were measured using accelerometers, charge amplifiers and a Norsonic 830 dual channel analyser. Due to the attenuation at the joists in the floor, the average vibration level for the floor was calculated using only three positions, one in each of the three bays nearest to the joint. The vibration levels of wall 10 were averaged for six random positions. The measured results show the ratio of the average floor vibration level to the average wall vibration level. Two predictions are also shown. The prediction calculated where the joists were ignored shows good agreement at low frequencies but does not have the correct slope at high frequencies. The main transmission path between floor 11 and wall 10 is through the fire stop. Introducing the joists gives a result which shows better agreement with the measured results at higher frequencies. The predicted result is still less than measured but the effect of the joist eccentricities have not been included and this would have increased the predicted values.

Figure 5.11 shows similar results to Figure 5.10 but for sound transmission from floor 11 to floor 12. The average vibration level for floor 12 was calculated in the same way as for floor 11 is as discussed above. The prediction which does not include the joists shows better agreement with the measured results.

Figure 5.12 shows measured and predicted vibration level differences for transmission from wall 9 to wall 10 with a plywood fire stop. The measurements were carried out using a hammer as a noise source, tapping over the surface of wall 9 for 25 seconds. The measurements were repeated 10 times and the accelerometers were moved after each position.

The results shown in Figure 5.12 have similar trends to those shown in Figure 5.10. The measured results increase rapidly with frequency and the predicted result which includes the effects of the joists shows best agreement. The eccentricity of the joists has not been considered and would have the effect of increasing the predicted results.

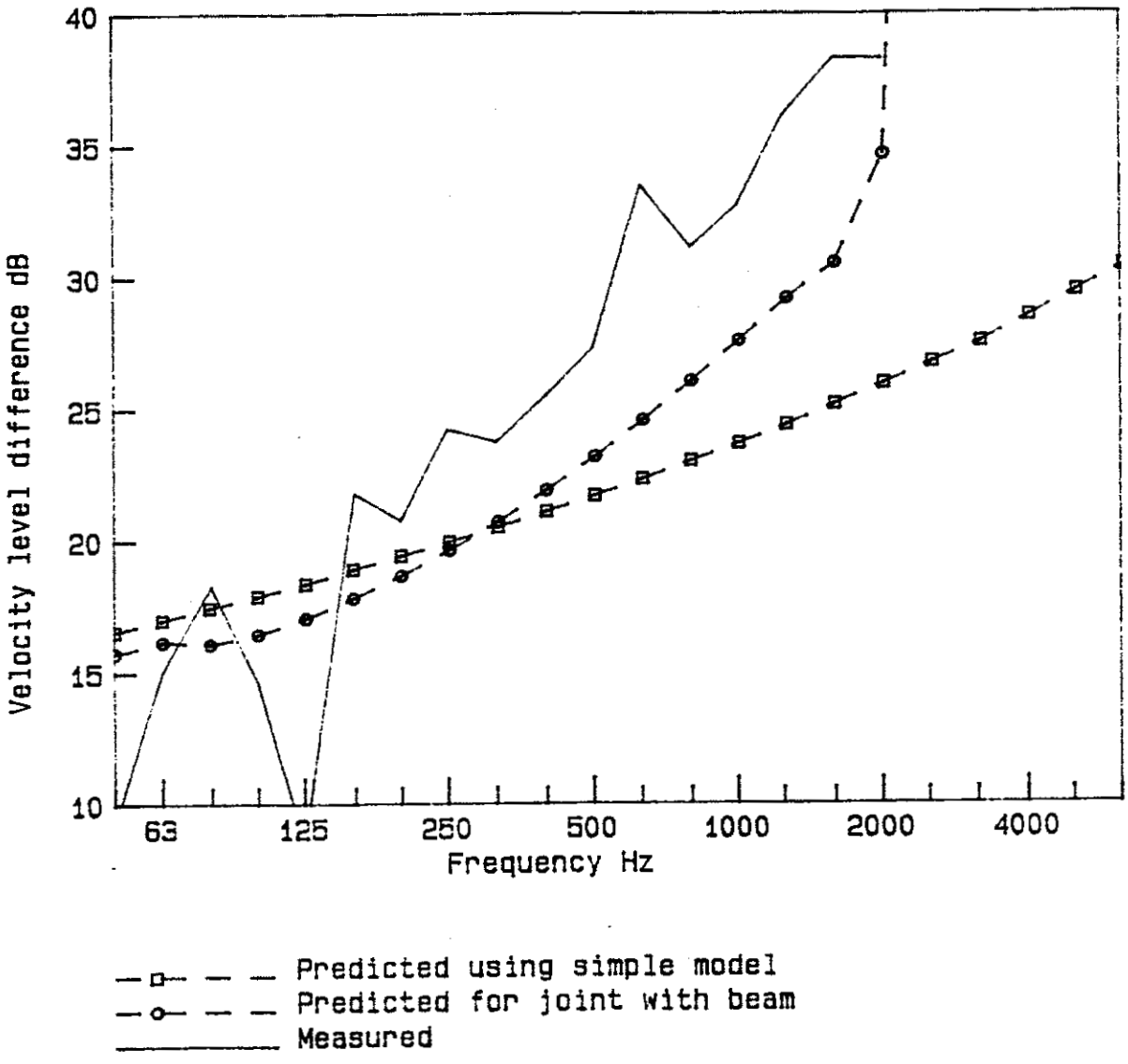

Figure 5.10. Measured and predicted structural vibration level difference for transmission from floor 11 to wall 10 with a plywood fire stop. (PPC FIG 41, 02 Nov. 94)

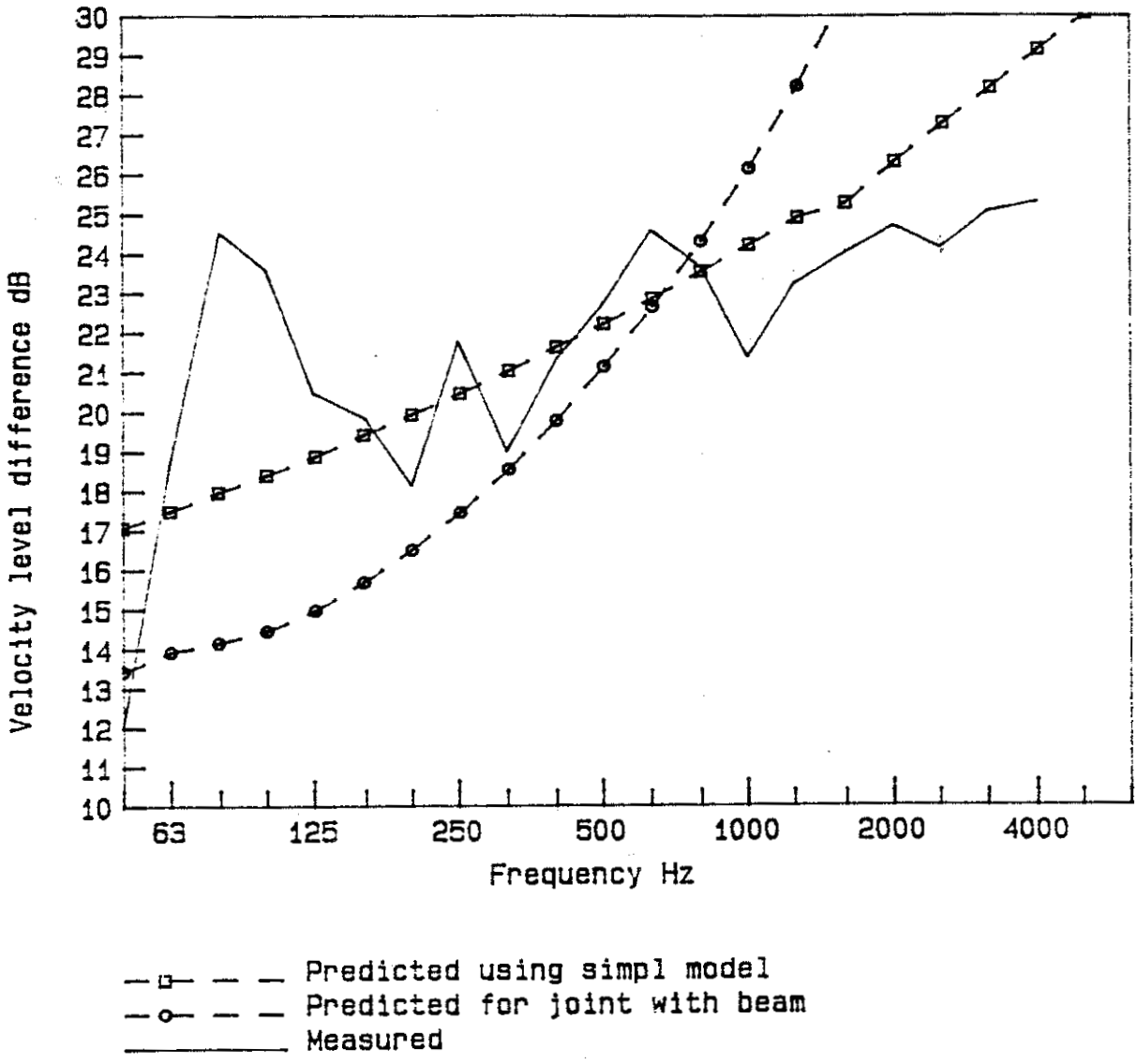

Figure 5.11. Measured and predicted structural vibration level difference for transmission from floor 11 to floor 12 with a plywood fire stop. (PPC FIG 40, 02 Nov. 94)

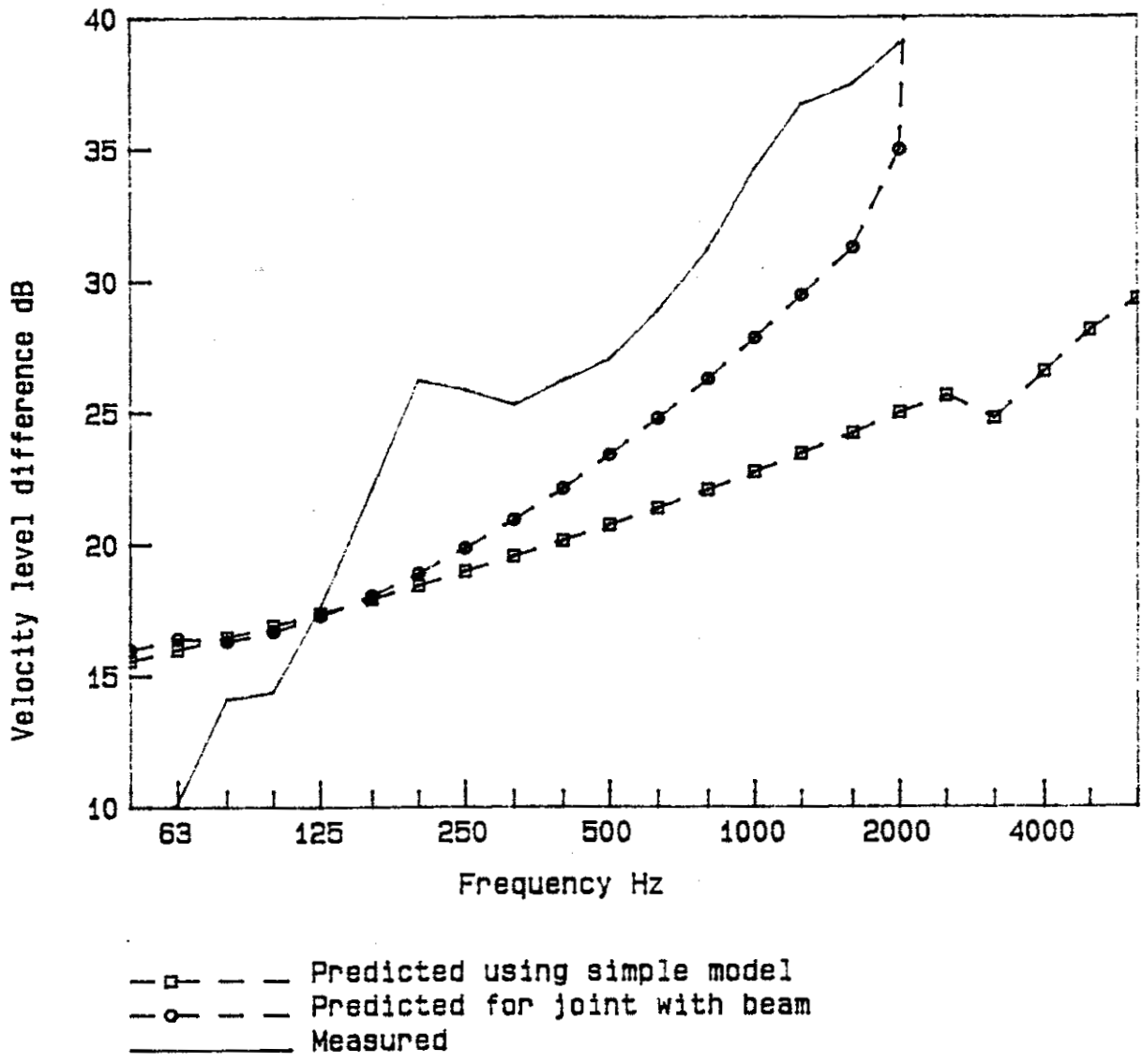

Figure 5.12. Measured and predicted structural vibration level difference for transmission from wall 9 to wall 10 with a plywood fire stop. (PPC FIG 36, 02 Nov. 94)

5.6 CONCLUSIONS

Sound transmission across fire stops has been successfully modelled and good agreement is found between measured and predicted results. The joint can be considered as a pinned joint so that in-plane motion can be ignored. The effect of the joists at the joint must be included if good agreement between measured and predicted vibration levels is to be achieved. The joists generally reduce transmission at higher frequencies and there is a cut of frequency, above which vibration transmission is negligible.

The results for vibration transmission between the floors is inconclusive.

6 VIBRATION PROPAGATION ACROSS FLOORS

6.1 INTRODUCTION

During measurements of vibration transmission across the fire stop, it was noticed that there was considerable attenuation from one bay of the timber floor to another. As this attenuation has an effect on the overall performance of the system, it was investigated further.

6.2 MEASUREMENTS

A tapping machine was placed on the plywood decking so that all the hammers fell in one bay. The vibration was then measured on each of the bays as shown in Figure 6.1. It can be seen that there is considerable attenuation of up to 30 dB at the mid frequencies.

In general, there is less attenuation with distance as the distance from the source increases so that the furthest bays all have similar level differences.

At very low frequencies, the level difference is small and the attenuation only starts at about 50 Hz. There is a very clear dip at 250 Hz and then a levelling off at the high frequencies above about 160 Hz.

6.3 MODAL FREQUENCIES

An analysis of the modes in the floors was carried out to see if modal effects could explain the effect. For there to be attenuation, the floor would need to be modelled as a number of separate subsystems. Each bay is then 0.4 x 4.54 m.

Given the material properties of the floor, the modal frequencies were generated and are given in Table 6.1 for all modes up to 50 Hz. The first mode in a single bay is at 116 Hz so that below this the floor must act as a single unit. If the floor behaves as a single unit, then it is a single subsystem and there should be uniform distribution of energy. This explains why there is little attenuation with distance at higher frequencies.

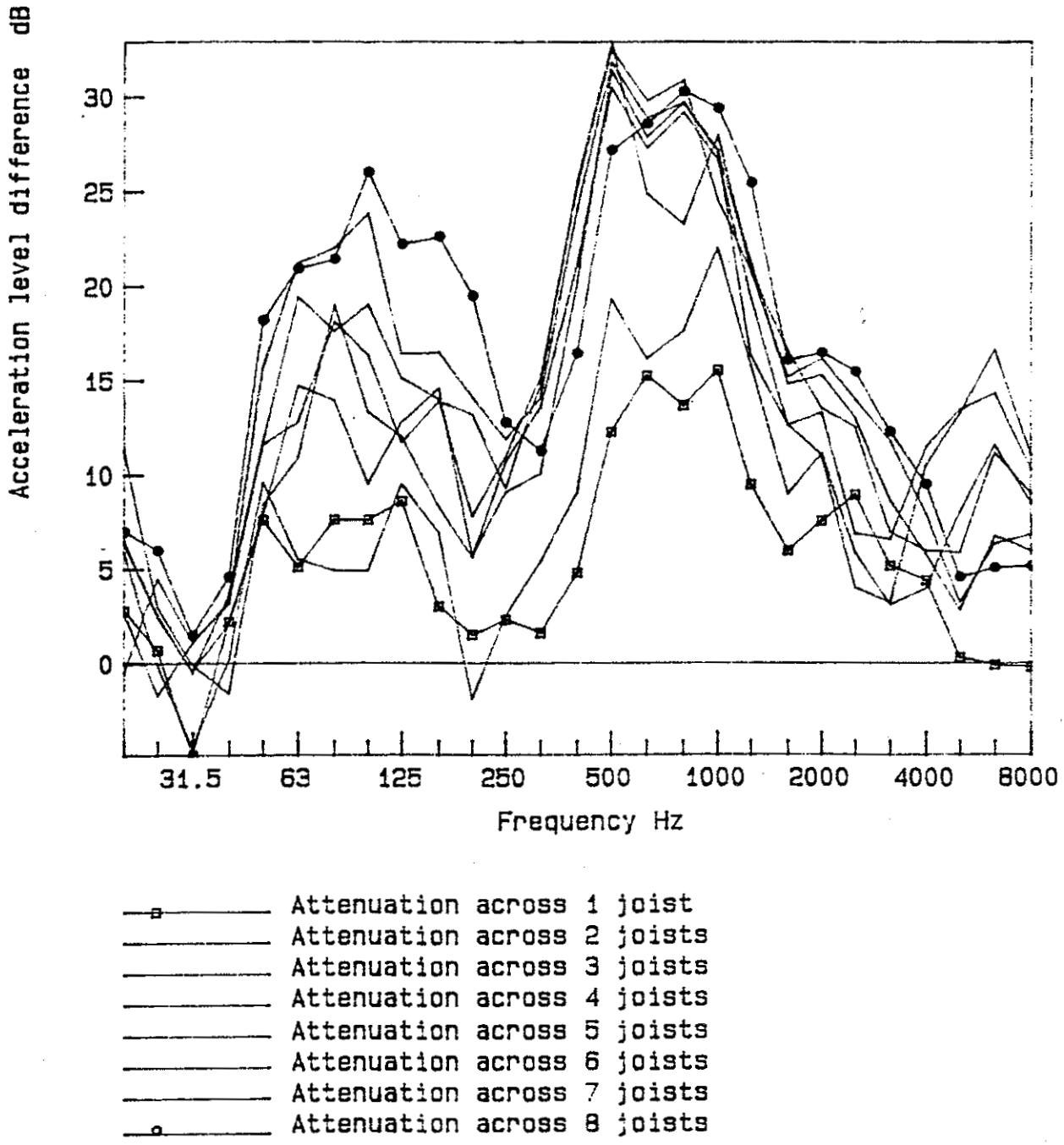

Figure 6.1. Measured attenuation across a timber floor past a series of timber joists. (PPC FIG 1, 26 Oct. 94)

	m	n	Frequency	Third octave band	Angle (degrees)
Mode	1	1	116.670 Hz	(band 125)	ang=85.0
Mode	1	2	119.366 Hz	(band 125)	ang=80.0
Mode	1	3	123.860 Hz	(band 125)	ang=75.2
Mode	1	4	130.150 Hz	(band 125)	ang=70.6
Mode	1	5	138.239 Hz	(band 125)	ang=66.2
Mode	1	6	148.124 Hz	(band 160)	ang=62.1
Mode	1	7	159.807 Hz	(band 160)	ang=58.3
Mode	1	8	173.288 Hz	(band 160)	ang=54.8
Mode	1	9	188.565 Hz	(band 200)	ang=51.6
Mode	1	10	205.640 Hz	(band 200)	ang=48.6
Mode	1	11	224.513 Hz	(band 200)	ang=45.9
Mode	1	12	245.183 Hz	(band 250)	ang=43.4
Mode	1	13	267.650 Hz	(band 250)	ang=41.1
Mode	1	14	291.915 Hz	(band 315)	ang=39.0
Mode	1	15	317.977 Hz	(band 315)	ang=37.1
Mode	1	16	345.836 Hz	(band 315)	ang=35.4
Mode	1	17	375.493 Hz	(band 400)	ang=33.7
Mode	1	18	406.947 Hz	(band 400)	ang=32.2
Mode	1	19	440.198 Hz	(band 400)	ang=30.9
Mode	1	20	475.247 Hz	(band 500)	ang=29.6
Mode	2	1	463.984 Hz	(band 500)	ang=87.5
Mode	2	2	466.680 Hz	(band 500)	ang=85.0
Mode	2	3	471.174 Hz	(band 500)	ang=82.5
Mode	2	4	477.465 Hz	(band 500)	ang=80.0
Mode	2	5	485.553 Hz	(band 500)	ang=77.6
Mode	2	6	495.438 Hz	(band 500)	ang=75.2

Table 6.1 Modes in a single floor bay.

One of the properties of the bay is that it is very long and narrow. If there are n half wavelengths in the l_x direction and m half wavelengths in the l_y direction, then k_x and k_y will be given by

$$k_x = \frac{\pi n}{l_x} \qquad k_y = \frac{\pi m}{l_y} \tag{6.1}$$

The angle at which waves will be incident on the boundary will then be given by

$$\theta = \tan^{-1}\frac{k_y}{k_x} = \tan^{-1}\frac{m l_x}{n l_y} \tag{6.2}$$

This angle is also listed in Table 6.1 for each mode.

For an individual bay of the floor being considered the angles for each of the modes up to 5000 Hz can be seen in Figure 6.2. It can be seen that there is a definite pattern, unlike a more rectangular floor where the pattern should be more random.

6.4 PREDICTED TRANSMISSION

For a system like the floor which consists of a series of plates separated by a beam the transmission between the plates can be computed using the method given by Cremer, Heckl and Ungar. Since their model assumes that the beam is symmetric, the calculations made were for the case where the joist was symmetrically located about the plates rather than on one side.

The transmission coefficients as a function of angle can be seen in Figure 6.3 for a number of discrete frequencies (125, 250, 500, 1000, 2000 Hz). There is a very small decrease in angle of maximum transmission as the frequency increases. One of the characteristics of the results is that the transmission coefficient is very high at one particular angle and is more or less zero at other angles. The angle at which transmission is taking place is around 40° irrespective of frequency. The consequence is that energy incident at this angle is transmitted whereas other angles are not. From Figure 6.2 it can be seen that there are modes with angles of incidence at 40° in the 250 Hz band and again at 1000, 2000 and 4000 Hz. At other frequencies, the angles are such that the transmission will be small and attenuation high as observed.

Starting with the known modal frequencies and angles, the transmission coefficient for each mode was computed as shown in Figure 6.4. This shows that there is high transmission at the frequencies 250, 1000 Hz, etc. These individual modal values were then averaged to give the band average transmission values shown in Figure 6.5 as transmission loss values. As expected, there is a low transmission loss at 250 and the other specific frequencies.

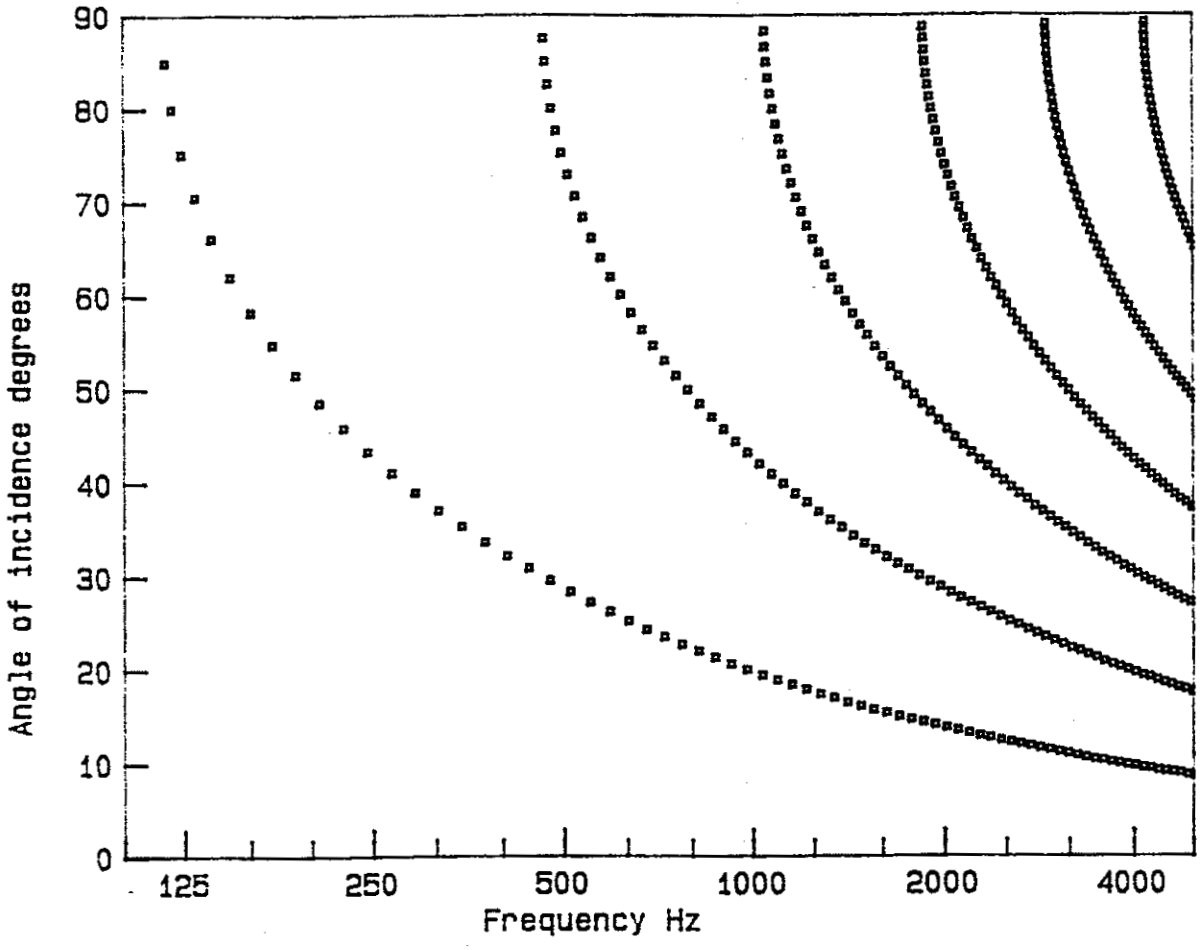

Figure 6.2. *Angles at which the modes in a 0.4 x 4.54 m panel are incident on the joist boundary (m is an arbitrary integer; see equations (6.1) and (6.2)). (PPC FIG 9, 28 Oct. 94)*

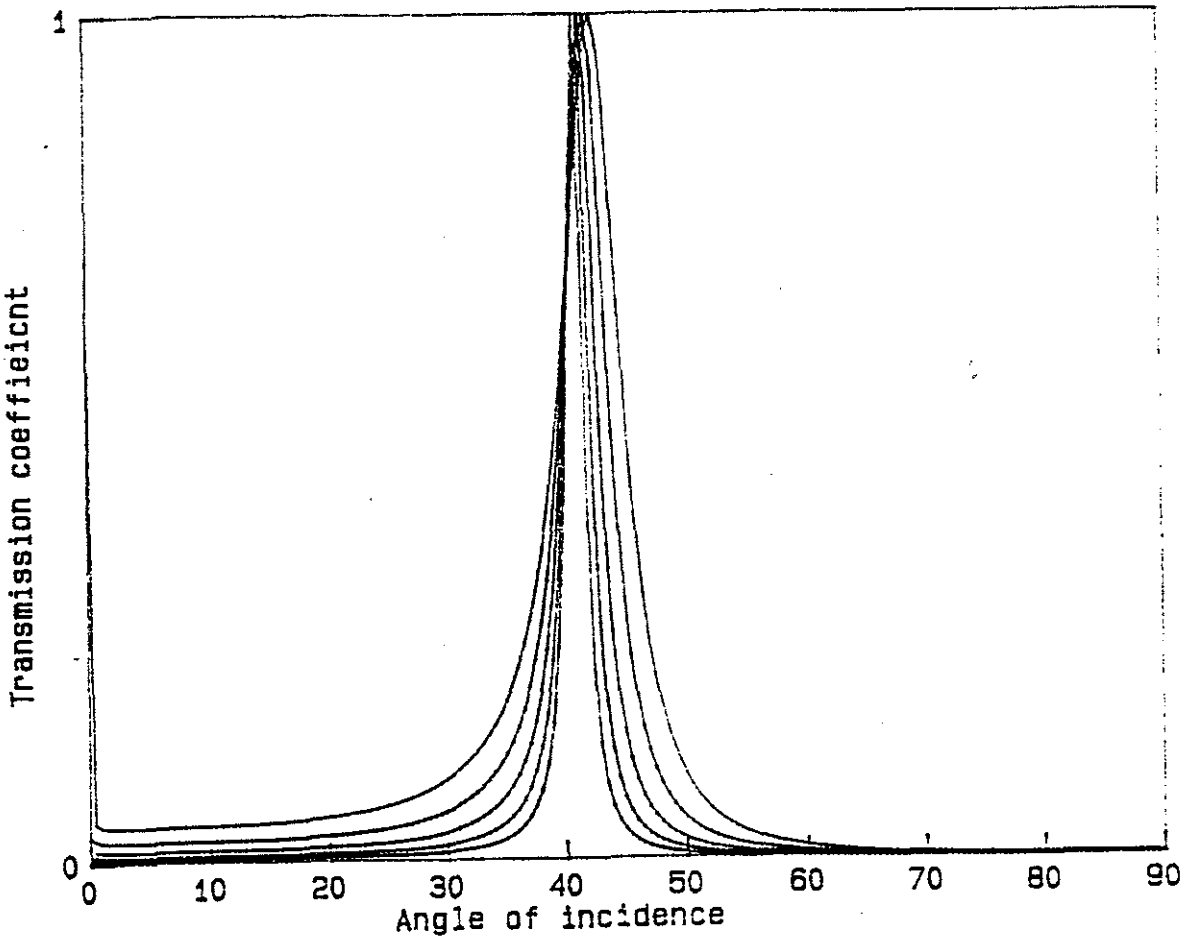

Figure 6.3. Transmission coefficient as a function of angle for a plate-beam-plate model at 125, 250, 500, 1000 and 2000 Hz. (PPC FIG 13, 31 Oct. 94)

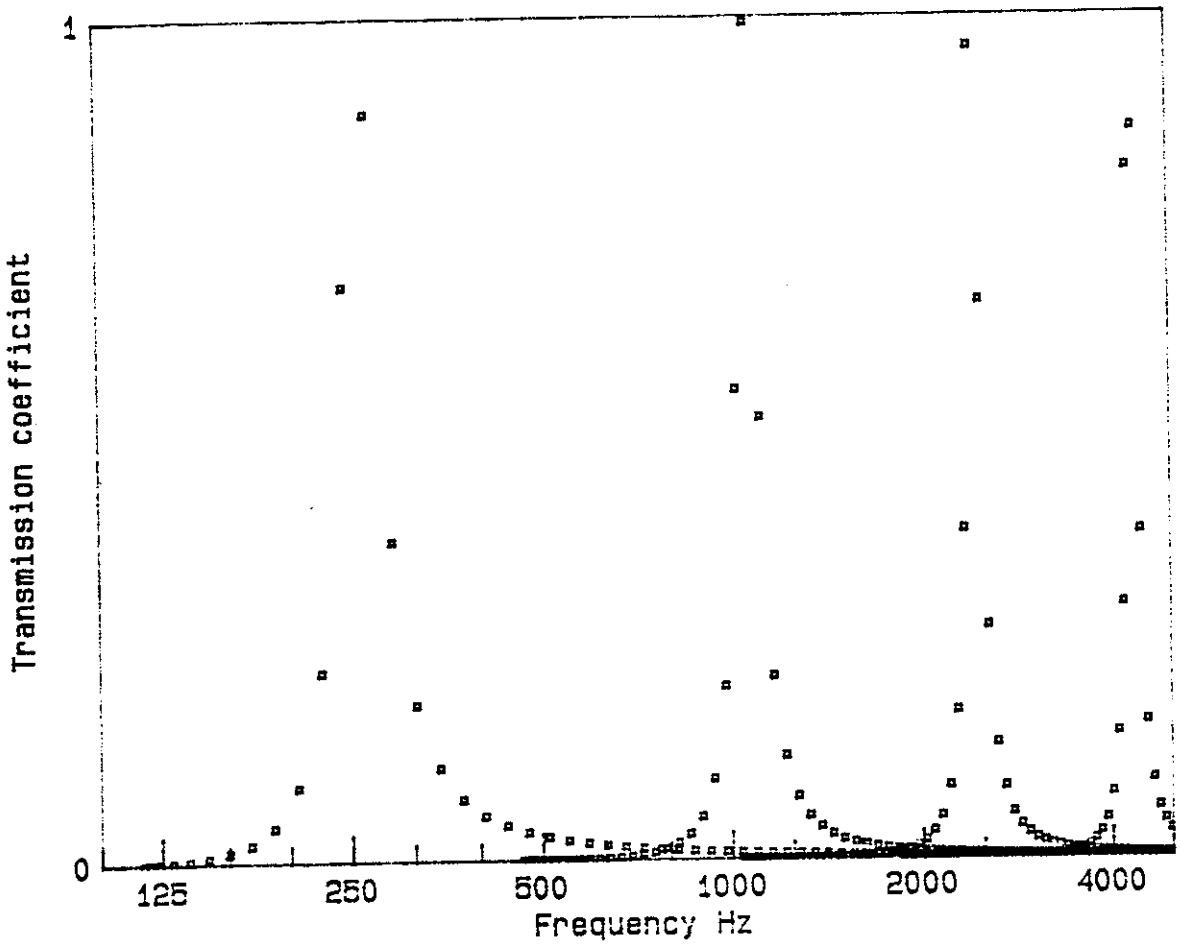

Figure 6.4. *Transmission coefficient for each mode in the 0.4 x 4.54 m panel section. (PPC FIG 10, 28 Oct. 94)*

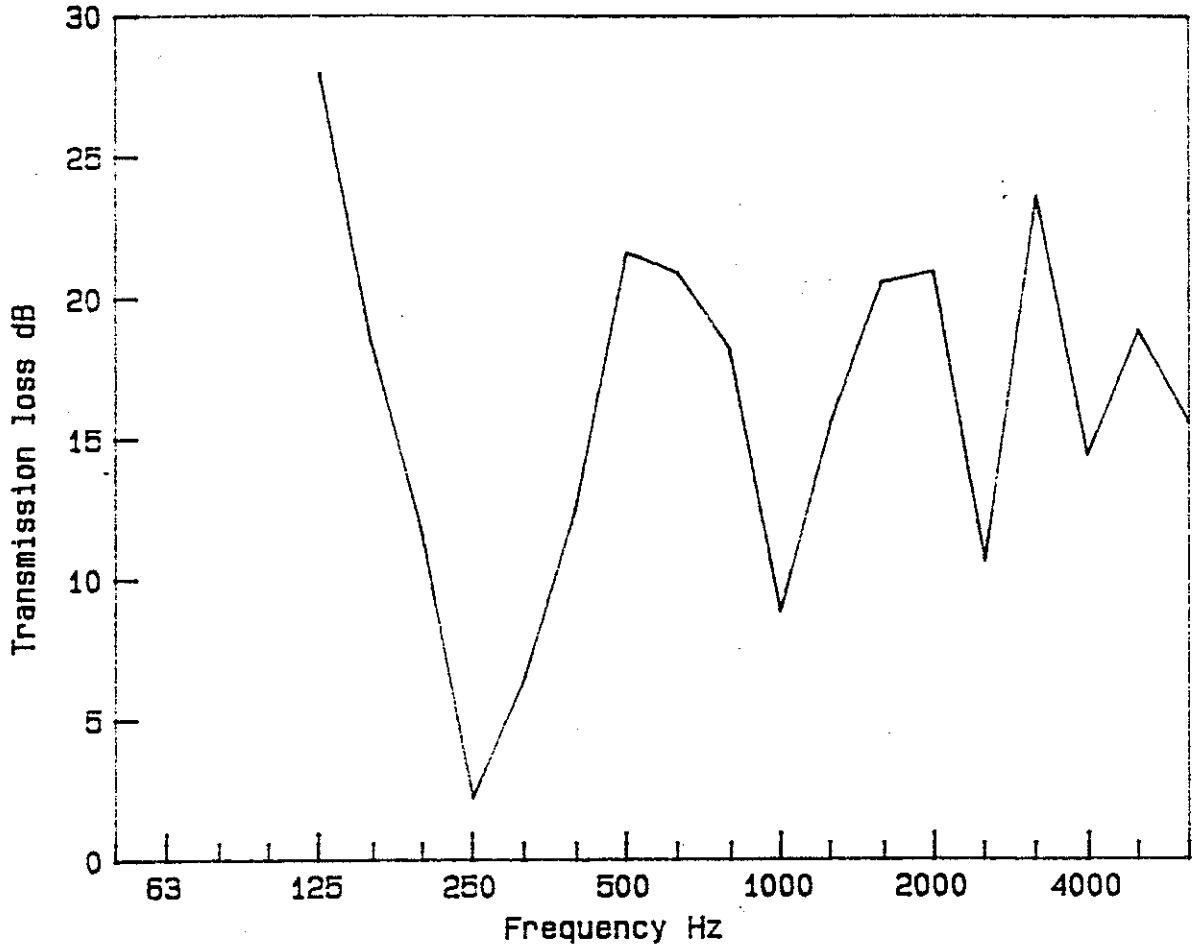

Figure 6.5. *Predicted band averaged transmission loss for a plate-beam-plate joint. (PPC FIG 12, 28 Oct. 94)*

6.5 PREDICTING ATTENUATION

As a final step, the predicted transmission loss values were input into a simple SEA model to predict the attenuation. The coupling was computed using equation (2.18) and the total loss factor was taken as the sum of the CLFs and the internal loss factor which was 0.015. The result is shown in Figure 6.6. It can be seen that the attenuation is much larger than measured and that the attenuation/bay is approximately constant. This is a consequence of the way the model was set up.

The model does give the correct trend of a dip at 250 Hz and other dips at the higher frequencies (though not always in the correct place).

The model is most likely to be accurate for transmission across the first bay where the assumptions in an SEA model are valid. The measured and predicted attenuation are given in Figure 6.7. The agreement is reasonable considering the extent to which SEA has been extended to deal with this type of system. At high frequencies, the assumption that the boundary is a line breaks down. The nails fixing the plywood to the joists were at about 150 mm centres. They are a half wavelength apart at about 800 Hz and a full wavelength at 2500 Hz. Therefore, at the higher frequencies the nails act as line connections and sound waves will pass between the nails. Therefore, the plate will act more like a single panel with no attenuation at these higher frequencies.

6.6 DISCUSSION

Although the simple model cannot predict the actual attenuation, it does help in the understanding of the mechanisms of transmission and attenuation. It is really only successful in predicting transmission across one bay. After traversing one joint, the energy is already aligned in the direction that gives transmission so that it could be argued that energy transmitted between the other plates should have a transmission coefficient of 1. This would greatly reduce the attenuation with distance.

The result of this revised prediction is shown in Figure 6.8. This gives much better agreement between the measured and predicted results in the range 125 to 1000 Hz. At higher frequencies, the line connection starts to become a series of point connections and the model becomes invalid.

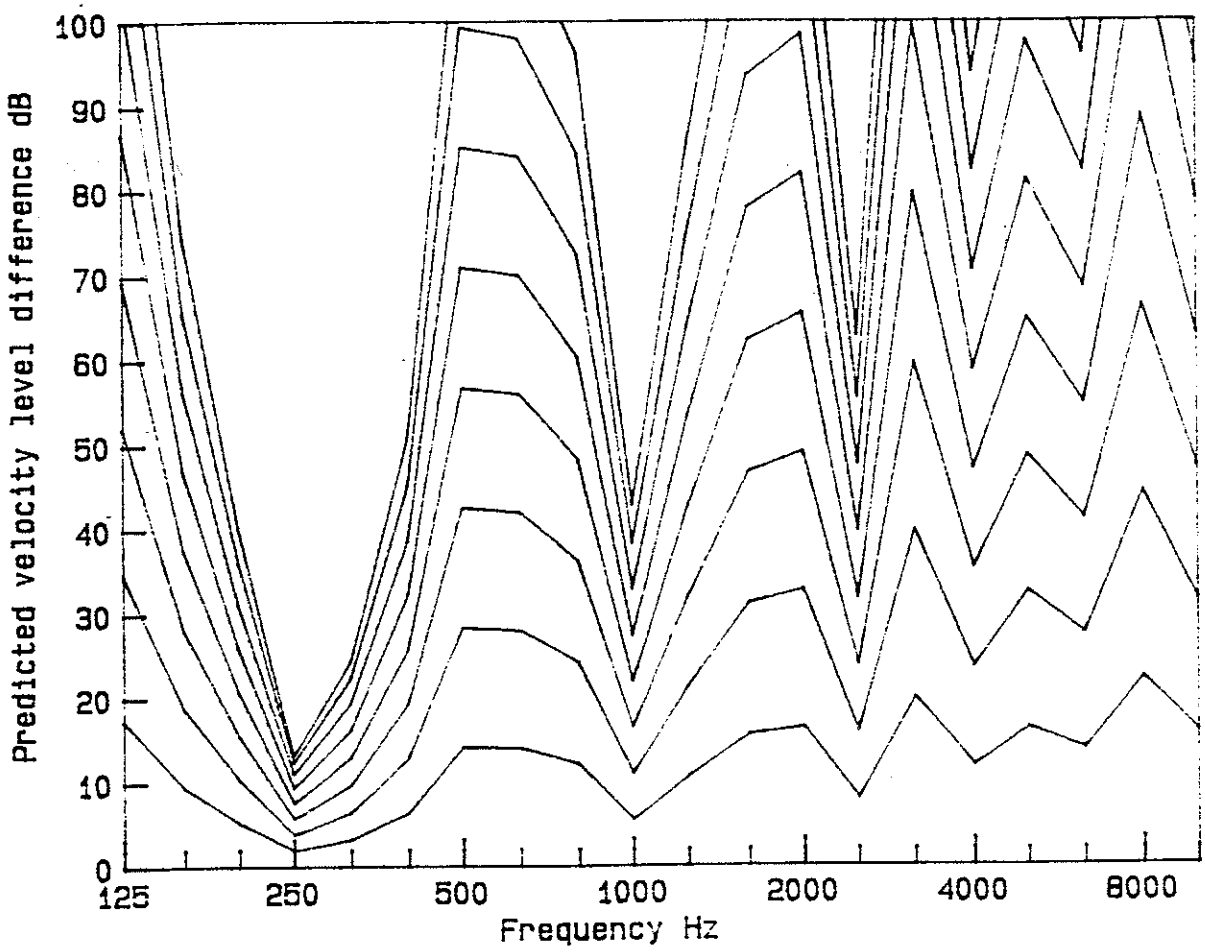

Figure 6.6. Predicted attenuation across the floor using the band averaged transmission coefficients. (PPC FIG 14, 31 Oct. 94)

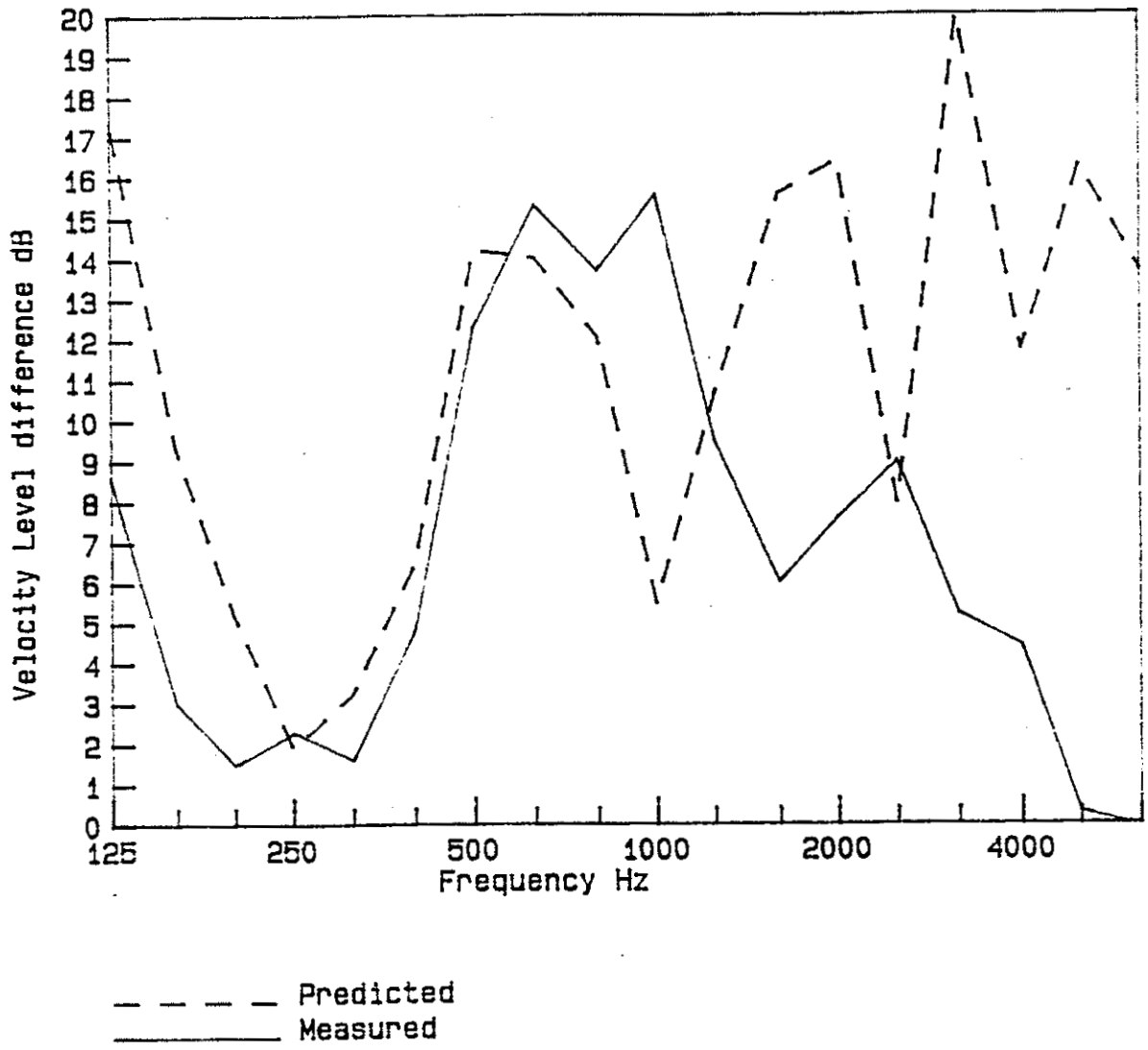

Figure 6.7. Measured and predicted attenuation across the first joist. (PPC FIG 15, 31 Oct. 94)

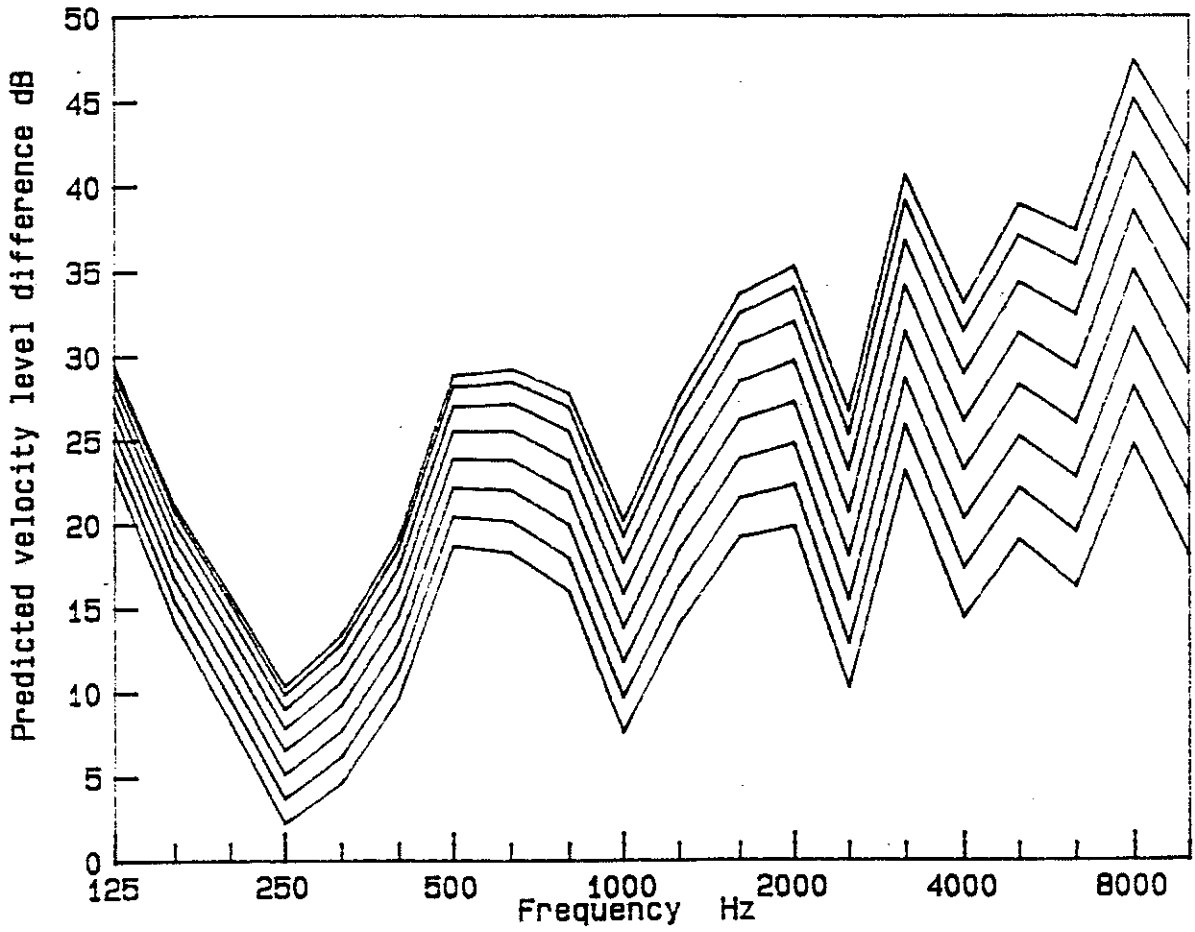

The transmision coefficient for the first joint is the band average
The other transmission coefficients are all 1

Figure 6.8. *Predicted attenuation across the floor where the band averaged transmission coefficients are used for the first joint and the transmission coefficients are assumed to be 1 for all other joints. (PPC FIG 16, 31 Oct. 94)*

7 CONCLUSIONS

7.1 SUMMARY OF CONCLUSIONS

Although this report can only summarize the work that was undertaken, the results obtained have shown that statistical energy analysis can be used with considerable success to predict transmission in complex building structures. There was generally good agreement between the measured and predicted results for all the constructions examined. Where the agreement was not as good, it can usually be explained by the approximations made to the model.

For airborne sound transmission through walls it was found that the transmission was dominated by non-resonant transmission into and out of the cavity below the critical frequency and by resonant transmission into and out of the cavity above the critical frequency. The equations that describe this path are given in the report and are simple enough to be evaluated by hand.

When fire stops are introduced, then additional flanking paths are introduced. These considerably increase transmission at the higher frequencies, with the dominant transmission path being that involving the floor in each room.

Studies were also undertaken into the effect of the floor joist at the junction of the wall and the floor and in vibration propagation across the floor. In each case, the trends that would be expected agreed well with the measured data. The joists at the joint have to be included for good agreement between the measured and predicted structural level difference results.

7.2 FUTURE RESEARCH

The results of this study have highlighted a number of areas for further study that arise as an immediate result of this study.

- The damping in the cavity is critical in determining the overall sound transmission. Attempts to measures this were not wholly successful and it needs to be studied further to find a reliable method of measurement and to obtain typical measured values. Ideally the measured damping obtained from cavity reverberation measures should be related to the quantity and material properties of absorption placed in the cavity.
- Prediction of sound transmission through the floor was only successful as there were resilient channels that eliminated the structural path. Further work is required on the coupling that would take place through the joists if rigid fixings were used.
- The attenuation of vibration that was measured across the floor also occurs across the wall. This effect has not been included in the model although its mechanisms are reasonably well described. This is likely to be important in determining the flanking transmission paths.
- The success of statistical energy analysis when applied to this particular form of construction suggests that it would be profitable to apply the same modelling techniques to other forms of construction such as multi-leaf lightweight constructions.

APPENDIX A

THE TEST FACILITY

This appendix gives construction and other details of the test facility. Further details are available from NRC.

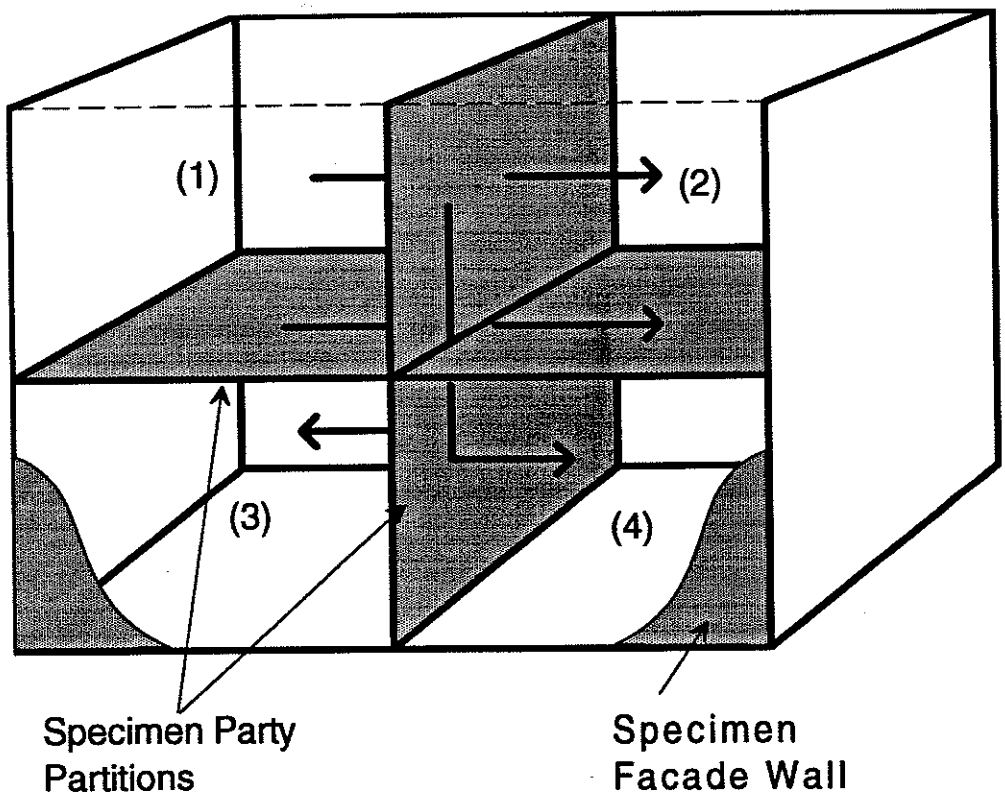

Figure A1. Schematic diagram of the flanking facility.

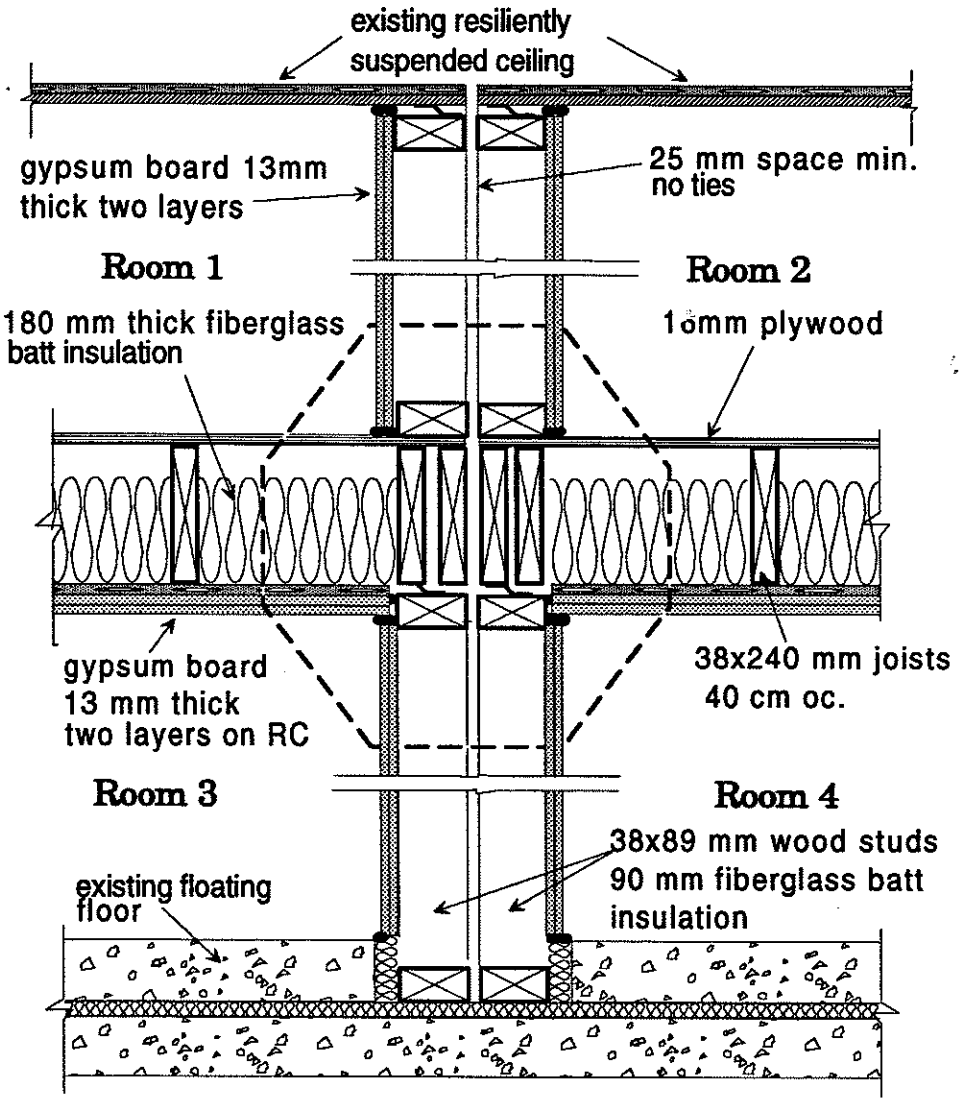

Figure A2. Section through the specimen showing construction details.

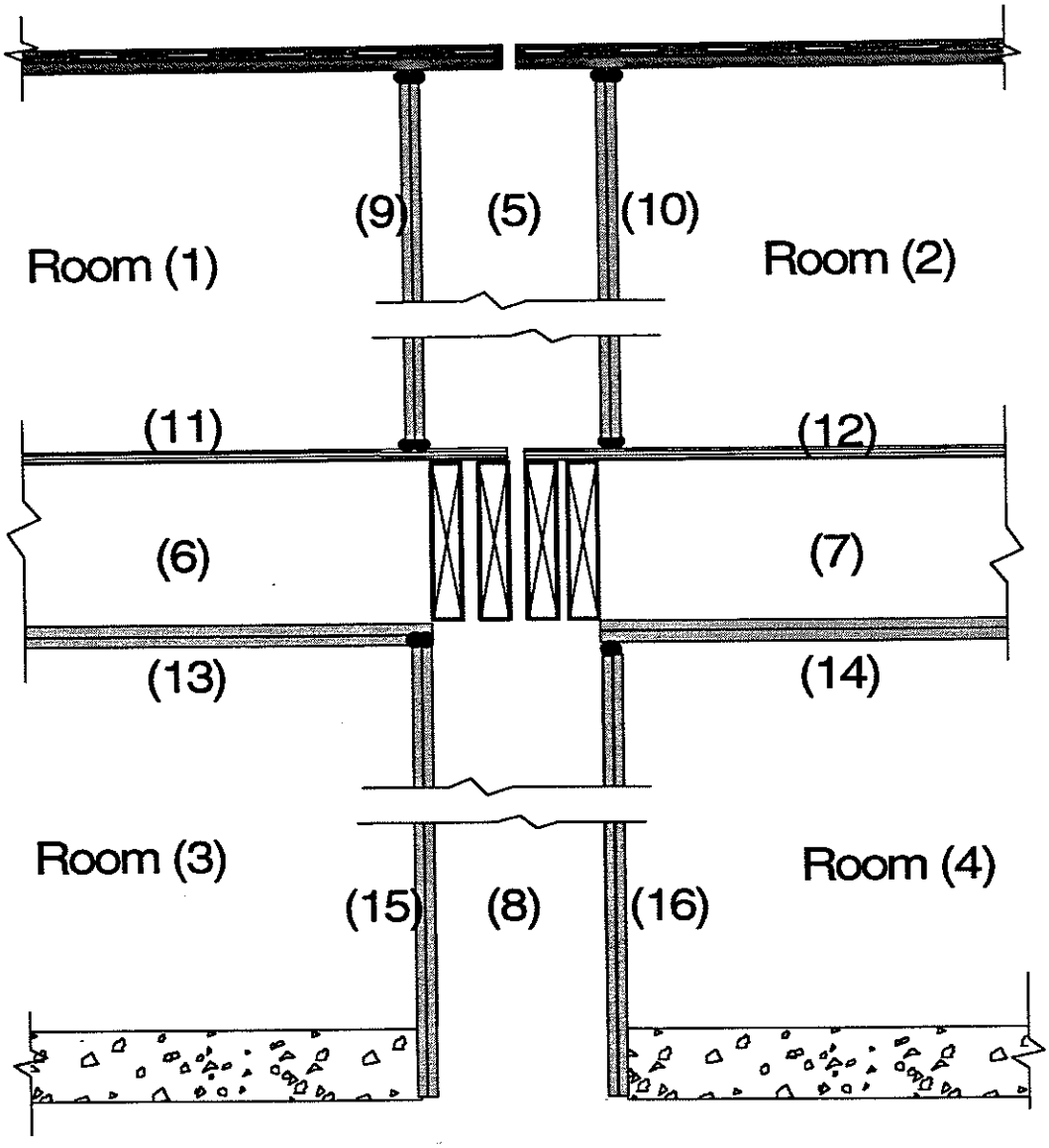

Figure A3. *Sketch of the section through the specimen showing the sub-systems that were modelled and their identification number.*

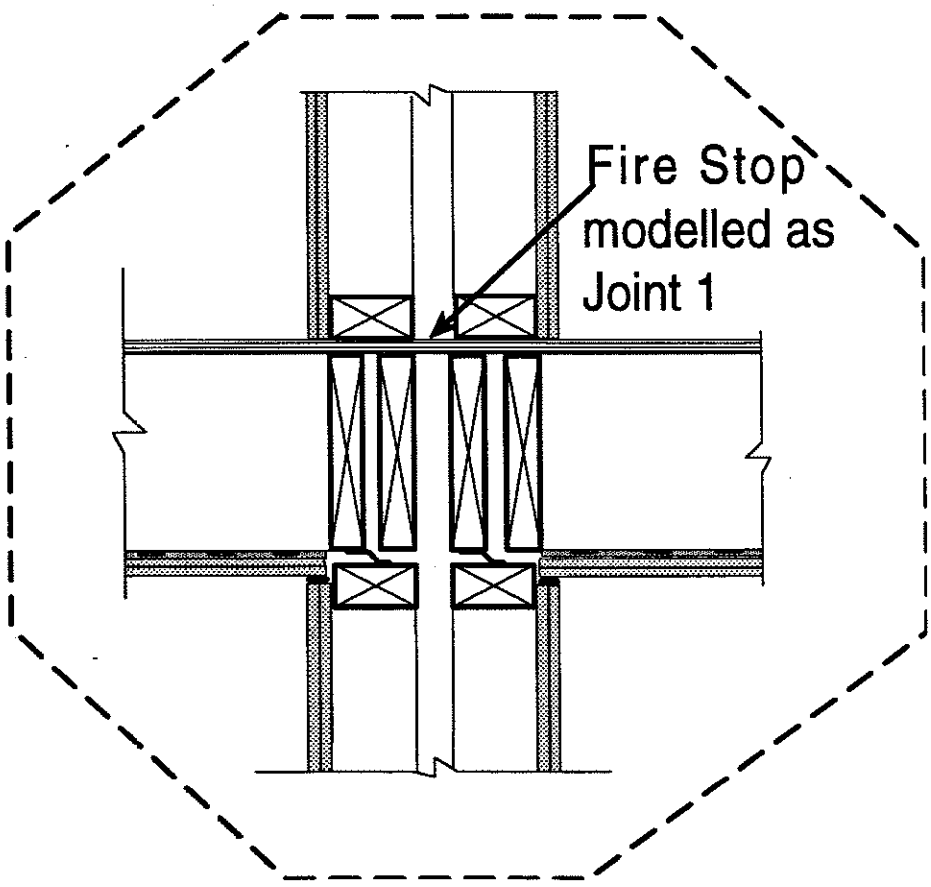

Figure A4. *Sketch of the joint involving the fire stop at the bottom of the party wall. This joint wall modelled as Joint 1.*

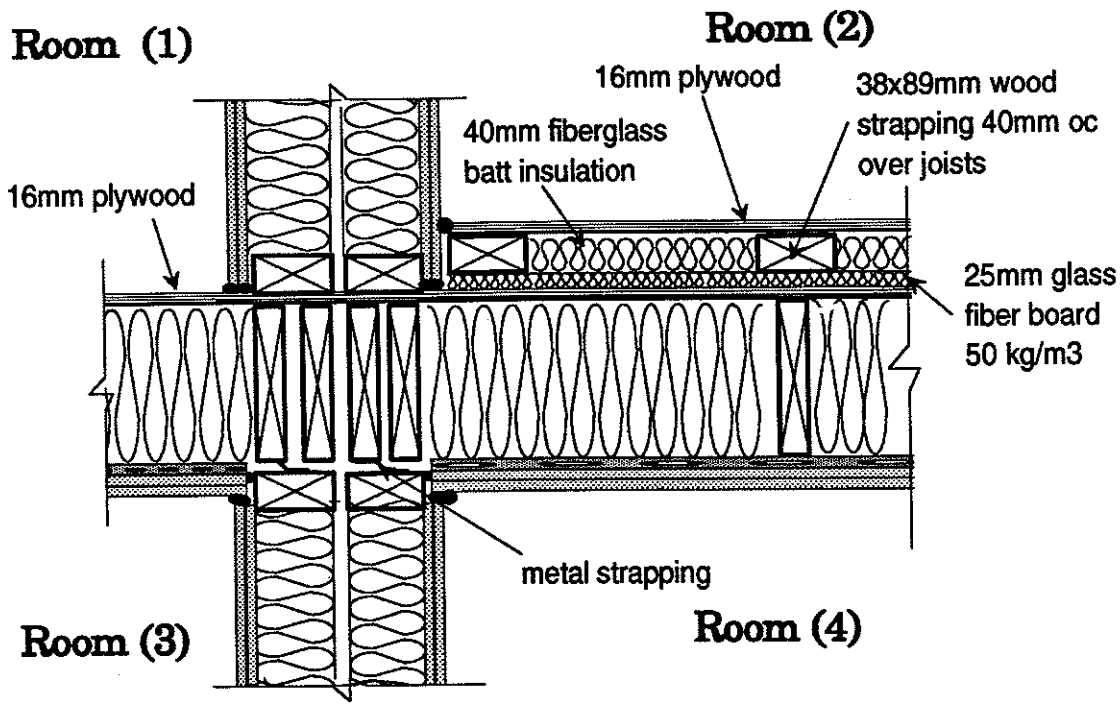

Figure A5. Sketch showing the floating floor installed in Room (2).

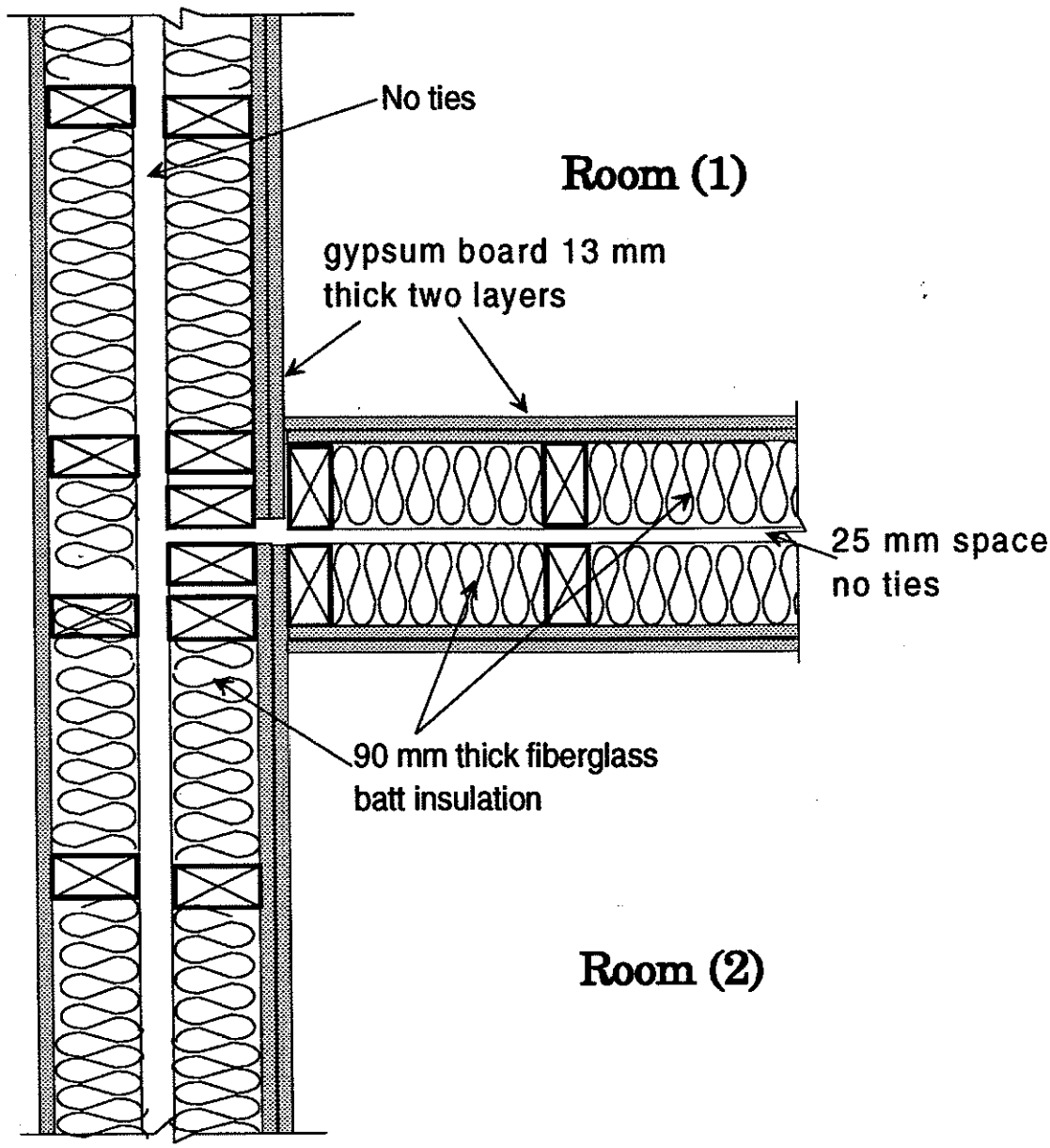

Figure A6. Plan section through the party and flanking walls of the upper rooms.

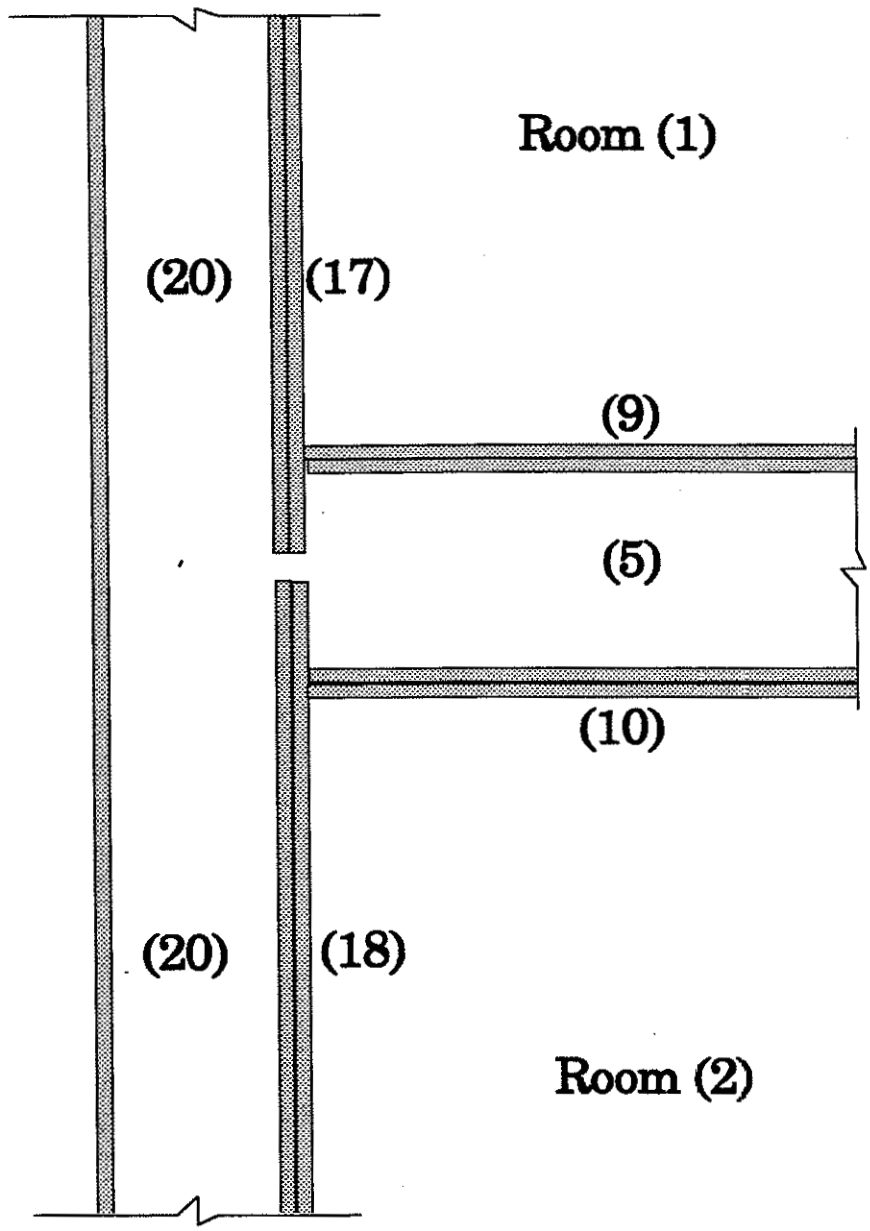

Figure A7. Sketch showing the sub-systems used to model the party and flanking walls of the upper rooms.

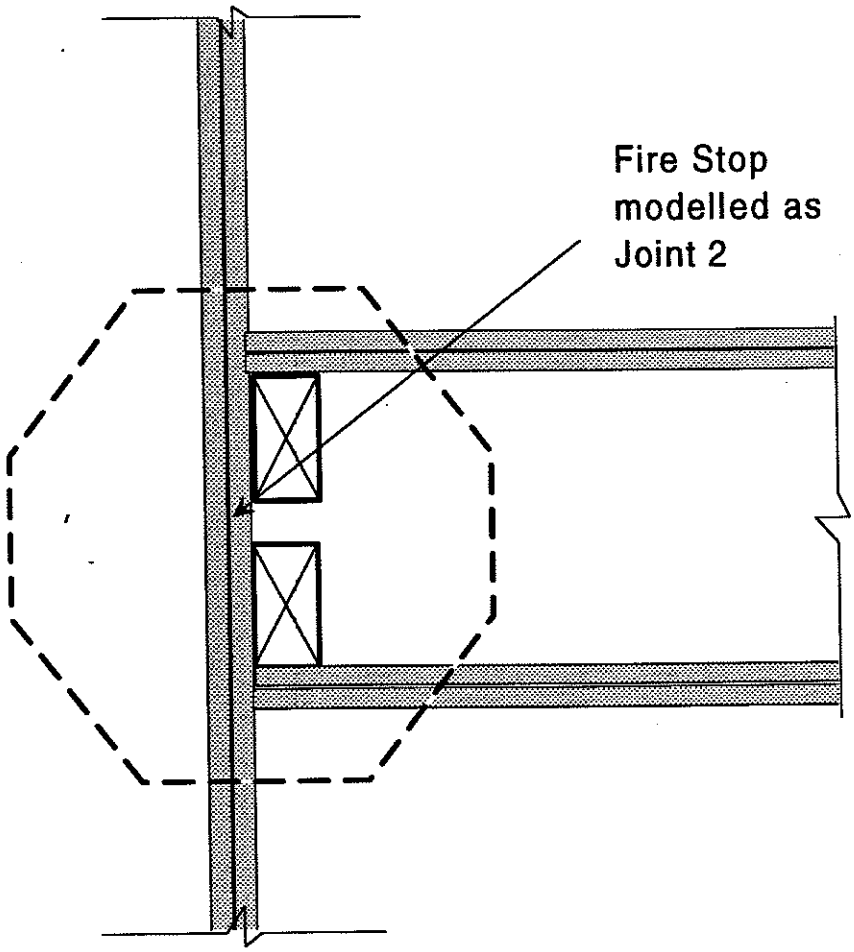

Figure A8. *Sketch showing the fire stop in the flanking wall which was modelled as Joint 2.*

APPENDIX B

The program listed below is the PPC program that was run to generate all the coupling and total loss factors.

THEMODEL.PPC

```
type PPC program to run a model for the basic system
type The program includes only the two upper rooms
type the upper wall and the floor
type
type It is assumed that the walls can be modelled as single plates

siz 27
inp #
50 63 80 100 125 160 200 250 315 400 500 630 800 1000
1250 1600 2000 2500 3150 4000 5000 6300 8000 10000 12500 16000 20000

x>f

$model=1
type Input    1 - steel   fire stop
type          2 - plywood fire stop
type          3 - plywood fire stop with floating floor
type          4 - gypsum  fire stop on wall
ask $model ?


/* choose either default perimeters of specific values */

$per5=#
$per6=#
$per7=#
$per8=#
$per17=#
$per18=#

/*
$per5=67.4
$per6=118.16
$per7=117.18
$per8=58.76
$per17=67.5
```

```
$per18=66.54


$per5=34
$per6=59
$per7=58
$per8=29
$per17=34
$per18=33
*/




if $model == 1 open model1.dat
if $model == 2 open model2.dat
if $model == 3 open model3.dat
if $model == 4 open model4.dat

eno 5
del * * 996,999
del * * 21,50
unj y y y


/* system record */
isy 3 4 4 0 2 1 0

/* subsystem data */
$gypsum=(0.026 3 19.2 0.2 2 3000 0.015)
$ply=(   0.016 3 7.22 0.2 2 1600 0.015)

isu  1 1 4.54 4.60 2.43  0
isu  2 1 4.52 4.11 2.43  0
isu  3 1 4.38 4.46 2.07  0
isu  4 1 4.37 3.96 2.07  0

isu  5 4 4.54 2.43 0.203 0
isu  6 4 4.54 4.60 0.240 0
isu  7 4 4.54 4.11 0.241 0
isu  8 4 4.64 2.07 0.203 0

isu  9 2 4.54 2.43 $gypsum
isu 10 2 4.54 2.43 $gypsum
isu 11 2 4.54 4.60 $ply
isu 12 2 4.54 4.11 $ply
```

```
isu 13 2 4.54 4.60 $gypsum
isu 14 2 4.54 4.11 $gypsum
isu 15 2 4.64 2.07 $gypsum
isu 16 2 4.64 2.07 $gypsum

isu 17 2 3.80 2.43 $gypsum
isu 18 2 3.70 2.43 $gypsum
isu 20 4 7.5  2.43 0.203 0


/* define CLFs */
/* room/cavity to structure */
clf 1  9 # $per5
clf 1 11 # $per6
clf 1 17 # $per17
clf 2 10 # $per5
if $model != 3 clf 2 12 # $per7
clf 2 18 # $per18
clf 5  9 # $per5
clf 5 10 # $per5

clf 3 13 # $per6
clf 3 15 # $per8
clf 4 16 # $per8
clf 4 14 # $per7
clf 6 11 # $per6
clf 6 13 # $per6
clf 7 12 # $per7
clf 7 14 # $per7
clf 8 15 # $per8
clf 8 16 # $per8
clf 20 17 # $per17
clf 20 18 # $per18

/* fix CLFs for peak at fc */
rec  1  9 21 pok 3150 [$3150 5.5 -] dst $last_key_2 $last_key_3 21
rec  1 11 21 pok 1600 [$1600 5.5 -] dst $last_key_2 $last_key_3 21
rec  1 17 21 pok 3150 [$3150 5.5 -] dst $last_key_2 $last_key_3 21
rec  2 10 21 pok 3150 [$3150 5.5 -] dst $last_key_2 $last_key_3 21
if $model != 3 rec  2 12 21 pok 1600 [$1600 5.5 -] dst $last_key_2
$last_key_3 21
rec  2 18 21 pok 3150 [$3150 5.5 -] dst $last_key_2 $last_key_3 21
rec  3 13 21 pok 3150 [$3150 5.5 -] dst $last_key_2 $last_key_3 21
rec  3 15 21 pok 3150 [$3150 5.5 -] dst $last_key_2 $last_key_3 21
rec  4 14 21 pok 3150 [$3150 5.5 -] dst $last_key_2 $last_key_3 21
rec  4 16 21 pok 3150 [$3150 5.5 -] dst $last_key_2 $last_key_3 21
rec  5  9 21 pok 3150 [$3150 5.5 -] dst $last_key_2 $last_key_3 21
rec  5 10 21 pok 3150 [$3150 5.5 -] dst $last_key_2 $last_key_3 21
rec  6 11 21 pok 1600 [$1600 5.5 -] dst $last_key_2 $last_key_3 21
```

```
rec  6 13 21 pok 3150 [$3150 5.5 -] dst $last_key_2 $last_key_3 21
rec  7 12 21 pok 1600 [$1600 5.5 -] dst $last_key_2 $last_key_3 21
rec  7 14 21 pok 3150 [$3150 5.5 -] dst $last_key_2 $last_key_3 21
rec  8 15 21 pok 3150 [$3150 5.5 -] dst $last_key_2 $last_key_3 21
rec  8 16 21 pok 3150 [$3150 5.5 -] dst $last_key_2 $last_key_3 21
rec  9  1 21 pok 3150 [$3150 5.5 -] dst $last_key_2 $last_key_3 21
rec  9  5 21 pok 3150 [$3150 5.5 -] dst $last_key_2 $last_key_3 21
rec 10  2 21 pok 3150 [$3150 5.5 -] dst $last_key_2 $last_key_3 21
rec 10  5 21 pok 3150 [$3150 5.5 -] dst $last_key_2 $last_key_3 21
rec 11  1 21 pok 1600 [$1600 5.5 -] dst $last_key_2 $last_key_3 21
rec 11  6 21 pok 1600 [$1600 5.5 -] dst $last_key_2 $last_key_3 21
if $model != 3 rec 12  2 21 pok 1600 [$1600 5.5 -] dst $last_key_2
$last_key_3 21
rec 12  7 21 pok 1600 [$1600 5.5 -] dst $last_key_2 $last_key_3 21
rec 13  3 21 pok 3150 [$3150 5.5 -] dst $last_key_2 $last_key_3 21
rec 13  6 21 pok 3150 [$3150 5.5 -] dst $last_key_2 $last_key_3 21
rec 14  4 21 pok 3150 [$3150 5.5 -] dst $last_key_2 $last_key_3 21
rec 14  7 21 pok 3150 [$3150 5.5 -] dst $last_key_2 $last_key_3 21
rec 15  3 21 pok 3150 [$3150 5.5 -] dst $last_key_2 $last_key_3 21
rec 15  8 21 pok 3150 [$3150 5.5 -] dst $last_key_2 $last_key_3 21
rec 16  4 21 pok 3150 [$3150 5.5 -] dst $last_key_2 $last_key_3 21
rec 16  8 21 pok 3150 [$3150 5.5 -] dst $last_key_2 $last_key_3 21
rec 17  1 21 pok 3150 [$3150 5.5 -] dst $last_key_2 $last_key_3 21
rec 18  2 21 pok 3150 [$3150 5.5 -] dst $last_key_2 $last_key_3 21


/* non resonant room to room */
clf 1  5  9 #
clf 2  5 10 #
clf 1  6 11 #
clf 3  6 13 #
if $model != 3 clf 2  7 12 #
clf 4  7 14 #
clf 3  8 15 #
clf 4  8 16 #
clf 1 20 17 #
clf 2 20 18 #

/* structural joints at corners */
clf 1 17 1 3.8
clf 2 18 1 3.7
if $model != 4 clf 9 17 1 2.43 clf 10 18 1 2.43
if $model == 4 clf 1  9 1 4.54 clf 2 10 1 4.54


if $model == 1 ijo 1 11 9 10 12 4.54 5 6 42      /* steel   fire stop
*/
if $model == 2 ijo 1 11 9 10 12 4.54 5 6 42200   /* ply     fire stop
*/
```

```
if $model == 3 ijo 1 11 9 10 12 4.54 5 6 42200  /* ply     fire stop
*/
if $model == 4 ijo 1 17 9 10 18 4.54 5 6 15900  /* gypsum fire stop
*/


/* input TLFs */
/* from measured gypsum RT */
lim 100 2000
inp #
0.285 0.275 0.189 0.145 0.120 0.110 0.105
0.073 0.063 0.055 0.035 0.035 0.035 0.033
dst 9 0 71
log line 10^x
lim 50 20000
1/x fre / 2.2 * log 10 * 120 +
sto  9 0 26
sto 10 0 26
sto 15 0 26
sto 16 0 26
sto 13 0 26
sto 14 0 26
sto 17 0 26
sto 18 0 26

/* assume the same for plywood */
sto 11 0 26
sto 12 0 26


/* input RT's of rooms */
inp #
0.7 0.63 0.75 1.19 1.25 1.48 1.65 1.51 1.62 1.75 1.83 1.54 1.45 1.45
1.38 1.32 1.28 1.30 1.32 1.28 1.21 1.07 1 1 1 1 1
dsto 1 0 71 1/x fre / 2.2 * log 10 * 120 + dst 1 0 26

inp #
0.52 0.74 0.83 1.1 1.3 1.42 1.35 1.38 1.44 1.71 1.74 1.53 1.42 1.36
1.24 1.21 1.17 1.14 1.21 1.18 1.13 1.0 1 1 1 1 1
dsto 2 0 71 1/x fre / 2.2 * log 10 * 120 + dst 2 0 26

inp #
0.45 0.70 1.08 1.27 1.44 1.72 1.61 1.47 1.70 1.88 1.85 1.84 1.59 1.50
1.38 1.35 1.35 1.26 1.27 1.37 1.32 1.23 1 1 1 1 1
dsto 3 0 71 1/x fre / 2.2 * log 10 * 120 + dst 3 0 26

inp #
0.48 0.47 1.05 1.02 1.14 1.45 1.45 1.45 1.69 1.96 1.70 1.67 1.48 1.38
1.33 1.32 1.32 1.30 1.30 1.35 1.31 1.19 1 1 1 1 1
```

```
dsto 4 0 71 1/x fre / 2.2 * log 10 * 120 + dst 4 0 26


/* cavity RT is 3/sqrt(f) */
2.2 fre / 3 fre sqrt / /
log 10 * 120 +
/* fix at 50 and 63 Hz */
pok 50 [$50 3 +]
pok 63 [$63 2 +]
pok 80 [$80 1 +]
sto 5 0 tlf
sto 6 0 tlf
sto 7 0 tlf
sto 8 0 tlf
sto 20 0 26

joi * # #

win 1 100
solve



/* compute TL values */

rec 1 1 30 rec 1 2 30 -
rec  2 0 71 11 * 0.161 / 45.3 / log 10 * +
dsto 1 2 31

rec 1 1 30 rec 1 3 30 -
rec 3 0 71  20.2 * 0.161 / 40.0 / log 10 * +
dsto 1 3 31

rec 1 1 30 rec 1 4 30 -
rec 4 0 71  10 * 0.161 / 35.3 / log 10 * +
dsto 1 4 31
```

REFERENCES

Cremer, L., Heckl, M. and Ungar, E. E., *Structure-borne sound.* Springer-Verlag, London (1973).

Leppington, F.G., Broadbent, E.G. and Heron, K.H., The acoustic radiation efficiency of rectangular panels. *Proceedings of the Royal Society of London* (1982), **A382**, 245-271.

Leppington, F.G., Broadbent, E.G. and Heron, K.H., Acoustic radiation from rectangular panels with constrained edges. *Proceedings of the Royal Society of London* (1984), **A393**, 67-84.

Leppington, F.G., Broadbent, E.G., Heron, K.H. and Mead, S.M., Resonant and non-resonant acoustic properties of elastic panels. I. The radiation problem. *Proceedings of the Royal Society of London* (1986), **A406**, 139-171.

Leppington, F.G., Heron, K.H., Broadbent, E.G. and Mead, S.M., Resonant and non-resonant acoustic properties of elastic panels. II. The transmission problem. *Proceedings of the Royal Society of London* (1987), **A412**, 309-337.

Maidanik, G., Response of ribbed panels to reverberant acoustic fields. *Journal of the Acoustical Society of America* (1962), **34**, 809-826.

Price, A.J. and Crocker, M.J. Sound transmission through double panels using statistical energy analysis. *Journal of the Acoustical Society of America* (1970), **47**, 683-693.

Sewell, E.C., Sound transmission through an infinite strip double partition. *Internal confidential note from the BRE.* Number 80/67, (1967).